PROCESS SIMULATION FOR CO_2 AND SO_2 CAPTURE BY USING FLY ASH AS SOLID SORBENT

BY

MAHINSASA RATHNAYAKE

A THESIS SUBMITTED IN PARTIAL FULFILLMENT OF THE REQUIREMENTS FOR THE DEGREE OF MASTER OF SCIENCE (ENGINEERING AND TECHNOLOGY)

SIRINDHORN INTERNATIONAL INSTITUTE OF TECHNOLOGY

THAMMASAT UNIVERSITY

ACADEMIC YEAR 2015

PROCESS SIMULATION FOR CO_2 AND SO_2 CAPTURE BY USING FLY ASH AS SOLID SORBENT

BY

MAHINSASA RATHNAYAKE

A THESIS SUBMITTED IN PARTIAL FULFILLMENT OF THE REQUIREMENTS FOR THE DEGREE OF MASTER OF SCIENCE (ENGINEERING AND TECHNOLOGY)

SIRINDHORN INTERNATIONAL INSTITUTE OF TECHNOLOGY

THAMMASAT UNIVERSITY

ACADEMIC YEAR 2015

PROCESS SIMULATION FOR CO_2 AND SO_2 CAPTURE BY USING FLY ASH AS SOLID SORBENT

A Thesis Presented

By

MAHINSASA RATHNAYAKE

Submitted to

Sirindhorn International Institute of Technology

Thammasat University

In partial fulfillment of the requirements for the degree of

MASTER OF SCIENCE (ENGINEERING AND TECHNOLOGY)

Approved as to style and content by

Advisor and
Chairperson of Thesis Committee _____

(Asst. Prof. Pisanu Toochinda, Ph.D.)

Committee Member and
Chairperson of Examination Committee _____

(Assoc. Prof. Luckhana Lawtrakul, Dr.rer.nat.)

Committee Member _____

(Asst. Prof. Anotai Suksangpanomrung, Ph.D.)

November 2015

Acknowledgements

I extend my sincere gratitude to my research advisor, Asst. Prof. (Dr.) Pisanu Toochinda for his valuable guidance and keen attention given throughout this master degree thesis. In addition, I want to show my genuine respect to the other Thesis committee members, Assoc. Prof. (Dr.) Luckhana Lawtrakul and Asst. Prof. (Dr.) Anotai Suksangpanomrung for always sharing their expertise with me which made me more knowledgeable and courageous during this thesis study.

Moreover, this master degree thesis study was supported by Electricity Generating Authority of Thailand (EGAT) and the National Research University Project of Thailand, Office of Higher Education Commission.

Finally, I must also thankfully remind the support given to me by my parents, my loving wife and my family members as well as by all the officials and colleagues in the School of Bio-Chemical Engineering Technology, Sirindhorn International Institute of Technology, Thammasat University, Thailand, in various ways to make this work successful.

Abstract

PROCESS SIMULATION FOR CO_2 AND SO_2 CAPTURE BY USING FLY ASH AS SOLID SORBENT

By

MAHINSASA RATHNAYAKE

Bachelor of the Science of Engineering, University of Ruhuna in Sri Lanka, 2010

Fly ash, a waste material from coal fired power plants, becomes an interesting solid sorbent due to their low cost and their applications after CO_2 capture. The performance of fly ash as a solid sorbent material for CO_2 capture via surface adsorption and carbonation reaction were evaluated using gas chromatogram analysis and EDTA titration respectively. At 30 ºC, 1 atm and 5 wt% moisture content, fly ash exhibited a total CO_2 capture capacity of 208 µmol/g sorbent. A scaled-up reactor system comprising of two tubular reactors in series by employing the annual quantity of qualified fly ash (1,800 ktonne/year) was proposed using Aspen plus process simulation software, which can capture a total amount of 16.48 ktonne CO_2/year equivalent to 0.09% of the annual CO_2 emission from Mae Moh coal fired power plant of the Electricity Generating Authority of Thailand (EGAT). Fly ash was suggested to be used as an admixture in cement after the CO_2 capture.

Unqualified fly ash can also serve as a solid sorbent to lower the load of the desulfurization unit in coal fired power plants at low temperatures. The SO_2 capture of fly ash via adsorption and sulfation reaction were evaluated using mass spectrometry and EDTA titration, respectively. The reversible SO_2 adsorption at low temperatures is not desirable for SO_2 capture. However, the reaction of irreversible SO_2 sulfation with fly ash boosts up at high temperatures and the highest yield of SO_2 capture was observed at 400 ºC. A scaled-up reactor system equipped with two tubular reactors in parallel was simulated in Aspen plus process simulation software using the annual intake of unqualified fly ash (200 ktonne/year), which can capture 4.882 ktonne SO_2/year equivalent to 0.37% of the annual SO_2 emission from Mae Moh coal fired power plant, Thailand. The effect of different parameters on this system will be discussed.

Keywords: CO_2 and SO_2 capture, fly ash, coal fired power plant, process simulation

Table of Contents

Chapter	Title	Page
	Signature Page	i
	Acknowledgements	ii
	Abstract	iii
	Table of Contents	iv
	List of Tables	vii
	List of Figures	viii
	List of Symbols	x
	List of Abbreviations and Chemical Formulas	xi
1	Introduction	1
	1.1 Introduction	1
	1.2 Statement of problems	2
	1.3 Objectives of the study	4
	1.4 Scope of the study	4
2	Literature Review	5
	2.1 Background of coal fired power plants	5
	2.1.1 Types of coal	5
	2.1.2 Coal combustion techniques	7
	2.1.3 Airborne emissions from coal fired power plants	12
	2.2 CO_2 capture techniques	17
	2.2.1 Chemical and physical properties of CO_2	17
	2.2.2 Environmental impact of CO_2 emission	18
	2.2.3 Conventional CO_2 capture techniques	19
	2.2.4 CO_2 capture using fly ash as a solid sorbent	25
	2.3 SO_2 removal techniques	28
	2.3.1 Chemical and physical properties of SO_2	28

2.3.2 Environmental impact of SO_2 emission 29
2.3.3 Conventional flue gas desulfurization techniques 30
2.3.4 SO_2 capture using fly ash as solid sorbent 37
2.3.5 Comparison of different reactor types for the desulfurization 43

3 Methodology 45
3.1 CO_2 capture using fly ash 45
3.1.1 Materials for CO_2 capture 45
3.1.2 Experimental procedure for CO_2 capture 45
3.1.3 Analysis techniques for CO_2 capture 47
3.1.4 Process simulation procedure for CO_2 capture 48
3.2 SO_2 capture using fly ash 50
3.2.1 Materials for SO_2 capture 50
3.2.2 Temperature programmed desorption (TPD) 50
3.2.3 Temperature programmed reaction (TPR) 51
3.2.4 Analysis techniques for SO_2 capture 52
3.2.5 Process simulation procedure for SO_2 capture 52

4 Results and Discussion 56
4.1 Properties of fly as 56
4.2 CO_2 capture using fly ash 56
4.2.1 Effect of moisture content for CO_2 capture capacity of fly ash 56
4.2.2 Effect of pressure for CO_2 capture capacity of fly ash 57
4.2.3 XRD characterization of fly ash before and after CO_2 capture 58
4.2.4 Effect of contact time for CO_2 capture performance of fly ash 59
4.2.5 Process simulation results for CO_2 capture 60
4.3 SO_2 capture using fly ash 61
4.3.1 SO_2 capture of fly ash at low temperatures 61
4.3.2 SO_2 capture over fly ash by sulfation reaction 62
4.3.3 XRD characterization of fly ash before and after SO_2 capture 63
4.2.2 Process simulation results for SO_2 capture 65

5 Conclusions and Recommendations 72
5.1 Conclusions 72
5.2 Recommendations 74

References 75

Appendices 85

Appendix A Physical properties of fly ash 86
Appendix B Chemical and physical properties of CO_2 87
Appendix C Chemical and physical properties of SO_2 88
Appendix D Calculation procedure for GC/MS results 89
Appendix E Calibration curve of CO_2 for gas chromatograph 90
Appendix F Calibration of SO_2 for mass spectrometry 91
Appendix G Calculation procedure for EDTA titration results 92

List of Tables

Tables		Page
2.1	Composition and properties of different stages of coal	6
2.2	Composition of airborne emissions from coal fired power plants	13
2.3	Standard regulations for chemical properties of coal fly ash to be used in cementitious applications	15
2.4	Standard regulation for physical properties of coal fly ash to be used in cementitious applications	15
2.5	Production data in 2008 for Mae Moh coal fired power plant	16
2.6	Summary of post-combustion CO_2 capture using solid sorbents	23
2.7	Summary of CO_2 capture using fly ash as solid sorbent	26
2.8	Summary of post combustion desulfurization using solid sorbents	35
2.9	Summary of SO_2 capture using fly ash as solid sorbent	39
2.10	Comparison of different desulfurization reactor units	44
3.1	Input data for the CO_2 capture simulation in Aspen plus software	48
3.2	Composition of flue gas input to the SO_2 capture simulation program	53
4.1	Major components of fly ash from Mae Moh coal fired power plant	56
4.2	Effect of moisture content for CO_2 capture performance of fly ash at 30 ºC, 1 atm, and contact time of 30 minutes	57
4.3	Effect of the adsorption pressure for CO_2 capture capacity of fly ash at 30 ºC, 0 wt% moisture content, and contact time of 30 minutes	58
4.4	Effect of contact time for CO_2 capture capacity of fly ash at 30 ºC, 1 atm and 0 wt% moisture	59
4.5	Process stream flow results from the Aspen plus simulation for the CO_2 capture process	60
4.6	Average SO_2 capture capacities of fly ash at low temperatures	61
4.7	Process stream results from the Aspen plus simulation for the scaled-up SO_2 capture system	70

List of Figures

Figures		Page
1.1	World fossil fuel reserves by region	1
2.1	Pulverized coal combustion technique	8
2.2	Circulating fluidized bed coal combustion technique	9
2.3	Integrated gasification combined cycle technique	10
2.4	Schematic diagram of a typical coal fired power plant	11
2.5	Lewis structure of CO_2	17
2.6	Environmental impact of CO_2 emission	18
2.7	Comparison of different post-combustion CO_2 control techniques	22
2.9	Two resonance Lewis structures of SO_2	28
2.10	Environmental impact of SO_2 emission	29
2.11	Comparison of conventional SO_2 control techniques	34
3.1	The experimental set-up for CO_2 capture	45
3.2	The experimental procedure for CO_2 capture	46
3.3	The steps of process simulation procedure for CO_2 capture	49
3.4	Aspen plus process flowsheet for the CO_2 capture simulation	49
3.5	The experimental setup for desulfurization	50
3.6	The experimental procedure for SO_2 capture	51
3.7	Process flowsheet for SO_2 capture process simulation in Aspen plus	54
3.8	Steps of SO_2 capture process simulation procedure	55
4.1	XRD patterns of the fresh fly ash before CO_2 capture and after CO_2 capture at 30 ºC, 1 atm, 5 wt % moisture	58
4.2	Mass spectrometry profiles of SO_2 (m/z = 64.0) and H_2O (m/z = 18.0) for temperature trogrammed reaction (TPR) over fly ash from 35 ºC - 600 ºC	62
4.3	XRD patterns of the fly ash samples (a: Fresh fly ash; b: After SO_2 capture at 330 ºC; c: After temperature programmed reaction from 35 ºC - 600 ºC)	64

4.4 Aspen plus sensitivity analysis results for the variation of reactor outlet pressure with respect to the total flue gas mass flow into the scaled-up packed bed reactor system 66
4.5 Aspen plus sensitivity analysis results for the variation of reactor outlet pressure with respect to the reactor bed void fraction in the scaled-up packed bed reactor system 67
4.6 Aspen plus sensitivity analysis results for the variation of reactor outlet pressure with respect to the reactor diameter in the scaled-up packed bed reactor system 68
4.7 Aspen plus sensitivity analysis results for the variation of reactor outlet pressure with respect to the reactor length in the scaled-up packed bed reactor system 69
5.1 Summary of the proposed CO_2 and SO_2 capture systems using fly ash 73

List of Symbols

Symbol	Unit	Property
A	s^{-1}	Pre-exponential factor
A_c	m^2	Cross sectional area
D	m	Diameter
D_p	m	Particle diameter in the bed
E_a	$KJmol^{-1}$	Activation energy
F_{A_o}	$mol.L^{-1}.s^{-1}$	Feed molar flow rate
G	$kg.m^{-2}.s^{-1}$	Superficial mass velocity ($G = \rho u$)
g_c	$kg.m.N^{-1}.s^{-2}$	Conversion factor (for metric system, $g_c = 1$)
k	s^{-1}	Reaction constant
L	m	Length
m	kg	Mass
n	mol	Mole quantity
P	atm	Pressure
P_o	atm	Inlet pressure to the reactor
R	$L.atm.K^{-1}.mol^{-1}$	Gas constant ($0.082\ L.atm.K^{-1}.mol^{-1}$)
$-r_{SO_2}$	$mol.L^{-1}.s^{-1}$	Rate of reaction
$[SO_2]$	$mol.L^{-1}$ (M)	Volume concentration of SO_2
T	K	Temperature
$T_{Reaction}$	K/ °C	Reaction Temperature
u	ms^{-1}	Superficial velocity
V	L	Volume
w	kg	Packed bed weight
X	Dimensionless	Conversion
ρ_o	$kg.m^{-3}$	Initial gas density
φ	Dimensionless	Void fraction
μ	$kg.m^{-1}.s^{-1}$	Viscosity of gas passing through the bed

List of Abbreviations and Chemical Formulas

Abbreviation / Formula	Definition
AFM	Atomic Force Microscopy
Al_2O_3	Aluminum Oxide
As	Arsenic
ASTM	American Society for Testing and Materials
BET	Brunauer–Emmett–Teller
C	Carbon
$CaCO_3$	Calcium Carbonate (Limestone)
CaO	Calcium Oxide (Free lime)
$Ca(OH)_2$	Calcium Hydroxide (hydrated lime)
$CaSO_3 \cdot ½H_2O$	Calcium Sulfate dihydrate
$CaSO_4$	Calcium Sulfite Anhydrite
$CaSO_4 \cdot 2H_2O$	Calcium Sulfite hemihydrate
Cd	Cadmium
CO	Carbon Monoxide
CO_2	Carbon Dioxide
DEA	Di-Ethanol Amine
DIPA	Di-isopropanol Amine
DRIFT	Diffuse Reflectance Infrared Fourier Transform Spectroscopy
EDS	Energy Dispersive X-Ray Spectroscopy
EDTA	Ethylene Diamine Tetra Acetic Acid
EGAT	Electricity Generating Authority of Thailand
ESP	Electrostatic Precipitator
Fe_2O_3	Iron Oxide (Ferric Oxide)
FGD	Flue Gas Desulfurization
GC	Gas Chromatograph
FTIR	Fourier Transform Infrared Spectroscopy

Abbreviation / Formula	Definition
GC/MS	Gas Chromatograph Mass Spectrometer
H	Hydrogen
H_2	Hydrogen Gas
H_2CO_3	Carbonic Acid
H_2O	Water
HCl	Hydrochloric Acid
HF	Hydrofluoric Acid
Hg	Mercury
HNO_3	Nitric Acid
H_2SO_3	Sulfurous Acid
H_2SO_4	Sulfuric Acid
ICDD-PDF	The International Centre for Diffraction Data - Powder Diffraction Files
IDEAL	Ideal Gas Property Method
IGCC	Integrated Gasification Combined Cycle
IR	Infrared
JCPDS	Joint Committee on Powder Diffraction Standards
K_2O	Potassium Oxide
KOH	Potassium Hydroxide
LOI	Loss On Ignition
m/z	Mass/Charge Ratio
max.	Maximum
MEA	Mono-Ethanol-Amine
MS	Mass Spectrometer
N	Nitrogen
N_2	Nitrogen Gas
Na_2O	Sodium Oxide
NaOH	Sodium Hydroxide

Abbreviation / Formula	Definition
NO_x	Nitrogen Oxides
OPC	Ordinary Portland Cement
Pb	Lead
PENG ROB	Peng-Robinson activity coefficient method
PID	Proportional–Integral–Derivative Controller
ppm	Particles per million
RH	Relative Humidity
Se	Selenium
SEM	Scanning Electron Microscopy
SiO_2	Silicon Dioxide
S	Sulfur
SO_2	Sulfur Dioxide
TCD	Thermal Conductivity Detector
[TETA]L	Tri-Ethylene Tetra Amine Lactate
TGA	Thermogravimetric Analysis
TPD	Temperature Programmed Desorption
TPR	Temperature Programmed Reaction
vol%	Volume Percentage
wt%	Weight Percentage
XPS	X-Ray Photoelectron Spectroscopy
XRD	X-Ray Diffraction
XRF	X-Ray Fluorescence
3-CPA	3-Chloro Propyl Amine

Chapter 1
Introduction

1.1 Introduction

Energy consumption expands day by day with the expansion of population and industrial activities in the entire world. Coal still plays a major role in the world energy supply and consumption representing nearly 30% of the world energy supply [1]. Utilization as a solid fuel to generate electricity, is the primary application of coal. The estimations reveal that, at least 40% of global electricity generation is supplied by using coal as the fuel source [2]. The global coal consumption was approximately 7.25 billion tonnes in 2010 and, it is predicted to be increased upto 9.05 billion tonnes by 2030 as per the prevailing trend [3].

According to the surveys, 892 billion tonnes of recoverable coal reserves have been scattered around the world in nearly 70 countries [4]. Figure 1.1 shows that, the largest coal reserves are available in the countries such as, North America, Russia, China and India. In addition, Asia Pacific region countries like Thailand also has a higher potential of coal reserves. Coal is responsible for nearly 25% of the total electricity supply in Thailand [5]. Thailand has proven reserves of lignite coal approximately 1,300 million tons which is composed of around 3% sulfur content and approximately 30% ash content [5].

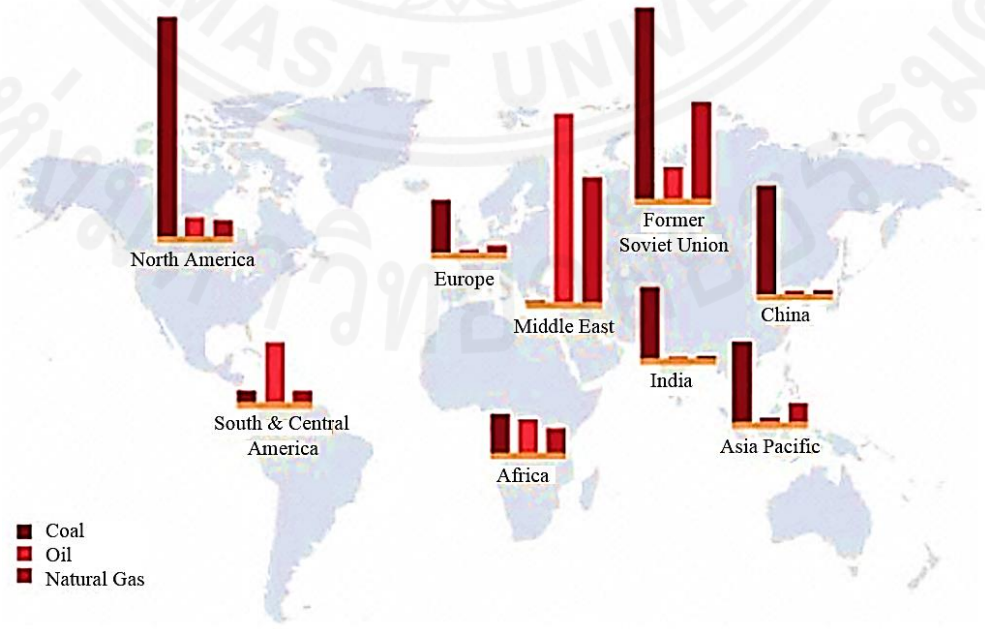

Figure 1.1: World fossil fuel reserves by region [4]

1.2 Statement of problems

Carbon dioxide (CO_2), is a major greenhouse gas which can reflect the infrared radiation of the sun back to the earth's surface. This phenomenon is known as the greenhouse effect. Accumulation of CO_2 in the atmosphere can cause global warming and climatic changes including melting of polar ice caps, unusual droughts, floods and storms as long term effects. The natural equilibrium cycle of CO_2 has been disturbed by various human activities coupled with the population growth and technological advancements. Hence, CO_2 concentration in the Earth's atmosphere has been significantly increasing. However, CO_2 concentration in the atmosphere still lies around 369 ppm and it is expected to rise upto 750 ppm by year 2100 if no proper actions are taken to control CO_2 emissions [6].

Approximately 40% of the global CO_2 emissions are caused by fossil fuel power plants where coal fired power plants are the main contributor [7]. There are no strict legislative regulations practiced so far, in order to limit CO_2 emissions from coal fired power plants. However, actions must be taken to mitigate the CO_2 emission from coal fired power plants because, consumption of coal is also increasing to provide required energy demand in the world. The conventional CO_2 control techniques are practically unmanageable and economically not viable since, they are subjected to high operational costs and difficulties in storage after capture [6-8]. Fly ash, a waste material coming out from coal fired power plants, has a certain potential for CO_2 capture [9]. However, there is a scarcity of previous studies which analyze the industrial scale CO_2 capture conditions and performance of pure fly ash.

Sulfur dioxide (SO_2) is a toxic gas with an irritating odor. When SO_2 get mixed with air, it oxidizes as well as dissolves in the water vapor in the air and forms sulfurous acid (H_2SO_3) and sulfuric acid (H_2SO_4) easily [10]. Therefore, SO_2 can be a major factor for the acid rain that is harmful for vegetation, agriculture and, corrosion of buildings and constructions [11]. SO_2 also contributes for the generation of smog in the atmosphere whereas, availability of SO_2 in the atmosphere can cause serious health hazards for the respiratory systems of all living beings [12]. Due to the higher toxicity and severity of environmental impacts, strict legislative regulations and emission standards have been stipulated by legal environmental authorities in order to control SO_2 emission from coal fired power plants upto permissible levels [13].

Sulfur content in coal varies with the quality of coal. However, even the best quality coal can contain a fair amount of sulfur in their compositions [14]. Therefore, urgent remedies are essential to eliminate SO_2 emission from coal fired power plants. Almost all of the conventional desulfurization techniques use natural materials such as limestone, hydrated lime, quick lime and dolomite as the chemical reagents, in order to take place the sulfation reactions between the reagent and SO_2 in the flue gas during the desulfurization process [15]. These desulfurization techniques suffer from high temperature operation, high material costs and high transportation costs of chemical reagents for large scale coal fired power plants [16, 17]. Existing studies report that, fly ash can also be used as a solid sorbent for SO_2 capture [18, 19]. Fewer studies discuss the capability and conditions for SO_2 removal using fly ash for large scale coal fired power plants. However, fly ash which has negligible material and transportation costs, can contribute for efficient SO_2 removal by lowering the load of the existing desulfurization unit for the flue gas emission from the coal fired power plant.

It is obvious that, further investigations are required to determine the CO_2 and SO_2 capture conditions and capture capacities of fly ash to verify the applicability of fly ash for industrial scale CO_2 and SO_2 capture. These investigations will be helpful in manipulating the coal fired electricity generation free from serious environmental issues while improving the waste management system of coal fired power plants in a more profitable approach. Therefore, utilization of fly ash as a solid sorbent for CO_2 and SO_2 capture would be an interesting research title equipped with the potential of further investigations.

1.3 Objectives of the study

The objectives of the entire study can be split up as follows.

1. Investigate the conditions for CO_2 capture and evaluate the CO_2 capture capacities using qualified fly ash as solid sorbent.

2. Estimate a scaled-up system for CO_2 capture using qualified fly ash as solid sorbent so that, fly ash can be further utilized for cementitious applications after CO_2 capture.

3. Determine the conditions and the capture capacities for desulfurization using unqualified fly ash as solid sorbent.

4. Propose a scaled-up system for SO_2 capture using unqualified fly ash as solid sorbent to lower the load of desulphurization unit in coal fired power plant.

1.4 Scope of the study

This study is focused on proposing a simulated CO_2 and SO_2 capture system using fly ash as solid sorbent. The purpose is not defined to replace the existing CO_2 and SO_2 removal techniques but, to effectively utilize fly ash as a supportive material towards CO_2 and SO_2 capture in order to maintain a more feasible environmental management for a coal fired power plant.

- The experimental and simulation studies are carried out by considering Mae Moh coal fired power plant in Thailand as the study model.

- The experiments cover the investigations for the conditions and capture capacities of fly ash as solid sorbent for CO_2 and SO_2 capture separately.

- The simulations from Aspen plus software are employed for the scaling-up process of the reactor systems for CO_2 and SO_2 capture separately.

Chapter 2

Literature Review

2.1 Background of coal fired power plants

2.1.1 Types of coal

Coal can be identified as a combustible sedimentary rock in black or brownish color. It is available on the Earth as rock layers, called as coal beds or coal seams. Coal is generated from fossilized carbon which forms when dead plant and animal matter is converted into peat [2]. This is a long periodic biological and geological process which takes place naturally. There are wide variations in the compositions of coal over the different grades of coal where, the physical properties also vary from each grade of coal to the other.

The main components in coal are carbon, hydrogen, oxygen, nitrogen, sulfur and incombustible ash [2, 20]. The incombustible ash within coal includes lot of heavy metal components such as arsenic (As), cadmium (Cd) and mercury (Hg) as well as several other mineral compounds like SiO_2, CaO, MgO, and Al_2O_3 [2]. There are seven different stages of coal starting from peat, lignite, sub-bituminous coal, bituminous coal, steam coal, anthracite and graphite. These different stages of coal can be either referred as the ranks or the grades of coal [2, 21].

Table 2.1 illustrates the average compositions and properties of different stages of coal. This classification of coal is developed based on the related properties of coal [2]. According to the Table 2.1, the carbon content and the calorific value of coal increase, with the change of the coal rank from lignite to anthracite. When the coal possesses better quality, the rank of coal becomes higher [22].

Anthracite is considered as the highest rank of coal while, lignite is the lowest rank. The moisture content, volatile matter and oxygen content is lower when the coal rank is higher, resulting coal in better quality. The quality of coal can also be determined by the composition of troublesome components in coal such as hydrogen, sulfur, nitrogen and incombustible ashes. When all these components are lower in content, coal can be considered as high quality coal. Hence, lignite includes more sulfur, nitrogen and ash particulates whereas, burning them creates more environmental issues. However, lignite can be easily ignited due to its' high volatile matter.

Table 2.1: Composition and properties of different stages of coal [2]

Coalification stage	**Moisture (%)**	**Volatile matter (%)***	**Carbon content (%)***	**Calorific value (kcal/kg)**	**Oxygen content (%)***
Peat	~ 75	69-63	< 60	3500 - 4000	>23
Lignite	35-55	63-53	65-70	4000 - 4200	23
Sub-bituminous C	30-38	53-50	70-72	4200 - 4600	20
Sub-bituminous B	25-30	50-46	72-74	4600 - 5000	18
Sub-bituminous A	18-25	46-42	74-76	5000 - 5500	16
High volatile bituminous C	12-18	46-42	76-78	5500 - 5900	12
High volatile bituminous B	10-12	42-38	78-80	5900 - 6300	10
High volatile bituminous A	8-10	38-31	80-82	6300 - 7000	8
Medium volatile bituminous C	8-10	31-22	82-86	7000 - 8000	4
Low volatile bituminous C	8-10	22-14	86-90	8000 - 8600	3
Semi-Anthracite	8-10	14-8	90	7800 - 8000	3.5
Anthracite	7-9	8-3	92	7600 - 7800	4.5
Meta-Anthracite	7-9	8-3	> 92	7600	5

* Dry ash free basis

The coal resource available in Thailand is a type of lignite coal which has a higher moisture content, sulfur content, and nitrogen content compared to lignite coal available in the Asian region [5, 14, 23, 24]. Eventhough, Thailand lignite coal has a better energy potential, it requires more emission control techniques in order to minimize the environmental impacts due to possible pollutant emissions [5, 14].

2.1.2 Coal combustion techniques

Since, coal is a natural organic fuel, organic matter consisted in coal is pyrolyzed when it is heated. Coal becomes volatile and a solid mixture of carbon and mineral matter remains after it gets pyrolyzed which is referred as char [25]. When coal is burnt in the presence of air, the volatile matter and carbon undergoes to the reactions with oxygen and releases heat energy. The coal combustion process can be separated into three stages. They are, 1. Releasing volatile matter due to heating of coal, 2. Burning of released volatile matter for heat emission and, 3. Burning of carbon in the remaining char [26].

Oxygen in the air diffuses into the char particles and the combustion reaction occurs on the surfaces of char particles. The rate of combustion reaction depends on the coal type, temperature, pressure, characteristics of char and air fuel ratio [25, 26]. Simultaneous to the primary reaction between carbon in coal and oxygen in the air, the other components in coal such as hydrogen, sulfur, and nitrogen can also react with oxygen to form the products such as, H_2O, SO_2, and NO_x respectively [27].

The combustion of bulk coal is difficult to be carried out and utterly inefficient because, the contact surface area between char and air is very low, when coal is in bulk form. Coal is ground into a fine powder (pulverization) and blown into the combustion chamber in order to increase the contact surface area. A high combustion temperature should be maintained between 1300°C to 1700°C, to assure that each particle of coal is ignited and the pyrolysis is taken place. The air is blown into the combustion chamber using an air blower. This is referred as pulverized coal combustion [26, 27]. This technique is the most conventional technique for coal combustion used by the majority of existing coal fired power plants in the world.

Pulverization is also applied in combustion processes of other types of solid fuels like biomass. However, the major drawback with pulverized coal combustion is the low combustion efficiency where the average thermal efficiency is usually lower than 30% [27]. More than half of the energy content in coal is wasted even if all the combustion conditions are maintained perfectly. Due to the lower efficiency level, more coal should be burnt to cater the power requirement. Consequently, more gaseous pollutants such as CO_2, CO, SO_2 and NO_x can be emitted in to the environment. Figure 2.1 shows the schematic arrangement of a pulverized coal combustion technique.

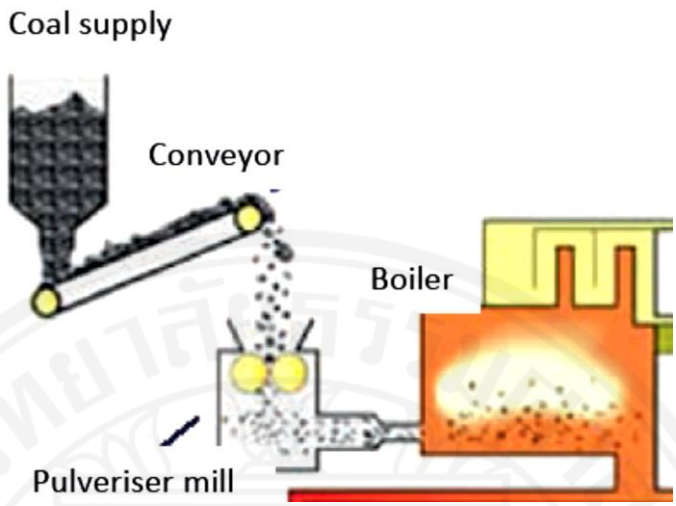

Figure 2.1: Pulverized coal combustion technique [4]

Fluidized bed coal combustion is an improved technology which is more advantageous over the conventional pulverized coal combustion. It involves higher combustion efficiencies and lesser pollution problems. When the air is blown upward through a bed of coal particles at a low velocity, the bed of particles remains stationary, that is referred as a fixed bed. However, the coal particles starts to suspend in the air stream when the air velocity is increased. The suspended particles start to behave like a boiling fluid at a certain air velocity which is called as fluidization [28].

If the air velocity is further increased, the bubbling will take place with the flow of air bubbles. The fluidized coal particles can blow out of the bed at very high air velocities. The particles which goes out of the bed, can be recycled by mixing with the air feed again. A combustion bed where recycling also takes place is called as a circulating fluidized bed [28]. Coal is crushed to sizes between 1–10 mm depending on the rank of coal fed into the combustion chamber in fluidized bed combustion [26]. Generally, the air velocity for fluidization is in the range of 1.2 ms^{-1} to 3.7 ms^{-1} [26]. Fluidized bed combustion can combust coal at low temperatures while reducing the formation of toxic nitrogen oxides (NO_x) [28].

In addition, sulfur dioxide can be more easily removed at a low cost during fluidized bed combustion where low quality coal and even a fuel mixture like coal and biomass mixture also can be undergone to combustion using this combustion technology [26]. Figure 2.2 shows the schematic arrangement of a circulating fluidized bed coal combustion.

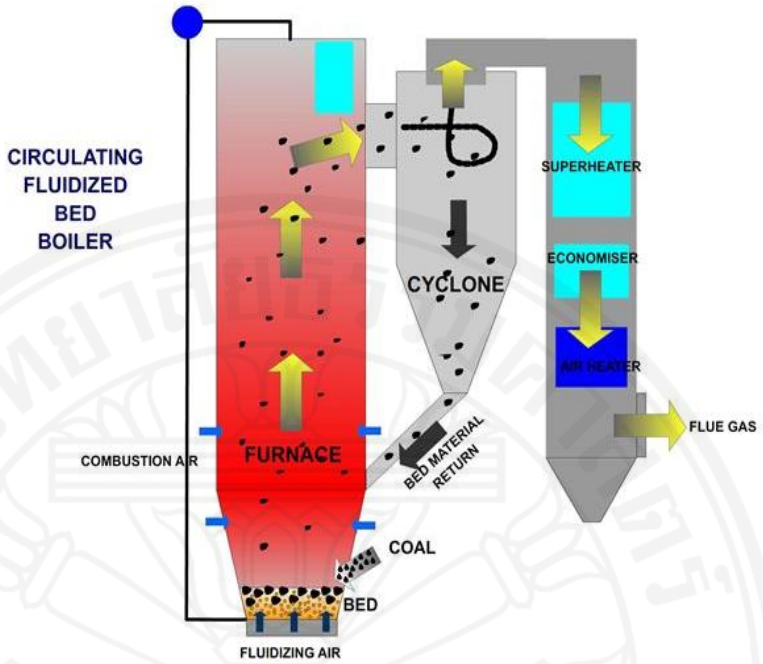

Figure 2.2: Circulating fluidized bed coal combustion technique [29]

The latest coal combustion technology is integrated gasification combined cycle (IGCC) combustion where, the coal is gasified prior to combustion. The coal gasification reaction takes place in the presence of a limited air amount, forming a mixture of carbon monoxide (CO) and hydrogen (H_2) which is called as synthesis gas [30]. The synthesis gas can be secondarily combusted as a fuel at higher efficiencies than solid fuel combustion [30]. The heat energy released during the gasification and the synthesis gas combustion can be combined and utilized as the total energy output.

On the other hand, the synthesis gas can be used to drive a gas turbine according to Brayton thermodynamic cycle while the thermal energy produced at initial gasification can be used to drive a steam turbine according to the Rankine thermodynamic cycle at the same time. Studies confirm that Brayton cycle is more efficient than Rankine cycle [31].

When the both thermodynamic cycles are operated simultaneously as a combined cycle, the overall combustion efficiency increases to be higher than other technologies [31]. The thermal efficiency of synthesis gas combustion cycle lies in the range of 40% - 50% and the overall efficiency increases upto 60% - 70% due to the combined cycle combustion [26, 30].

However, the installation and capital costs to establish a coal fired power plant with IGCC combustion technology is higher in several times compared to the installation cost of a conventional pulverized coal fired power plant. Furthermore, low quality coal is difficult to be burnt using this technique because, gasification does not happen perfectly due to the higher moisture content in low grade coal [26]. There are few IGCC coal fired power plants available in the world due to these economic limitations. Figure 2.3 shows the arrangement of IGCC combustion technique.

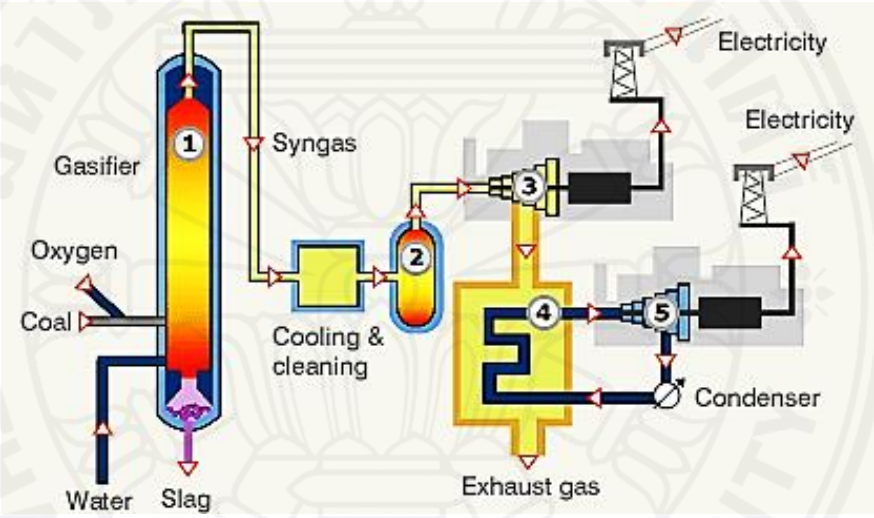

Figure 2.3: Integrated gasification combined cycle technique [32]

The primary function of a coal fired power plant is, the energy conversion process for electricity generation using the chemical energy contained in coal. Figure 2.4 illustrates a schematic diagram of a pulverized coal fired power plant [33]. At first, coal is crushed in to small pieces (pulverized) and it is fed to the combustion chamber through a hopper. The equipment that includes the combustion chamber is named as the boiler. The boiler has a tube arrangement and water is flowed through the tubes in a water tube boiler system.

When the combustion of coal takes place inside the combustion chamber, the generated heat is transferred to the water inside the boiler tubes and, steam is generated. The generated steam is injected to a steam turbine where huge number of turbine blades have been situated. The steam is partially condensed due to the impact on turbine blades inside the turbine and the kinetic energy in pressurized steam is converted to the mechanical energy of the turbine shaft.

The mechanical energy of the rotating turbine shaft is converted to electricity by means of an alternator, referred as a generator. Thereafter, the generated electricity in the power plant can be transformed into a higher voltage by transformers and distributed to required areas using distribution lines. The steam accumulated inside the steam turbine is condensed entirely through a steam condenser where the steam is condensed by cooling water. A cooling tower cools and circulates warm water received after the steam condensation. The make-up water required for the cooling tower can be obtained from river water. The condensed steam by the condenser is recirculated through the boiler tubes and pressurized steam can be regenerated continuously.

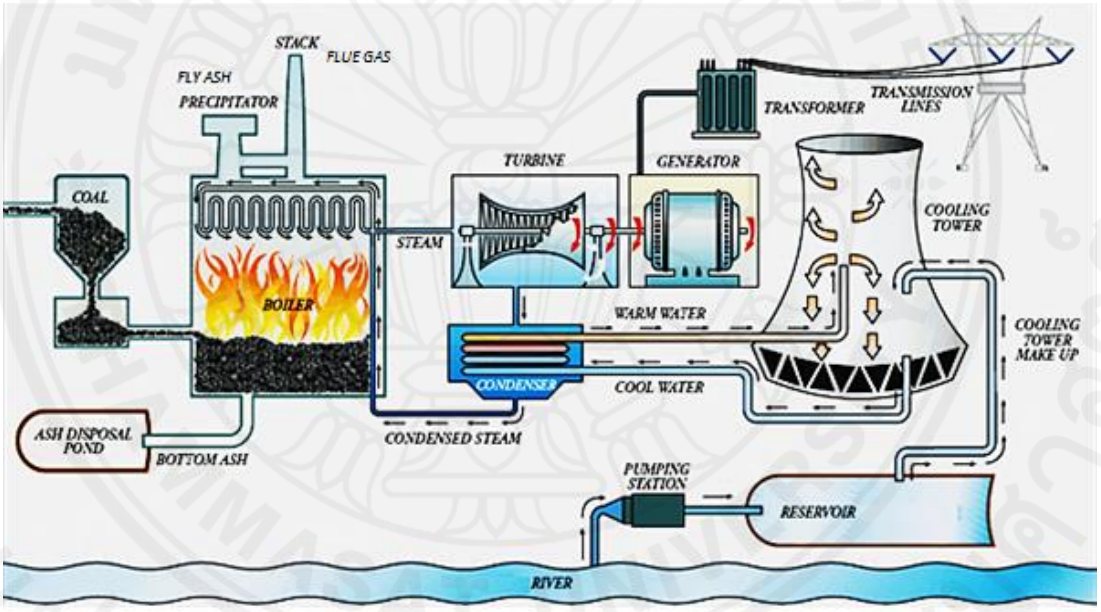

Figure 2.4: Schematic diagram of a typical coal fired power plant [33]

The incombustible ash that remains in the coal combustion chamber is collected to the ash disposal pond at the bottom of the combustion chamber. The disposable unburnt ash is called as bottom ash, which is one of the solid waste materials coming out from a coal fired power plant. The gaseous products formed due to the combustion reactions of different components in the coal, climb up from the combustion chamber during the combustion process. Therefore, a chimney stack with a standard height is fixed to the combustion chamber to release these gaseous products coming out from combustion chamber with the excess air. This entire gaseous emission coming out from a coal fired power plant is called as the flue gas.

While this flue gas coming out through the stack, the fine particulate matter which is released by the surface of unburnt coal also get mixed with the flue gas. Therefore, a particulate precipitator is installed in the pathway of flue gas chimney stack by trapping the fine particulate matter in order to prevent them getting released to the atmosphere with the flue gas. This precipitated fine particulate matter is referred as fly ash which is another solid waste material collected as a byproduct from a coal fired power plant.

The overall process described for the layout of a pulverized coal fired plant is exactly similar to the process in a fluidized bed coal fired power plant except the only difference between the two combustion techniques which is, the coal burns on a fluidized bed inside the boiler with a better contact between the air and coal in fluidized bed combustion. In IGCC coal fired power plant, a gas turbine is set up with power generation unit and gas condensing unit are incorporated in addition to the steam turbine system of pulverized coal fired power plant.

2.1.3 Airborne emissions from coal fired power plants

The major elements in coal are carbon (C), hydrogen (H), nitrogen (N), sulfur (S), and incombustible ash. Each component reacts with oxygen in the air forming different gaseous products and particulate matter during the combustion process of coal. The most problematic emissions of a coal fired power plant are the gaseous products. Releasing flue gas into the atmosphere by every coal fired power plant in the world can contribute to create lot of environmental issues. Generally, the temperature of flue gas released from pulverized coal fired power plants varies in the range of 110 °C – 150 °C and the pressure of flue gas lies around 1 atm - 1.2 atm [34, 35]. The environmental impact and sustainability of coal fired power plants depend on their quantities of harmful emissions.

Table 2.2 demonstrates the average compositions of airborne emissions in the flue gas from pulverized coal fired power plants and IGCC coal fired power plants. Eventhough, CO_2 emission is comparatively higher in flue gas, statutory regulations have not been established to limit CO_2 emissions from coal fired power plants. However, strict legislative requirements persist to control NO_x and SO_2 emissions from coal fired power plants upto permissible levels.

Table 2.2: Composition of airborne emissions from coal fired power plants [35]

Component	**Pulverized coal fired power plant**	**Integrated gasification combined cycle (IGCC) coal fired power plant**	**Emission standard in Thailand**	**Emission standard in China**
CO_2	~ 12 vol%	~ 7 vol%	-	-
NO_x /(ppm)	500 – 800	10 – 100	500	200
SO_2 /(ppm)	200 – 1500	10 – 200	320	200
Moisture	~ 6 vol%	~ 14 vol%	-	-
O_2	~ 6 vol%	~ 12 vol%	-	-
N_2	~ 76 vol%	~ 66 vol%	-	-
Particulates / (g/m^3)	5 – 20	<< 0.02	0.12	0.03

The emission standards stipulated as per the factory act by the ministry of industry, Thailand, for major pollutant gas emissions such as NO_x and SO_2 from Mae Moh coal fired power plant are 500 ppm and 320 ppm respectively [36]. These standards are less strict than the standards stipulated for Chinese lignite coal fired power plants [37]. Low NO_x burners and wet limestone forced oxidation flue gas desulfurization (FGD) units have been installed in Mae Moh coal fired power plant to reduce NO_x and SO_2 emissions [38]. However, the existing FGD units meet operational difficulties to handle the high load of SO_2 emission from many coal combustion units in Mae Moh coal fired power plant [38]. Therefore, urgent remedies are required to lower the load of desulfurization units in Mae Moh coal fired power plant, Thailand.

Particulate matter is the other airborne emission from a coal fired power plant. Fine particles of solid and liquid matter of organic or inorganic compounds in coal, suspended in flue gas is referred as particulate matter. Particulate matter should be trapped from flue gas before it is released to the atmosphere. After separation of particulate matter it is called as coal fly ash. Coal fired power plants are equipped with fly ash collection equipment such as Electrostatic precipitators (ESP), fabric filters, mechanical collectors and ionized wet (Venturi) scrubbers [39]. Ionized wet scrubbers are used in Mae Moh coal fired power plant, Thailand which can considerably trap toxic elements like As, Hg, Se, Pb, and Mn available in particulate matter [14].

Microscopic analysis reveals that fly ash can be considered as solid particles spherical in shape and some particles in fly ash have thin-walled hollow geometry called as cenospheres where, the size of fly ash particles are usually ranging from 1 to 100 microns in diameter [40, 41]. The physical properties of fly ash has been indicated in Appendix A. Generally, fly ash obtains tan color and dark gray color which is mainly composed of SiO_2, Al_2O_3, Fe_2O_3, CaO, MgO, Na_2O and K_2O. These components have high thermal stability and uniform properties at high temperatures [42]. They can easily react with free lime in the presence of water and this reaction is called hydration of fly ash [43]. The product of hydrated fly ash is a gel similar to cementitious materials which can be used to bind inert materials together [44]. Furthermore, elements such as arsenic, mercury and selenium included in coal become volatile at high temperatures and condense on the surface of fly ash particles [42].

The common application of coal fly ash is the usage as cementitious materials in construction activities. Fly ash is directly used as a replacement for ordinary Portland cement (OPC) in concrete for concrete pipes and structures in roadway, pavement and dam constructions as well as, it can be applied as an admixture in cement at certain mixing proportions [24]. Many studies reveal that, fly ash can significantly improve physical properties of concrete such as, compressive strength, permeability, and resistance to alkali silicate reactivity [40-42, 45, 46].

Standard specification of ASTM C618 and TIS 231 must be referred for the physical and chemical properties of fly ash in order to be used in concrete [46]. The fly ash which fulfills the standard specifications of ASTM C618 and TIS 2135, is called as qualified fly ash. On the other hand, fly ash that does not meet the same specifications are called as unqualified fly ash. Table 2.3 and Table 2.4 show the standard requirements for physical and chemical properties of fly ash in order to qualify for cementitious applications according to TIS 2135 standard specification respectively. The major chemical properties of fly ash required to be checked before using for cementitious applications, are composition of SiO_2, CaO content, SO_3 content, moisture content, loss on ignition (LOI), and alkali content. In addition, the major physical properties of fly ash are fineness, strength activity index water requirement, and autoclave expansion. Usually, a portion of fly ash coming out from a coal fired power plant would not meet these standard requirements becoming unqualified fly ash.

Table 2.3: Standard regulations for chemical properties of coal fly ash to be used in cementitious applications [46]

No	Chemical properties of fly ash	Standard regulation			
		First class	Second class		Third class
			Type a	Type b	
1.	Silicon dioxide (SiO_2), min %	30.0	30.0	30.0	30.0
2.	Calcium oxide, %	-	< 10.0	> 10.0	-
3.	Sulfur trioxide (SO_3), max. %	5.0	5.0	5.0	5.0
4.	Moisture content, max. %	3.0	3.0	2.0	2.0
5.	LOI content, max. %	6.0	6.0	6.0	12.0
6.	Alkali content (Na_2O + 0.658K_2O), max. %				
	1.1 when SO_3 between 3.0 to 5.0 %	1.5	1.5	1.5	1.5
	1.2 when SO_3 less than 3.0 %	4.0	4.0	4.0	4.0

Table 2.4: Standard regulation for physical properties of coal fly ash to be used in cementitious applications [46]

No	Physical properties of fly ash	Standard regulation			
		First class	Second class		Third class
			Type a	Type b	
1.	Fineness (select a method)				
	Amount retained on 45-μm-mesh sieve, max. %	10	50	55	65
	Or Blaine fineness, min. cm^2/g	6000	2300	2000	1600
2.	Strength activity index with OPC type 1				
	7-day, min. % of the control	85	70	70	60
	28-day, min. % of the control	95	75	75	70
	91-day, min. % of the control	100	85	85	75
3.	Water requirement, Max. % of the control	102	102	105	108
4.	Autoclave expansion, max. %	0.8	0.8	0.8	0.8

The unqualified fly ash is not desirable to be added in cementitious and concrete applications because, the chemical composition and physical properties of this fly ash may hinder the properties of cement and concrete mixtures especially, the high free lime content in unqualified fly ash can cause failure in concrete structures due to excessive expansion [46]. Hence, the unqualified fly ash would remain merely as a waste material generated within a coal fired power plant.

Studies report that fly ash can be utilized as a solid sorbent with a considerable performance for CO_2 capture and SO_2 capture [47-50]. If qualified fly ash is used for SO_2 capture, the sulfur content can exceed the standard limit and the fly ash becomes illegible for cementitious applications after SO_2 capture. Therefore, SO_2 capture is recommended to be carried out only using the unqualified fly ash quantities generated in the coal fired power plant. On the other hand, the excessive expansion problem in fly ash derived concrete due to the high free lime content in fly ash, can be reduced after CO_2 capture since, free lime available in fly ash can undergo carbonation during CO_2 capture so that, both qualified and unqualified fly ash can be used for CO_2 capture [46, 51].

Table 2.5 indicates annual production data of emissions in 2008 obtained from Mae Moh coal fired power plant of the Electricity Generating Authority of Thailand (EGAT). 2000 ktonne/year of fly ash has been produced annually whereas, the total CO_2 emission is 18,174.18 ktonne/year and total SO_2 emission after existing desulfurization unit is 21.55 ktonne/year. However, the total SO_2 amount in the flue gas without any control from Mae Moh coal fired power plant, Thailand has been reported as 1,314 ktonne/year [38].

Table 2.5: Production data in 2008 for Mae Moh coal fired power plant

Material	**Annual production (ktonne/year)**
Fly ash	2,000
CO_2 emission	18,174.18
SO_2 emission (with control)	21.55
SO_2 emission (without control)	1,314

2.2 CO_2 capture techniques

2.2.1 Chemical and physical properties of CO_2

Carbon dioxide (CO_2) is a colorless gas which has a molecular weight of 44.01 g/mol. CO_2 is odorless at low concentrations and it gives a sharp acidic odor at high concentrations. CO_2 can also be considered as a non-flammable and slightly acidic liquefied gas which has a pH value around 6.35. At standard temperature and pressure, the density of CO_2 is nearly 1.98 kgm^{-3} that is about 1.67 times of the density of air. Therefore, CO_2 is heavier than air. The major chemical and physical properties of CO_2 has been indicated in Appendix B. [52]

Figure 2.5 shows the Lewis structure of CO_2. When the Lewis structure of CO_2 is considered, it has a steric number of 2 and the geometric shape of molecule is linear with a bond angle of 180°. The CO_2 molecule is centrosymmetric. Consequently, CO_2 can be considered as a non-polar gas. The molecular structure of CO_2 reveals that, it is comparatively a stable gas. It cannot be thermally decomposed below 2000 °C. The bond length in CO_2 is approximately 116.3 pm. Only two vibrational bands in the CO_2 molecule that can be observed in IR spectrum. They are an antisymmetric stretching mode at 2349 cm^{-1} and a bending mode near 666 cm^{-1}. [52]

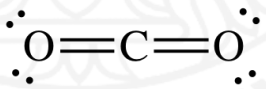

Figure 2.5: Lewis structure of CO_2 [52]

CO_2 is soluble in water but, it does not get ionized completely within water forming carbonic acid (H_2CO_3) which is a weak acid. The freezing point of CO_2 at atmospheric pressure is approximately -78.5 °C and at this temperature, CO_2 directly turns into solid state from gas state. There is no liquid state for CO_2 at the pressures below 520 kPa. When CO_2 becomes solid states, it is called as dry ice. At higher pressures, the solid state of CO_2 is amorphous called as carbonia. However, at very high pressures above critical point of CO_2 (7.38 MPa at 31.1 °C), it behaves as a super critical fluid. This is known as super critical carbon dioxide. [52]

2.2.2 Environmental impact of CO_2 emission

Carbon dioxide (CO_2) is a major greenhouse gas. Eventhough, it is transparent to light, it can reflect the infrared radiation of the sun back to the earth's surface due to its' vibrational frequencies of the molecule bonds at the infrared range [52]. This phenomena is known as the greenhouse effect. Therefore, long term accumulation of CO_2 in the atmosphere can cause global warming and climate changes affiliated to several other environmental impacts including melting of polar ice caps, unusual droughts, floods, and storms. There is a natural equilibrium cycle of CO_2 on the Earth. All the living beings exhale CO_2 into the atmosphere during their respiration process. Meanwhile, flora consumes CO_2 in the atmosphere to produce food via the photosynthesis process in the presence of sunlight. Therefore, CO_2 concentration in the atmosphere is controlled naturally. However, deforestation due to urbanization and CO_2 emission by industrial processes have been rapidly expanding with the population growth on the Earth since the industrial revolution. These circumstances have disrupted the natural equilibrium cycle of CO_2. As a result, CO_2 concentration in the Earth's atmosphere is continuously rising year by year.

CO_2 concentration in the atmosphere still lies around 369 ppm and it is expected to rise up to 750 ppm by the year 2100 if any action is not taken to control artificial CO_2 emissions [6]. Major sources that should be responsible for CO_2 emission into the atmosphere are electrical power generation plants especially including coal fired power plants, emissions from vehicles due to transportation and industrial activities such as heating applications and manufacturing. These three major sources share the responsibility of CO_2 emission among them as 39% from electrical generation plants, 23% from transportation, and 22% from industry respectively [53].

Environmental impact of CO_2 emission

Long term effects...	**Solutions are required...**

A major greenhouse gas and causes greenhouse effect.
Long term accumulation atmosphere can cause global warming.
Climate changes including melting of polar ice caps, unusual droughts and floods storms.

Figure 2.6: Environmental impact of CO_2 emission

2.2.3 Conventional CO_2 capture techniques

CO_2 emission into the atmosphere should be controlled to mitigate the harmful environmental impacts due to CO_2 accumulation. The conventional methods are focused on collecting CO_2 as a bulk gas and storing in suitable places, such as disposal in deep oceans, depleted oil and gas fields, deep saline formations (aquifers) and recovery of enhanced oil, gas, and coal-bed methane [54]. However, the sequestrated CO_2 in these natural places can slowly release back to the atmosphere while, they create many operational difficulties including huge transportation costs [7].

Pre-combustion CO_2 capture techniques such as selecting better quality coal for combustion, and following a more efficient coal combustion technology can help to reduce the CO_2 emission from coal fired power plants up to a certain level [6]. However, the huge quantity of CO_2 emission from a large scale coal fired power plant cannot be significantly controlled by pre-combustion methods. Therefore, CO_2 control after combustion is essentially required for the effective emission control in a coal fired power plant. Post-combustion techniques capture CO_2 in the flue gas coming out from the coal combustion chamber before releasing to the atmosphere. CO_2 capture using a chemical process becomes more advantageous because, CO_2 can be stored in an irreversible state within the specific material which is used for CO_2 capture. The major chemical and physical CO_2 capture methods can be indicated as membrane separation, cryogenic separation, absorption by liquid solvents (chemical solvent method), and adsorption by solid sorbents [6, 8].

A membrane is a material with solid porous structure which separates one component from the other components when a gas mixture is flowed through the membrane material [8]. Membranes for CO_2 capture usually consist of thin polymeric films such as polyimide, poly-dimethyl-phenylene oxide, poly-ether-sulfone and poly-acrylonitrile with poly-ethylene glycol as well as, inorganic membrane materials like alumina, activated carbon, silicon carbide, and zeolites [8]. Most of these membrane materials are very expensive and the separation of CO_2 takes place based on the relative flow rate of CO_2 through the membrane material resulting low fraction and the purity of the captured CO_2 which also requires a more complicated operation [6, 8]. Cryogenic separation consists of multistage compression by cooling down CO_2 in the flue gas in order to liquefy or solidify CO_2 to be separated from the gas phase.

After compression of the gas, further separation process is required with a distillation column to remove any impurities available with CO_2 [6, 8]. Condensation of CO_2 by cooling down to a very low temperature is integrated with high energy consumption and high operating costs.

CO_2 capture technique through chemical absorption includes a reaction between CO_2 and a chemical solvent forming a weakly bonded intermediate compound. This intermediate compound can be regenerated into the original solvent and CO_2 after CO_2 capture by applying heat [6, 34]. Most of the chemical solvents used in this method are different amine solutions such as, mono-ethanol-amine (MEA) and di-isopropanol amine (DIPA) [6]. These chemicals are corrosive and their regeneration process is energy intensive. Storage of captured CO_2 after regeneration process is also another hassle. Therefore, CO_2 capture by chemical solvent absorption also suffers from several disadvantages like solvent degradation due to SO_2 and O_2 in flue gas, high equipment corrosion rate and high operational cost for high energy consumption [6, 55].

Adsorption is a physical sequestration process that involves the attachment of a gas or liquid into a solid surface which is called as the solid sorbent or adsorbent. The gas which undergoes to the adsorption process is termed as adsorbate. For commercial solid sorbents, regeneration of the adsorbent is required. There are two main possibilities for regeneration of CO_2 capture solid sorbents such as temperature swing adsorption and pressure swing adsorption [8]. The pressure swing adsorption would seem to be a more suitable operation for the impregnated solid sorbents like amines, due to the sensitivity of the surface amine groups to temperature changes [8]. However, during the post-combustion CO_2 capture, compressing the enormous volume of flue gases would not be economical [8]. Thus, capture should take place at normal pressure and the regeneration of the sorbents at a reduced pressure.

Vacuum swing adsorption is more suitable for CO_2 capture with physisorption type adsorbents like zeolite and mesoporous carbon materials in order to yield a concentrated CO_2 stream without dilution [8]. The commercial solid sorbents for CO_2 capture such as amines, zeolite and mesoporous carbon materials are high surface area materials which are reusable [53]. However, the CO_2 capture with these commercial solid sorbents are very expensive because of their high price as well as their requirement in large quantities for the adsorption process [55].

The porous sites available on the solid sorbents, promote weak intermolecular forces (Van der Waals forces) with the gas molecules referred as physical adsorption (physisorption) [56]. The adsorbed gas molecules can leave the solid surface due to pressure reduction or temperature increase (desorption) resulting, physisorption is a reversible process. [9]. In addition to the physisorption, certain compounds available in the solid sorbent, can form irreversible chemical reactions with the gas molecules by either covalent bonding or ionic bonding which is called as chemical adsorption (chemisorption) [49]. The chemical reaction can consist of several reaction steps including surface reaction, internal diffusion, and external diffusion during the mechanism of chemisorption process [57].

The commercial solid sorbents incur additional operational and transportation costs in order to transfer the solid sorbents from the industrial area to a resevior for reusing the solid sorbents by the desorption process after CO_2 capture [55]. The material and energy costs play a huge role for the CO_2 capture using solid sorbents. Consequently, more efforts are required to reduce material costs and energy consumptions. Energy cost can be brought down by process heat integration, efficient consumption of energy, simultaneous removal of other pollutant gases in the flue gas like SO_2 and using the most energy efficient way of operation [58]. However, low cost solid sorbents seems to be more desireble for CO_2 capture.

Kaolin, a kind of a clay which is one of the commercially available low cost sorbent material for CO_2 capture [55]. Mullite, is a waste material coming from the aluminum industry that displays various Al to Si ratios with the capability of using as a solid sorbent for CO_2 capture [55]. Activated carbon, limestone and dolomite are also possible natural solid sorbents [9, 59, 60]. Baggase and rice chaff are two widely available waste materials that can be utilized as CO_2 capture solid sordents because, these agricultural wastes include amines in their compositions which can boost CO_2 capture [55]. However, landfilling is the only way to dispose these solid sorbents after CO_2 capture. Therefore, the disposal of these low cost solid sorbents after CO_2 capture can be the practical problem associated with these low cost solid sorbents. Figure 2.7 illustrates a comparison of different post-combustion CO_2 control techniques and Table 2.6 shows the highlighted facts in the literature regarding post-combustion CO_2 capture using different solid sorbents.

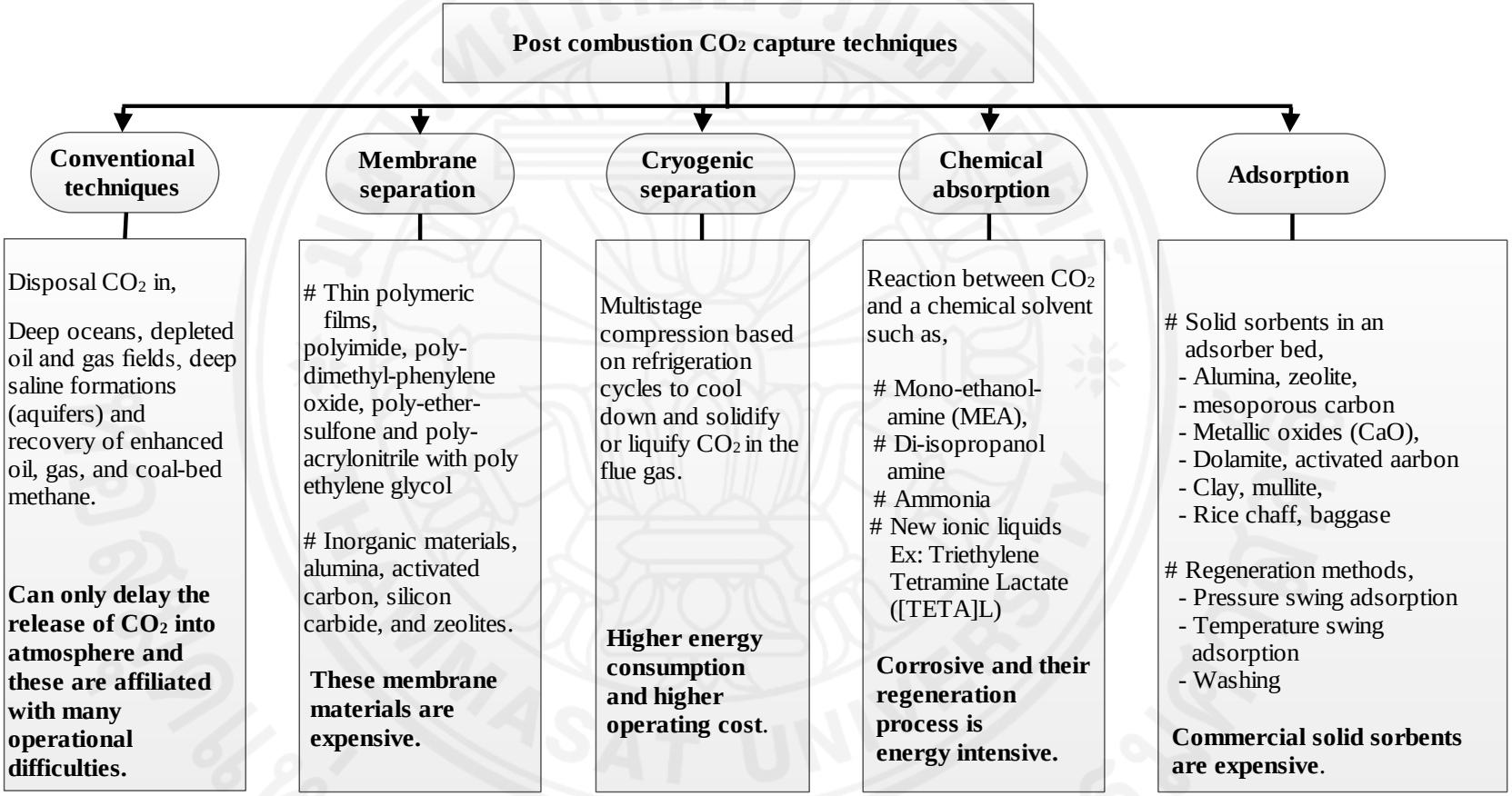

Figure 2.7: Comparison of different post-combustion CO_2 control techniques

Table 2.6: Summary of post-combustion CO_2 capture using solid sorbents

Ref.	Solid sorbent	Conditions	Experimental techniques	Results
[55]	Amine-enriched solid sorbent (MEA & DEA) supported by kaolin, mullite, bagasse and Rice chaff	Sample size : 2 g $T_{Adsorption}$: 303 K $T_{Desorption}$: 393 K Pressure : 1 atm N_2 flow rate for desorption : 30 mL/min Experiment was conducted in a tubular column.	The gas samples were analyzed for the amount of CO_2 by gas chromatography (GC). CO_2 adsorbate over the sorbent was characterized by smart diffused reflectance infrared Fourier transform spectroscopy with an infrared spectrophotometer.	CO_2 capture capacities, kaolin : 734 µmol/g , mullite : 593 µmol/g , bagasse : 351 µmol/g , rice chaff : 329 µmol/g The solid sorbent is disposable and cannot be reused. The presence of more amine groups enhances CO_2 capture performance. But, additional treatments with NaOH are required.
[53]	Nitrogen enriched activated carbon sorbent	Amines were incorporated into activated carbon by wet impregnation method. Isothermal test at 25 ºC Non-isothermal test: upto 100 ºC at 0.5 ºC/min rate. Pressure : 1 atm	Surface functionalities was observed using DRIFT spectra. CO_2 adsorption and desorption performances were analyzed using TGA. Sorbent surface area was determined via BET equation.	Maximum capture capacity: 73 mg CO_2/g for raw activated carbon Impregnation with amines reduces microporous volume and CO_2 capture capacity. The thermal stability increases with the amine impregnation.

Cont'd from Table 2.6

Ref.	Solid sorbent	Conditions	Experimental techniques	Results
[60]	Natural limestone	A pilot-scale dual fluidized bed system. Artificial flue gas was used with 8 vol% CO_2. T: 0 - 800 ºC Initial bed mass : 3 kg Carbonation period: 70 min	Gas samples were analyzed in (GC/MS).	Overall sorbent conversion: ~ 46.9%. The presence of steam increased carbonation conversion. Time period for high CO_2 capture efficiency was lessened after each cycle of CO_2 capture.
[59]	Kinetic Study with limestone and dolomite	CO_2 partial pressure: 0 - 0.1 MPa Feed gas mixture of CO_2, N_2 and He using mass flow controllers to adjust concentration of CO_2 $CaCO_3$ decomposition, T : 850 °C , P : 1 atm Sample mass : 8 – 11 mg	2 fixed-bed TGA, one operated at atmospheric pressure (50 °C/min) and the other under pressurized conditions (20 °C/min). A grain model with kinetic control for the kinetic study.	Kinetic control applies only in the initial stage of carbonation. The carbonation reaction was first order only for CO_2 partial pressure driving forces less than 10 kPa, abruptly changing to zero order for higher CO_2 partial pressures. The activation energies were found to be 29 ± 4 kJ/mol for limestone and 24 ± 6 kJ/mol for dolomite.

2.2.4 CO_2 capture using fly ash as a solid sorbent

Fly ash with standard properties as per ASTM C618 and TIS 2135 standard specifications can be utilized as admixture in cement and concret for roadway, pavement and dam constructions [41, 42, 46]. Studies also show that fly ash coming out from a coal fired power plant can be utilized for CO_2 capture as a solid sorbent [49, 54]. Therefore, fly ash is an interesting CO_2 capture solid sorbent with post capture applications.

Literature reports that, CO_2 adsorption capacity of 174.5 μmol/g sorbent at 25°C and 1 atm pressure can be obtained when treated amine enriched fly ash carbon was used for CO_2 capture [54]. A CO_2 capture capacity of 31.2 mg CO_2/g sorbent has been observed when, coal fly ashes with high unburned carbon content were studied for CO_2 capture at a range of 30 - 120 $^{\circ}$C temperature and 1 atm pressure [49]. CO_2 capture capacity decreases with increasing temperature and CO_2 adsorption capacity increases when activated amines are impregnated on fly ash [49].

Fly ash mostly consists of amorphous and crystelline compounds like SiO_2, Al_2O_3, FeO, CaO, MgO and free lime. These components in fly ash contribute to increse the surface area of fly ash and thermal stability with uniform properties [42]. During the CO_2 capture process, the adsorption of CO_2 over fly ash as well as the carbonation reaction can take place between CaO (free lime) and CO_2 to form the carbonate compound [60]. As a result, the capture performance can be increased. Reaction 2.1 indicates the carbonation reaction which can occur during the CO_2 capture process due to free lime contained in fly ash.

$$CO_2 + CaO \rightarrow CaCO_3 \qquad \text{Reaction 2.1}$$

An additional advantage would be the reduction of free lime content in fly ash after CO_2 capture as a result of the carbonation reaction. Free lime can increase the excessive expansion and cause defects in concrete constructions where original fly ash is used as an admixture [46]. Consequently, CO_2 capture using fly ash can provide useful post capture applications. However, clear evidences are scarce in existing studies regarding the usage of coal fly ash for industrial scale CO_2 capture. Table 2.7 shows the summary of few existing studies on CO_2 capture using fly ash as solid sorbent.

Table 2.7: Summary of CO_2 capture using fly ash as solid sorbent

Ref.	Solid sorbent	Conditions	Experimental techniques	Results
[54]	Treated amine enriched fly ash carbon	10 g of fly ash carbon concentrate was treated with a 500 mL 1×10^{-3} molar 3-CPAHCL salt solution with and without 1×10^{-2} molar KOH. T : 30 °C , P : 1 atm CO_2 capture carried out in the DRIFTS/TPD reactor systems.	The chemical CO_2 capture capacities were determined by the combination of DRIFTS, TPD and MS analyses. The amount of nitrogen in the surface of the sorbent was determined by XPS analysis.	Capture capacity of 174.5 μmol/g sorbent with the highest amine concentrated fly ash with surface area of 27 m^2/g. Capture capacity of commercial sorbents with surface area 1000 – 1700 m^2/g: 1800 – 2000 μmol/g
[49]	Coal fly ashes with high unburned carbon content	2 Samples of fly ash (FA1 and FA2) An acid ($HCl/HNO_3/HF$) digestion step to remove ash and concentrate carbon in the sorbent samples. T : 30 - 120 °C , P : 1 atm CO_2 capture experiments were conducted in a TGA. Sample size : 10 mg CO_2/ N_2 flow rate : 100 mL/min	CO_2 adsorption capacities were analyzed using the TGA. Weight change of the sorbents was recorded and used to determine the adsorption capacities of the samples.	At 30 ºC, CO_2 capture capacity : 40.3 mg/g (FA1) , 43.5 mg/g (FA2) CO_2 adsorption capacities increase when activated amines are impregnated (40.3 mg/g). The highest adsorption capacity was at 30 °C. CO_2 capture capacity decreases with increasing temperature.

Cont'd from Table 2.7

Ref.	Solid sorbent	Conditions	Experimental techniques	Results
[50]	Fly ash derived solid amine sorbent	CO_2 capture experiments were conducted in the TGA. Sample size : 50 mg CO_2/N_2 flow rate : 80 mL/min T : Room temperature , P : 1 atm Desorption temperature : 100 °C Sorption time : 30 min	N_2 adsorption isotherms were measured and surface area of sorbent was calculated by BET method. CO_2 sorption performance was evaluated by using TGA by the mass change. SEM images and FTIR spectra was obtained.	The best sorbent gave a sorption capacity: 145.0 mg/g at 90 °C. Sorption capacity increased with temperature from 30 °C (77.6 mg/g) to 90 °C, and dropped thereafter. Diffusion of CO_2 in the sorbent active sites can be the kinetic control step.
[9]	Coal fly ash derived carbon materials	CO_2 capture experiments were conducted in an alumina crucible. Sample size : 10 mg CO_2/N_2 flow rate : 20 mL/min T : 75 °C , P : 1 atm Desorption temperature : 75 °C Sorption time : 40 min	CO_2 adsorption capacities were evaluated by using TGA by the mass change. Temperature programmed adsorption (TPA) was conducted from room temperature to 100 °C at a rate of 0.25 °C/min	CO_2 adsorption capacities from 4 wt% to 6 wt% at 75 °C, by impregnating with amines. Amine loaded adsorbents increased the CO_2 adsorption capacity and decreased the time taken to reach equilibrium.

2.3 SO_2 removal techniques

2.3.1 Chemical and physical properties of SO_2

Sulfur dioxide (SO_2) is a colorless gas which has a strong and sharp suffocating odor. SO_2 becomes a liquid when compressed under pressure and it dissolves in water very easily. Molar mass of SO_2 is 64. 06 $gmol^{-1}$. At the atmospheric pressure, the melting point is -72.7 °C and boiling point is -10 °C. Sulfur dioxide (SO_2) is an acid gas that has a pH value of roughly about 1.81. Density of SO_2 in gas form is 2.927 kgm^{-3} and it is heavier than CO_2 when the both are in a gas mixture. SO_2 can dissolve in the water vapor present in the air and further oxidizes to form sulfurous acid (H_2SO_3) and sulfuric acid (H_2SO_4) easily. The major chemical and physical properties of SO_2 has been indicated in Appendix C. [10]

Figure 2.9 illustrates the two resonance Lewis structures of SO_2. According to the Lewis structures, SO_2 becomes a bent molecule with the bond angle of 119°. The sulfur – oxygen bond has a bond length of 143.1 pm and the bond order is 1.5. The sulfur atom in a SO_2 molecule, has an oxidation state of +4 and a formal charge of +1. The molecular shape of SO_2 molecule is dihedral and consequently it can be considered as a polar gas. [61]

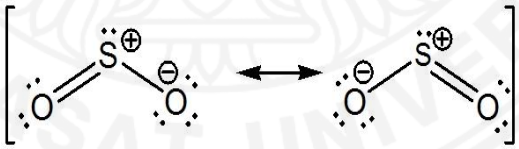

Figure 2.9: Two resonance Lewis structures of SO_2 [61]

SO_2 is released into the atmosphere during volcanic eruption naturally. However, SO_2 is artificially emitted when sulfur contents in fuels like coal, diesel, petrol and other hydrocarbons react with oxygen in the air during combustion processes. Oxidized sulfur first transforms to SO_2 and further oxidation converts into SO_3. Both chemicals are called sulfur oxides, symbolized as SO_x (SO_2 and SO_3) [61]. The frequent emissions of sulfur into the atmosphere is in the form of SO_2.

2.3.2 Environmental impact of SO_2 emission

When the SO_2 concentration in the air is higher than 5 mgm^{-3} (1.9 ppm), the air turns into an irritating odor [10]. Sulfur dioxide (SO_2) accumulation contributes to the generation of smog in the atmosphere and, long term exposure to SO_2 in the air can cause serious health hazards for the respiratory systems of all living beings. The impacts of SO_2 can be divided into issues raised by long term exposure to SO_2 and short term exposure to SO_2. Long term accumulation of SO_2 in the atmosphere causes oxidation reactions of SO_2 with air, water vapor and solid particles in the atmosphere. Therefore, SO_2 can be a major factor for the acid rain that is harmful for vegetation, agriculture and corrodes buildings and constructions [11]. Short term exposure to high concentrations of SO_2 can result insufficient oxygenation in the blood and accumulation of fluids in the lungs which is life threatening in minutes [10].

Figure 2.10 briefly outlines the long term environmental impacts of SO_2 and impacts of short term exposure to SO_2. The severity of these impacts reflects how urgent the remedies are required to control SO_2 emission from various sources. Coal fired power plants are a major source which is highly responsible for a significant proportion of SO_2 emission into the atmosphere. The global SO_2 emission into atmosphere has been estimated to be several million tons per year [11, 17].

Environmental impact of SO_2 emission

Long term accumulation	**Short term exposure (1-6 hours)**
# A major factor for the acid rain, that is harmful for vegetation, agriculture and corrodes buildings and constructions. # Contributes to the generation of smog in the atmosphere. # Long term exposure can cause serious health hazards for the respiratory systems of all living beings.	# To concentrations as low as 1 ppm may produce a reversible decrease in lung function. # To about 20 ppm is objectionably irritating. # To about 100 ppm is considered immediately dangerous to life and health. # To about 500 ppm is so objectionable that a person cannot inhale a single deep breath.

Figure 2.10: Environmental impact of SO_2 emission [10]

2.3.3 Conventional flue gas desulfurization techniques

The approaches for SO_2 emission reduction in coal fired power plants can be separated into two stages as pre-combustion and post-combustion desulfurization. The pre-combustion desulfurization strategies are based on reducing the sulfur contained in the coal by means of fuel blending or fuel switching to a lower sulfur coal and utilizing a more efficient coal combustion technology like fluidized bed combustion [39]. Eventhough, SO_2 content in flue gas is very low compared to the quantity of CO_2 emitted from a coal fired power plant, even a very small amount of SO_2 emission to the atmosphere can be more hazardous than a large scale CO_2 emission. Therefore, the post-combustion technologies are essentially required for the complete elimination of SO_2 emission from flue gas.

According to the legislative regulations, it is mandatory to have post combustion flue gas desulfurization especially for a coal-fired power plant in order to control SO_2 emission [62]. The major conventional desulfurization techniques can be mainly pointed out as wet flue gas desulfurization and dry flue gas desulfurization [17]. Generally, all these techniques involve in a desulfurization reaction with SO_2 using a chemical reagent, absorbent or a solid sorbent. The widely used chemical reagents are different forms of lime such as $CaCO_3$ (limestone), CaO (free lime) or $Ca(OH)_2$ (hydrated lime). As a result of the desulfurization reaction between SO_2 in the flue gas and chemical reagents, the product coming out from the desulfurization unit is possibly different forms of $CaSO_4$ [16, 17, 39]. The form of $CaSO_4$ from each desulfurization technique depends on the conditions and the type of chemical reagents used in the desulfurization process.

Conventional wet flue gas desulfurization systems utilize a wet slurry of $CaCO_3$ (limestone) as the chemical reagent [17]. Mostly, the desulfurization process takes place inside an absorber tower where the wet limestone slurry is sprayed in the counter-current direction to the flue gas flow. When the hot flue gas enters the absorber tower, it is cooled down and saturated by the wet limestone slurry. The average temperature inside the absorber tower lies around 60 - 70 °C. As the initial reaction step, SO_2 available in flue gas reacts with the wet slurry of $CaCO_3$ and forms calcium sulfite hemihydrate ($CaSO_3 \cdot \frac{1}{2}H_2O$) [17, 39].

Thereafter, when flue gas flows towards the slurry spraying area, the desulfurization reaction process incorporates forced oxidation in the presence of more oxygen in order to convert calcium sulfite hemihydrate ($CaSO_3 \cdot ½H_2O$) into calcium sulfate dihydrate ($CaSO_4 \cdot 2H_2O$) from SO_2 in the flue gas. Therefore, $CaSO_4 \cdot 2H_2O$ (gypsum) is produced as the product in this overall desulfurization process [17, 39, 63]. Wet flue gas desulfurization can achieve high SO_2 removal efficiencies approximately 98% based on the quality of coal and other coal fired plant conditions [39]. However, wet flue gas desulfurization suffers from high consumption of chemical reagents, high transportation and utility costs due to the complexity of operation. Reactions 2.2 to 2.4 indicate the overall reaction process during wet flue gas desulfurization.

$$CaCO_3 + SO_2 + ½\ H_2O \rightarrow CaSO_3 \cdot ½H_2O + CO_2 \qquad \text{Reaction 2.2}$$

$$CaSO_3 \cdot ½H_2O + ½\ O_2 + 3/2\ H_2O \rightarrow CaSO_4 \cdot 2H_2O \qquad \text{Reaction 2.3}$$

The overall reaction,

$$CaCO_3 + SO_2 + ½\ O_2 + 2H_2O \rightarrow CaSO_4 \cdot 2H_2O + CO_2 \qquad \text{Reaction 2.4}$$

Dry flue gas desulfurization can be further categorized into several methods such as, semi-dry flue gas desulfurization, circulating dry scrubbing and dry sorbent injection. In semi-dry flue gas desulfurization technique, a spray dryer absorption system is used where the limestone slurry is atomized and sprayed into the hot flue gas in order to absorb SO_2 available in the flue gas [16]. The spray dryer is connected to a dust collection system equipped with either electrostatic precipitators (ESP) or fabric filters and, the output dry material from the spray dryer is collected by this dust collection system [16]. This output dry material is composed of products of the desulfurization reaction and fly ash which was available in the flue gas. Therefore, in comparison to the wet flue gas desulfurization, extremely low particulate matter is available in the output flue gas coming out from the semi-dry flue gas desulfurization technique. As well, a part of this output dry material can be recycled with the initial limestone slurry so that, the consumption of limestone would be minimized. The average operating temperature range lies over 200 °C [16].

Due to the initial wet slurry of limestone, under moist flue gas conditions, the same reaction process shown in reactions 2.2 to 2.4 can take place by leaving the product as $CaSO_4 \cdot 2H_2O$. If the desulfurization occurs under completely dry conditions over 700 °C, the reaction process follows the sequence indicated by reactions 2.5 to 2.7. However, SO_2 removal efficiency can be achieved upto 96% using semi-dry flue gas desulfurization method for low sulfur coal (<2%) fired power plants. [16]

$$CaCO_3 + SO_2 \rightarrow CaSO_3 + CO_2 \qquad \text{Reaction 2.5}$$

$$CaSO_3 + \tfrac{1}{2} O_2 \rightarrow CaSO_4 \qquad \text{Reaction 2.6}$$

The overall reaction,

$$CaCO_3 + SO_2 + \tfrac{1}{2} O_2 \rightarrow CaSO_4 + CO_2 \qquad \text{Reaction 2.7}$$

In circulating dry scrubbing, a fluidized bed is used in order to efficiently contact the chemical reagent with the SO_2 available in the flue gas. Frequently, $Ca(OH)_2$ (hydrated lime) is used as the chemical reagent for this technique. The mixing of reactants is promoted by means of the fluidized bed and water spray is utilized to optimize the moisture content of the reagent for the desulfurization reaction [16, 39]. The products of the desulfurization reaction depends on the moisture level of reactants and in wet conditions, it follows the reaction process indicated by reactions 2.8 to 2.10. The solid output is collected using a dust collection system and it mostly contains the reaction products, fly ash in the flue gas and unreacted $Ca(OH)_2$ [39]. The capital cost is lower than wet flue gas desulfurization and semi dry flue gas desulfurization since, a waste water treatment facility is not required for the low temperature operation.

$$2Ca(OH)_2 + 2SO_2 \rightarrow 2CaSO_3 \cdot \tfrac{1}{2}H_2O + H_2O \qquad \text{Reaction 2.8}$$

$$CaSO_3 \cdot \tfrac{1}{2}H_2O + \tfrac{1}{2} O_2 + 3/2\ H_2O \rightarrow CaSO_4 \cdot 2H_2O \qquad \text{Reaction 2.9}$$

The overall reaction,

$$2Ca(OH)_2 + 2SO_2 + \tfrac{1}{2} O_2 + \tfrac{1}{2}H_2O \rightarrow CaSO_3 \cdot \tfrac{1}{2}H_2O + CaSO_4 \cdot 2H_2O \qquad \text{Reaction 2.10}$$

The flue gas desulfurization technique with the lowest cost is dry sorbent injection or adsorption by a solid sorbent [39]. SO_2 available in the flue gas undergoes to the desulfurization reaction with the solid sorbent packed in a reactor or injected to the flue gas stream. The major solid sorbent used in this technique is CaO or different materials composed of CaO [16, 39]. The desulfurization reaction follows the process illustrated by reactions 2.11 to 2.13. The SO_2 removal efficiency lies between 50-70% based on other coal fired plant conditions and the solid sorbent used. However, this technique incorporates high temperatures over 700 °C to occur the particular reactions under dry conditions [16, 39].

$$CaO + SO_2 \rightarrow CaSO_3 \qquad \text{Reaction 2.11}$$

$$CaSO_3 + \tfrac{1}{2} O_2 \rightarrow CaSO_4 \qquad \text{Reaction 2.12}$$

The overall reaction,

$$CaO + SO_2 + \tfrac{1}{2} O_2 \rightarrow CaSO_4 \qquad \text{Reaction 2.13}$$

This technique is easier in operation and the consumption of solid sorbents is lesser compared to other techniques. The commonly used materials as chemical reagents in flue gas desulfurization are derived from limestone, magnesium-enriched lime, dolomite, seawater and soda ash [64, 65]. In addition, there are prevailing studies that show the commercial solid sorbents like zeolites also can be used for desulfurization via adsorption [66]. These materials are natural resources and they are used in lot of other industrial applications as major raw materials. Therefore, major drawbacks of using the conventional chemical reagents for desulfurization are, the high natural resources consumption, high transportation costs and, disturbance on other industrial applications due to excessive utilization. As a result, future investigations are required in order to develop low cost solid sorbent materials which can help to reduce the load of the desulfurization units using these natural chemical resources. Figure 2.11 demonstrates a comparison of different conventional SO_2 control techniques. As well, Table 2.8 illustrates a summary of existing studies on post combustion flue gas desulfurization using solid sorbents.

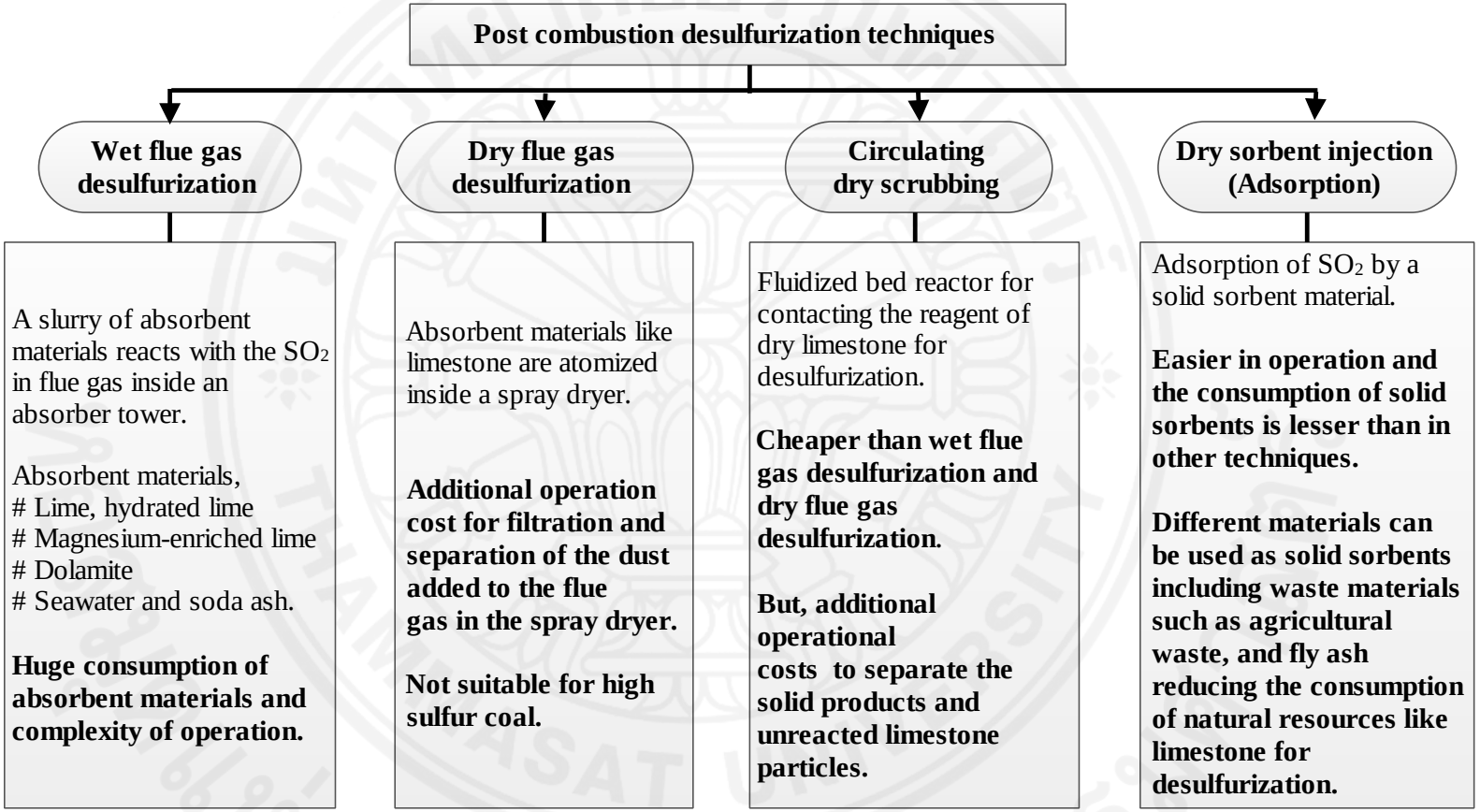

Figure 2.11: Comparison of conventional SO_2 control techniques

Table 2.8: Summary of post combustion desulfurization using solid sorbents

Ref.	Solid sorbent	Conditions	Experimental techniques	Results
[67]	SO_2 sorption by limestone	Sample size : 10 mg Mean particle size : 545 µm SO_2 flow rate : 20 mL/min $T_{Reaction}$: 750 - 950 °C P : 1 atm The experiment was performed in TGA.	TGA (Heating rate: 30 $^oC\ min^{-1}$) Kinetic model was developed based on Arrhenius equation, rate laws, and mass balance.	The reaction rate and conversion increased with T until 850 ^oC, and considerably dropped after that, because, reaction mechanism changes above 850 ^oC due to sintering of the limestone. Pre-exponential factor : 0.822 s^{-1} Activation energy: 4.446 $kJmol^{-1}$
[65]	SO_2 sorption by MgO	Samples : Single-crystal MgO with a plane shape of 5mm x 5mm x 0.5mm $T_{Reaction}$: 550, 650, 750 °C N_2/SO_2 flow rate: 100 mL/min Reaction of MgO with SO_2, O_2 was taken place in the TGA.	TGA (Heating rate: 50 $^oC\ min^{-1}$) Surface morphology of the single crystals before and after reaction was explored using AFM. The sulfur distribution on the reacted single-crystal surface was measured using SEM equipped with EDS analysis.	The product $MgSO_4$ forms three-dimensional cone-shaped islands rather than a uniform product layer on the MgO surface when the reaction temperature increases. Adsorption, reaction, diffusion and product molecule nucleation act as steps during the reaction mechanism respectively.

Cont'd from Table 2.8

Ref.	Solid sorbent	Conditions	Experimental techniques	Results
[66]	SO_2 sorption using zeolite	Commercially available zeolites Sample size: 2.0 g T : Room temperature Fixed bed glass adsorber used for gas mixing with zeolite. (N_2 + SO_2) flow rate: 60 L/hr SO_2 concentration : 1050 ppm	Infrared non-dispersive SO_2 analyzer with online recording to find the amount of SO_2 adsorbed during the experiments.	Sorbent should contact with flue gases for long period of time to be fully saturated by SO_2 and fluidized bed contactor should be employed. SO_2 adsorption capacity: From 0.5 - 2.0 mg of SO_2/g of zeolite to 38 mg of SO_2/g of zeolite when temperature increased.
[64]	SO_2 sorption by dolomite	Average particle size : 650 μm Sample size: 10 mg. $T_{Reaction}$: 600 - 900 °C SO_2 flow rate : 20 mL/min SO_2 volumetric fraction : 20% Air flow rate : 80 mL/min Isothermal experiments were performed in TGA. (Heating rate : 30 °Cmin^{-1})	Reaction rate was found based on the TG and DTG curves. XRD in a 2θ range of 20–70º, to analyze chemical compositions of the natural dolomite and the reaction solid products.	Reaction is very fast initially and then, becomes slower due to diffusion resistance by pore plugging. Both CaO and MgO react with SO_2. Reaction rate increases up to 850 ºC, Above 850 ºC, sintering happens. T < 850 ºC, Pre-exponential factor: 1.410 s^{-1}, Activation energy: 8.8 kJ/mol

2.3.4 SO_2 capture using fly ash as solid sorbent

Existing studies show that fly ash coming out from a coal fired power plant can be utilized for desulfurization as a solid sorbent. Solid sorbent prepared by coal fly ash synthesized with CaO and $CaSO_4$ has delivered SO_2 capture capacities from 53.6 to 244.7 mg /g sorbent at temperature range of 60 - 300 ˚C and 1 atm pressure [47]. Generally, the desulfurization performance increases with the surface area of the sorbent and the desulphurization temperature [47, 68]. Furthermore, existing investigations prove that, coal fly ash can be mixed with commercial solid sorbents like zeolite for simultaneous CO_2 and SO_2 capture. In a similar study, a SO_2 capture performance of 38 mg SO_2/g sorbent has been obtained at 700 ^oC and the sorbent should have contact with the flue gas for longer period of time as well as thermal activation of sorbent is required for better SO_2 adsorption [66].

Since, fly ash mostly consists of CaO (free lime), apart from the SO_2 adsorption over fly ash, sulfation reaction between SO_2 and CaO (free lime) can take place by forming $CaSO_4$ during the SO_2 capture process [69]. As a result, the total desulfurization activity can be increased when a satisfactory contact time is given for the flue gas over the fly ash solid sorbent. Reaction 2.14 indicates the sulfation reaction which takes place during the SO_2 capture process using free lime (CaO) contained fly ash as solid sorbent.

$$CaO + SO_2 + \frac{1}{2} O_2 \rightarrow CaSO_4 \qquad \text{Reaction 2.14}$$

Due to the possibility of exceeding standard properties of fly ash required to be used in concrete, qualified fly ash is not recommended to be used for SO_2 capture. However, considerable amounts of unqualified fly ash are often generated within coal fired power plants. These unqualified fly ash quantities available in coal fired power plants can be incorporated for desulfurization without imposing any risk on post capture applications of qualified fly ash. The existing studies about the utilization of coal fly ash for SO_2 capture reveal that, a complicated reaction mechanism takes place between fly ash sorbent and SO_2 during the desulfurization process. This reaction mechanism is not simply controlled by the surface reaction step between SO_2 and the free lime (CaO) available in fly ash.

The existing investigations provide many evidences that, SO_2 undergoes adsorption into the fly ash sorbent surface and allows the surface reaction to take place initially where, ash diffusion becomes the rate limiting step thereafter [68-70]. Eventhough. A rapid reaction rate can be observed initially during the surface reaction limiting step, the rate becomes slower during the ash diffusion step. The development of product ($CaSO_4$) layer on the sorbent surface and pore plugging phenomena also ocurr at this step [68-70].

Using unqualified fly ash for SO_2 capture is advantageous for a coal fired power plant in many ways. Fly ash with high free lime can contribute to make the entire desulfurization system of the coal fired power plants more economical due to the low temperature operation, negligible transportation cost and zero material cost. In addition, fly ash can help to reduce the load of desulfurization unit for the flue gas emission in the same place. The common CO_2 capture materials would not be an attractive combined solutions for a coal fired power plant emission control while, fly ash becomes an interesting combined solution for both CO_2 and SO_2 control. Utilization of waste materials generated in the same vicinity for hazardous emission control of CO_2 and SO_2 would help to reduce the emission control cost. As well, it would make the waste management system in the coal fired power plant more profitable and feasible.

Table 2.9 breifly explains a summary of the exsisting studies related to SO_2 capture using fly ash as a solid sorbent in laboratory scale.

Table 2.9: Summary of SO_2 capture using fly ash as solid sorbent

Ref	Solid sorbent	Conditions	Experimental techniques	Results
[69]	SO_2 sorption using CaO/fly ash (At 1: 4 ratio)	Sample size : 15 mg $T_{Reaction}$: 400 – 800 °C Gas flow: 200 mL/min Gas phase composition : SO_2 : 2000 ppm, O_2 : 5 vol%, balance : N_2 Experiments were carried out in a TGA	TGA to measure the calcium conversion due to sulfation. The kinetic model was developed based on shrinking unreacted core model (reaction + diffusion)	Initially, the chemical reaction is the rate limiting step. Activation energies, (diffusion) : 49.3 $kJmol^{-1}$ > (reaction) : 13.9 $kJmol^{-1}$ Pre-exponential factor: 178 min^{-1} Inter particle and product layer diffusion dominates the chemical reaction when time > 20 min.
[71]	SO_2 sorption using $Ca(OH)_2$ / fly ash sorbent added with $CaSO_4$. $2H_2O$	$T_{Reaction}$: 57˚C, RH : 80% Gas composition: 5000 ppm SO_2, 12% CO_2, 2% O_2 and balance N_2 Gas flow: 1000 mL/min Experiment was performed in a fixed bed reactor.	Nitrogen adsorption data and the BET standard method to find pore size distribution and specific surface area of the sorbent. The reacted sorbent was analyzed by the in TGA to find the amount of reacted SO_2 to form $CaSO_4$.	Specific surface area of sorbent : 11.3 - 38.8 m^2/g Maximum $Ca(OH)_2$ utilization : 0.012 mol SO_2/g $Ca(OH)_2$ $Ca(OH)_2$ utilization increases with the sorbent hydration time. $Ca(OH)_2$ utilization slightly reduces with increasing $CaSO_4$ content.

Cont'd from Table 2.9

Ref	Solid sorbent	Conditions	Experimental techniques	Results
[72]	SO_2 sorption by fly ash/ $Ca(OH)_2$ / $CaSO_4$ sorbent	Composition of sorbent: $Ca(OH)_2$: 30% , $CaSO_4$: 30% , coal fly ash: 40% Sample size: 23-26 g Experiment was conducted in a tubular reactor, 40 mm diameter and 150 mm long. Gas composition: 2250 ppm SO_2, 700 ppm NO_x, 6% O_2, 13% CO_2, 10% H_2O and N_2 as a balance Gas flow rate : 1 Liter/min $T_{Reaction}$: 130 °C	Nondispersive IR spectroscopy for the amount of SO_2 and CO_2 Atmospheric chemical luminescence technique for of NO_x amount Paramagnetic susceptibility technique for O_2 content The amount of water molecule adsorbed on the sorbent was measured with a quartz spring balance. Nitrogen adsorption based on the BET method to find surface area XRD measurement to identify the products (Cu Kα , 2θ : 5 - 90°)	Maximum desulfurization activity : 0.8 mol SO_2/mol sorbent Desulfurization activity increased with the inlet NO_x concentration up to 500 ppm and remained constant above that. The NO_x removal increased with an increase in the SO_2 concentration up to 1500-2000 ppm and then gradually decreased as the SO_2 concentration increased further. SO_2 and NO_x removal increased with the increase in the moisture content of the flue gas. Removal of SO_2 and NO_x increased until 75 °C, thereafter, stayed constant at higher temperatures than 75 °C.

Cont'd from Table 2.9

Ref	Solid sorbent	Conditions	Experimental techniques	Results
[73]	SO_2 sorption by CaO / fly ash / $CaSO_4$ sorbent	Sorbent: CaO: 5g, $CaSO_4$: 7.4g, coal fly ash: 13.7g Sample size : 25 g Experiment conducted in a fixed-bed reactor system. 500 ppm $\leq C_{SO2} \leq$ 2000 ppm, 250 ppm $\leq C_{NOx} \leq$ 750 ppm, $T_{Reaction}$: 60-80 °C RH : 50-70%	Portable flue gas analyzer to measure C_{SO2} before and after the sorption process. Matlab software for simulations to solve partial differential equations in the developed kinetic model.	FGD reaction is initially controlled by reaction rate and became ash-diffusion limiting due to the gradual increase in solid product production. Activation energies, (diffusion) : 45,000 J/mol > (reaction) : 15,052 J/mol The orders of reaction for SO_2 (g) and NO_x (g) were found to be 1 and 0.73, respectively.
[74]	SO_2 sorption by CaO / fly ash / $CaSO_4$ as the sorbent	Sample size : 10 mg Gas composition : SO_2 : 4000 ppm, balance N_2 Gas flow rate : 150 mL/s $T_{Reaction}$: 60 – 140 °C	X-ray spectrometer, to find the weight percentage of Ca in sorbent. TGA, to study the sulfation reaction between the sorbent and SO_2. A kinetic model was developed using Arrhenius equation and reaction rate laws.	Initial rate of the sulfation reaction increases with increasing $T_{Reaction}$. The highest initial rate at 140 ºC Reaction rate drops with reaction time Activation energy : 22.9 kJ/mol is lower than pure CaO (41.8 kJ/mol) and $Ca(OH)_2$ (133.9 kJ/mol) Pre-exponential factor : 64.4 min^{-1}

Cont'd from Table 2.9

Ref	Solid sorbent	Conditions	Experimental techniques	Results
[75]	SO_2 sorption by fly ash/ $Ca(OH)_2$ sorbent	Composition of sorbent : $Ca(OH)_2$ / fly ash : 70/30 wt Sample Size : 30 mg Experiments carried out using a differential fixed-bed reactor. Total gas flow rate: 4 L/min. Gas composition : SO_2 : 1000 ppm, and N_2 $T_{Reaction}$: 60 – 80 ºC RH : 70%	N_2 adsorption with BET method to find surface area of sorbent. Conversion of sorbent was determined from its SO_3^{2-}/Ca^{2+} molar ratio. SO_3^{2-}content was determined by iodometric titration, and the Ca^{2+} content by EDTA titration. XRD patterns of unreacted and reacted sorbent for 0, 10 and 60 min reaction times to study the products. SEM micrograph to observe pore volume distributions of a typical $Ca(OH)_2$ / Fly ash sorbent particle.	The particle size distribution of the sorbent : 0.6-60.6 μm , D_{mean} : 10.3 μm BET surface area : 38.0 m^2/g The reaction product is $CaSO_3 \cdot 0.5H_2O$ Reaction is rapid in the initial period, but conversion levels off after 10 min. At 60ºC, the 1 h conversion of sorbent : 0.60 (0.19 for pure $Ca(OH)_2$ sorbent) The initial reaction rate and the maximum conversion of the sorbent increased significantly with increasing relative humidity. The sulfation rate is limited by chemical reaction on the sorbent grain surface. It is also affected due to the surface coverage by product.

2.3.5 Comparison of different reactor types for the desulfurization

Table 2.10 shows a comparison of advantages and disadvantages among fixed bed reactors, fluidized bed reactors and conventional reactors with a solid reagent stream for desulfurization process [15, 57, 76]. According to the comparison, the packed bed reactors are more suitable for expensive solid sorbents and catalytic reaction. When the solid sorbent quantity increases in the packed bed, plugging can occur due to product layer development hence, reducing the efficiency of desulfurization. Therefore, fluidized bed reactors provide better gas/solid, and solid/solid contact areas so that, the conversion of the desulfurization reactions comparatively becomes higher. However, the conventional reactors with reagent stream yield very high efficiencies of desulfurization eventhough, the operation is quite difficult and costly.

Table 2.10: Comparison of different desulfurization reactor units

Reactor type	In terms of desulfurization	
	Advantages	Disadvantages
Packed bed / fixed bed reactor	More suitable for expensive adsorbents. Designing process and is simple and operating cost is lower. Scaling-up is more reliable with experimentation. The residence time for the reaction is higher for the stationary adsorbent layer.	Plugging occurs due to product layer development over adsorbent and heat gradients are not uniform. Difficulty in the replacement of the adsorbent and SO_2 removal efficiencies fall down 40-50% for large scale desulfurization.
Fluidized bed reactor	Can prevent plugging the product layer within the adsorbent used. Heat and mass transfer are more efficient due to high gas/solid, and solid/solid contact areas. Shut down of the desulfurization process is not needed for the replacement of the adsorbent. Higher SO_2 removal efficiencies upto 98%	Increasing the flue gas flow rate may affect to reduce SO_2 residence time in the adsorbent. Designing process and experimentation are complicated and more expensive. Scaling-up is difficult. Catalysts, supports, promoters of a reaction can be deactivated due to impacts of fluidization.
Reactor with reagent stream	Feasibility to maintain required moisture level within the reactor. Higher SO_2 removal efficiencies upto 95% in large scale desulfurization.	Additional equipment for stream handling makes capital cost higher as well as difficulties in maintenance. The requirement of additional separation of product in the reactor can increase more energy consumption.

Chapter 3
Methodology

3.1 CO_2 capture using fly ash

3.1.1 Materials for CO_2 capture

Fly ash was collected from Mae Moh coal fired power plant of the electricity generating authority of Thailand (EGAT). Fly ash samples were dried at room temperature for 48 hours and at 110 °C temperature for 8 hours in order to remove the moisture completely. In the experiments, 99.8 vol% carbon dioxide (CO_2) gas (Praxair, Thailand) was used for CO_2 capture and 99.995 vol% nitrogen gas (Praxair, Thailand) was used for purging.

3.1.2 Experimental procedure for CO_2 capture

Figure 3.1 illustrates the experimental set up for CO_2 capture experiments using fly ash as solid sorbent. CO_2 capture was conducted in a tubular reactor. 99.8 vol% CO_2 gas was flowed into the reactor for 1 hour by maintaining the pressure and the temperature in the reactor at 30 °C. After the CO_2 capture process, 99.995 vol% nitrogen gas was fed into the reactor with a volume flow rate of 30 mL/min for 30 minutes in order to remove the physically adsorbed CO_2 (desorption process). The temperature in the reactor was increased upto 150 ºC and kept for 1 hour to ensure all of the adsorbed CO_2 are desorbed. The temperature was maintained using a furnace (model TF150) with PID controller. The gas samples were taken from the sampling port and the CO_2 capture capacities via physical adsorption (Appendix D) and carbonation were analyzed separately.

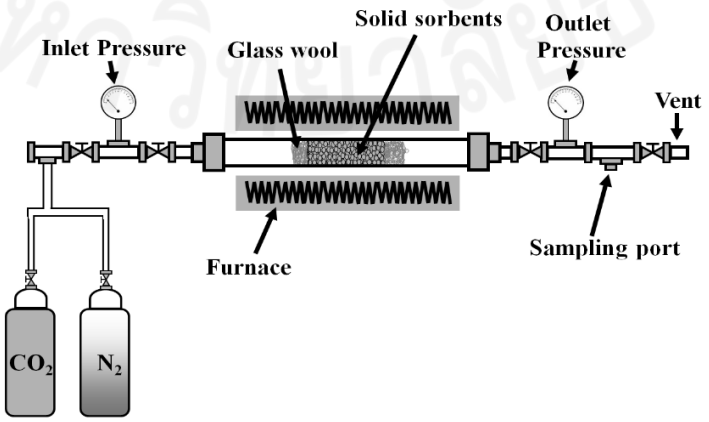

Figure 3.1: The experimental set-up for CO_2 capture

Initially, the effect of the moisture content in fly ash to the CO_2 capture performance was investigated by varying the moisture content at 0 wt%, 5 wt% and 10 wt% while keeping the pressure at 1 atm and the contact time between fly ash and CO_2 inside the tubular reactor at 30 min. Similarly, the effect of pressure was determined by varying pressure at 1 atm, 1.2 atm and 1.5 atm while keeping the moisture content at 0 wt% and the contact time between fly ash and CO_2 inside the tubular reactor at 30 min. Moreover, the effect of contact time was evaluated by varying the contact time at 1 min, 5 min and 30 min while maintaining the moisture content at 0 wt% and the pressure at 1 atm. Figure 3.2 summarizes the full experimental procedure for CO_2 capture.

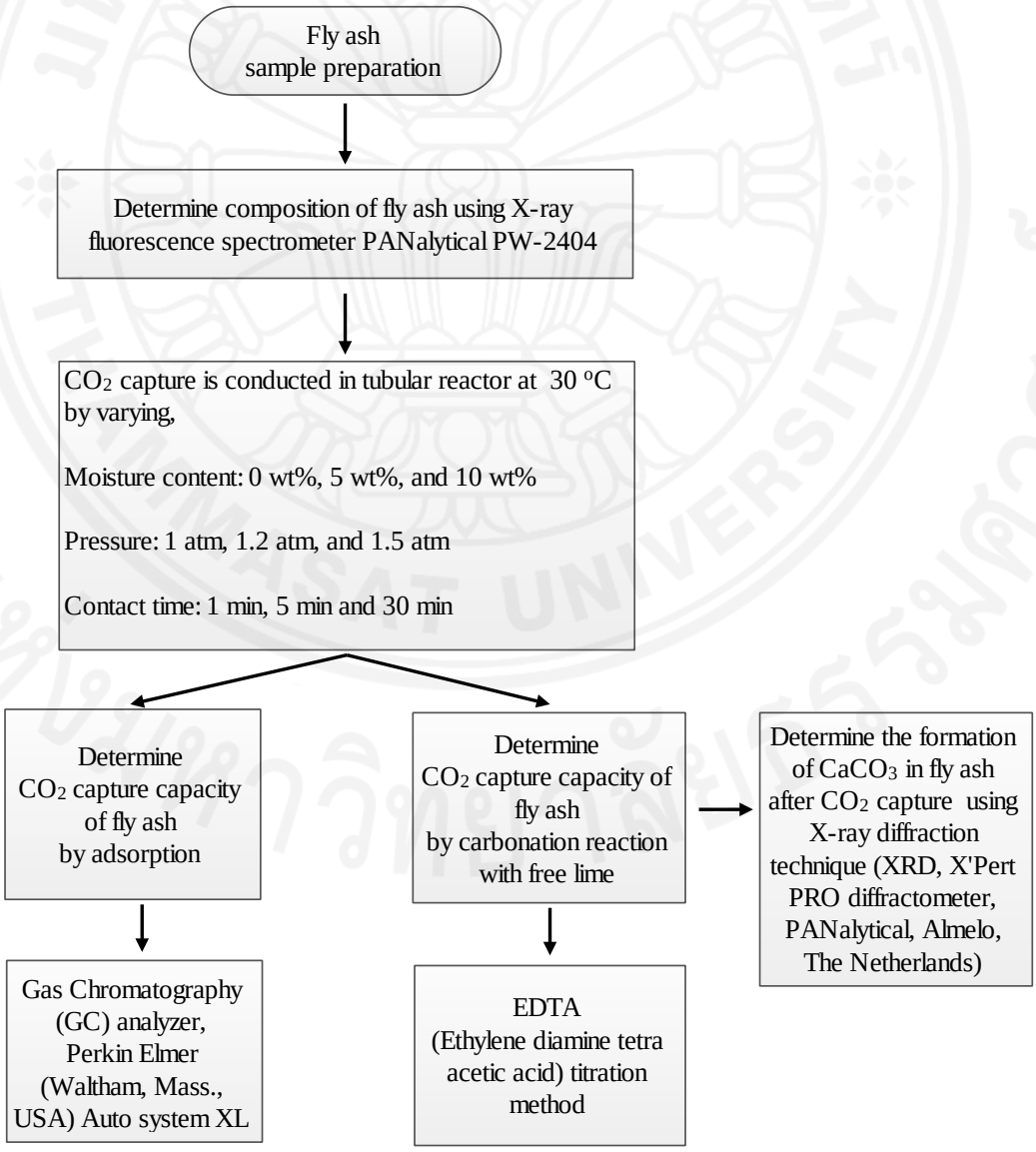

Figure 3.2: The experimental procedure for CO_2 capture

3.1.3 Analysis techniques for CO_2 capture

The chemical compositions of fly ash samples were analyzed by using X-ray fluorescence spectrometer PANalytical PW-2404. The formation of $CaCO_3$ in fly ash after CO_2 capture was analyzed by the X-ray diffraction technique (XRD, X'Pert PRO diffractometer, PANalytical, Almelo, The Netherlands) using Cu $K\alpha_1$ radiation, 10°- 80° 2-theta, 0.02° step size, 0.5 sec step time. The XRD patterns were compared with the powder diffraction files-2003 ICDD PDF database for phase identification.

The CO_2 capture capacity via adsorption over fly ash was evaluated using the Perkin Elmer (Waltham, Mass., USA) Auto system XL gas chromatography (GC) with Porapak Q column (Supelco, Bellefonte, PA, USA) coupled with a thermal conductivity detector (TCD). The gas samples obtained from the sampling port in the experimental set up, were injected into the GC using a gas tight syringe. In the GC analyzer the carrier gas is used to transport the gas samples through the column. The column involves subsequent separation of gas species in the sample and the charged gases are identified by the TCD detecter. The intensity of the detector output signal is indicated in the computer monitor with the relative peaks for each gas species.

EDTA (Ethylene diamine tetra acetic acid) titration method was utilized to determine the amount of CO_2 reacted with free lime during the CO_2 capture. The solid samples of the fresh fly ash and fly ash after CO_2 capture were diluted in deionized water overnight so that, the calcium ions completely dissolved in the liquid for titration process. The dissolved fly ash samples were filtered using filter papers (Whatman^{TM}, Cat No. 1093-110, UK). The standard solution was prepared using EDTA (≥99%, Ajax Finechem Pty Ltd.) at the concentration of 0.025 Molar ($moldm^{-3}$) diluting in deionized water. Ammonium chloride (≥99.5%, Sigma Aldrich) and ammonium hydroxide (28 %, Sigma Aldrich) were diluted in deionized water as the buffer solution with the pH value of 10. Eriochrome Black T (Panreac) was used as the indicator. 1 mL of the buffer solution and a drop of the indicator were added to the sample solution and, titration was carried out for the sample solution with the standard EDTA solution. The volume of the EDTA solution consumed to change red colour of the sample into blue color in each titration was marked. The amount of CO_2 captured by carbonation reaction is equal to the difference of free Ca^{2+} ions between the fresh fly ash and the fly ash after CO_2 capture. Calculation procedure has been indicated in Appendix E.

3.1.4 Process simulation procedure for CO_2 capture

The simulation for the scaled-up reactor system for CO_2 capture was executed using Aspen plus process simulation software. The production data from Mae Moh coal fired power plant of the Electricity Generating Authority of Thailand (EGAT) in year 2008 were utilized as input data for the feed.

RStoic reactor model (stoichiometric reactor) was applied to model the CO_2 capture reactor system coupled with the PENG ROB (Peng-Robinson activity coefficient method) thermodynamic property method in Aspen plus software. Experimental results for the composition of fly ash were used to define the required chemical components for the simulation program in Aspen plus software.

Table 3.1 indicates the input data used for the CO_2 capture process simulation in Aspen plus software.

Table 3.1: Input data for the CO_2 capture simulation in Aspen plus software

Input data parameter	Value
Flue gas temperature	150 ºC
Flue gas pressure	1 atm
Reactor temperature	30 ºC
Reactor pressure	1 atm
Moisture content in fly ash and flue gas	5 wt%
Qualified fly ash mass flow rate (90 wt% of total)	1,800 ktonne/year
CaO content in fly ash (16.52 wt% + 1.7 wt%)	327.96 ktonne/year
CO_2 mass flow rate	18,174.18 ktonne/year
Experimental CO_2 capture capacity at 5 wt% moisture, 30 ºC, 1 atm and contact time of 1 min	208 μmol CO_2/g fly ash

Few assumptions were made for modeling the CO_2 capture process in Aspen plus software. The temperature and the pressure were selected as 30 ºC and 1 atm respectively. In addition, moisture content in fly ash and flue gas was assumed to be 5 wt%. According to the experimental results, the CO_2 capture of fly ash by adsorption is very small compared to the CO_2 capture via carbonation reaction.

Therefore, it was assumed that, carbonation reaction represents the total CO_2 capture at 30 ºC, 1 atm, 5 wt% moisture content, and 1 min contact time in the CO_2 capture reactor system which amounts to 208 µmol CO_2/g fly ash. Reaction 3.1 indicates the carbonation reaction between free lime in fly ash (CaO) and CO_2.

$$CaO + CO_2 \rightarrow CaCO_3 \qquad \text{Reaction 3.1}$$

The conversion of the carbonation reaction was assumed to be equal to the total experimental CO_2 capture capacity at the selected conditions. Figure 3.3 summarizes the steps for CO_2 capture process simulation in Aspen plus software.

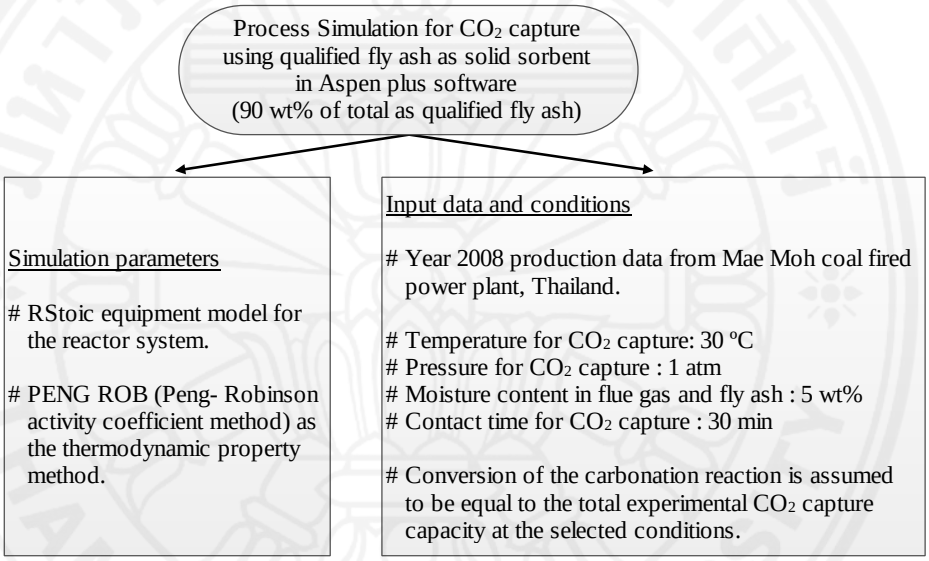

Figure 3.3: The steps of process simulation procedure for CO_2 capture

Two reactors in series were occupied for the simulation of CO_2 capture reactor system. The total qualified fly ash quantity (1800 ktonne/year) was equally split into two streams at 900 ktonne/year as the fly ash feed for each reactor. Figure 3.4 demonstrates the Aspen plus process flowsheet for the simulation of CO_2 capture.

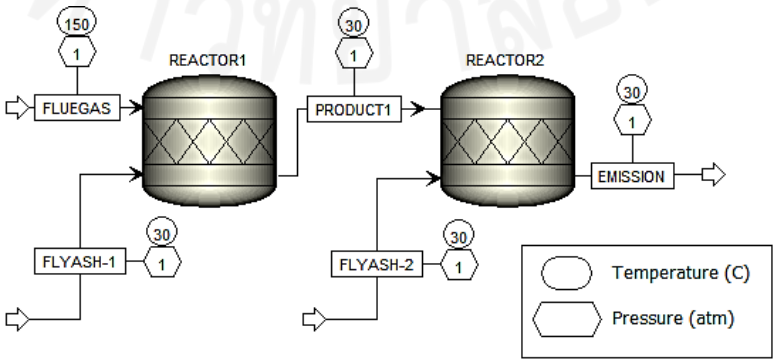

Figure 3.4: Aspen plus process flowsheet for the CO_2 capture simulation

3.2 SO_2 capture using fly ash

3.2.1 Materials for SO_2 capture

Fly ash was collected from Mae Moh coal fired power plant, Thailand and, fly ash samples from the same batch were directly used as the sorbent material in the SO_2 capture experiments. Sulfur dioxide gas (4.3 vol% of SO_2 in N_2, Linde, Thailand) was used as the feed gas for SO_2 capture and, 99.999 vol% nitrogen gas (Praxair, Thailand) was used for purging.

3.2.2 Temperature programmed desorption (TPD)

Figure 3.5 illustrates the experimental set-up used for temperature programmed desorption (TPD) experiment. Initially, 1g of fly ash was placed in the middle of the tubular reactor using quartz wool and 99.999 vol% nitrogen gas was fed into the reactor with a flow rate of 50 mL/min for 15 minutes in order to purge the air inside the reactor. Fly ash in the reactor was exposed to SO_2 gas (4.3 vol% of SO_2 in N_2) at a flow rate of 30 mL/min for 30 minutes at 50 ºC and 100 ºC separately. After the SO_2 capture, TPD process was performed for the SO_2 captured fly ash samples at 50 ºC and 100 ºC by increasing the desorption temperature from 50 ºC to 200 ºC at a rate of 10 ºC per minute while flowing 99.999 vol% nitrogen gas into the reactor at a flow rate of 30 mL/min. The temperature was maintained using a furnace (model TF150) with PID controller. The real time mass spectrometry (MS) profiles were observed for the TPD process.

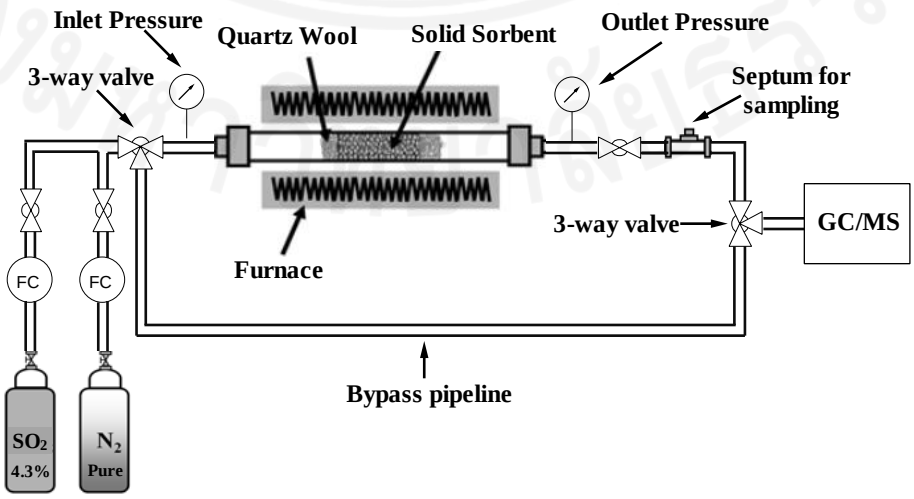

Figure 3.5: The experimental setup for desulfurization

3.2.3 Temperature programmed reaction (TPR)

Temperature programmed reaction (TPR) was carried out in the same experimental set-up as shown in Figure 3.5. The tubular reactor was loaded with 1g of fly ash in the middle using quartz wool. The air inside the reactor was purged using 99.999 vol% nitrogen gas with a flow rate of 50 mL/min for 15 minutes at 35 ºC and 4.3 vol% of SO_2 gas in N_2 was fed at a flow rate of 30 mL/min through the tubular reactor at 35 ºC. After the mass spectrometry profile of SO_2 flow was stabilized, the temperature was increased from 35 ºC to 600 ˚C at a rate of 10 ºC per minute while flowing 4.3 vol% of SO_2 in N_2. The temperature was maintained using a furnace (model TF150) with PID controller. The real time mass spectrometry (MS) profile of the outgoing gas flow from reactor was observed at uniformly increasing temperatures. Figure 3.6 sums up the full experimental procedure for SO_2 capture.

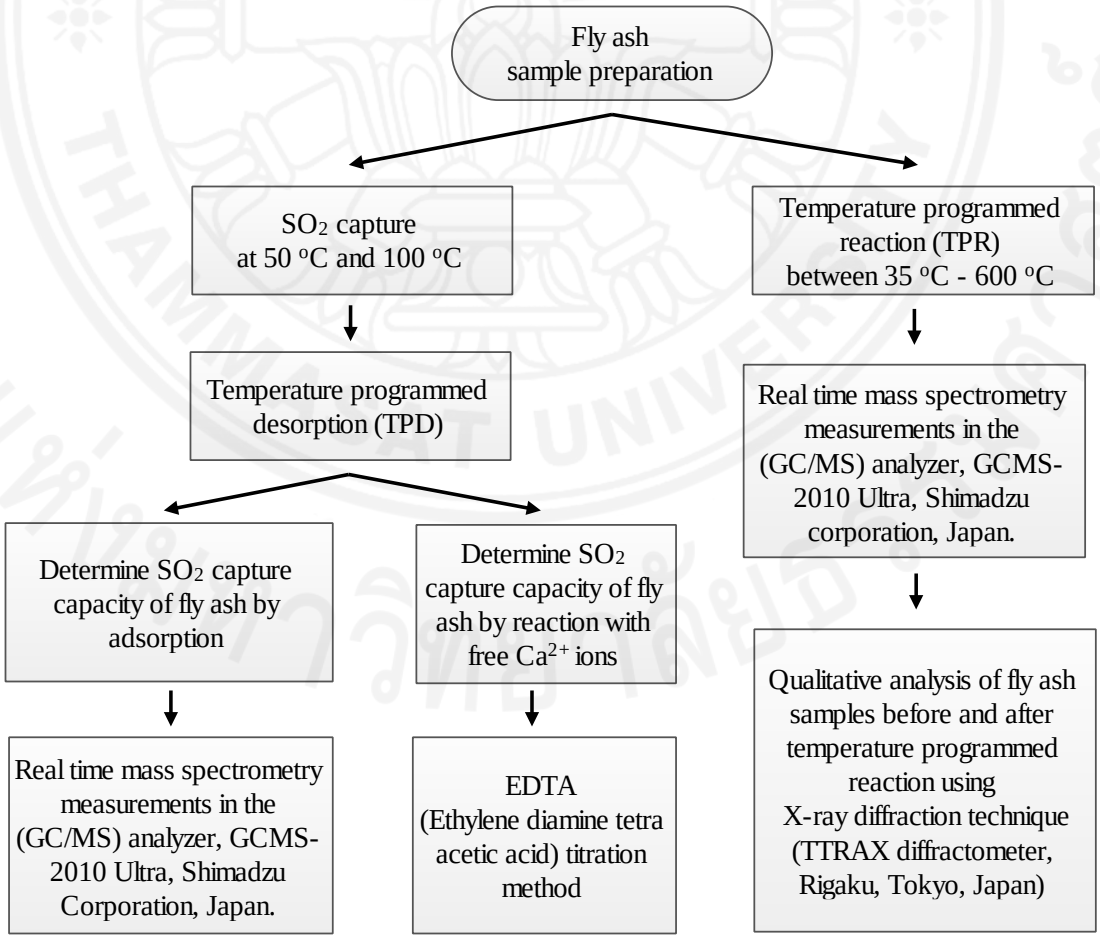

Figure 3.6: The experimental procedure for SO_2 capture

3.2.4 Analysis techniques for SO_2 capture

The fly ash samples before and after SO_2 capture, were characterized by the X-ray diffraction technique (TTRAX diffractometer, Rigaku, Tokyo, Japan) with Cu $K\alpha_1$ radiation, at 50 kV, 300 mA, 15°-65° 2-theta, 0.01° step size, scan speed 3°/min, and using monochromator to remove noise generated from iron particles in the fly ash sample. The recorded XRD patterns were compared with the powder diffraction files-2003 ICDD PDF database for phase identification.

The real time mass spectrometry measurements were performed using the gas chromatography and mass spectrometry (GC/MS) analyzer, GCMS-2010 Ultra, Shimadzu Corporation, Japan. The SO_2 capture capacities by adsorption were calculated based on the manual peak integration of peak intensities at m/z = 64 in the mass spectrometry profiles after calibrating the mass spectrometry profile with a 1 ml standard pulse of SO_2 at 4.3 vol% concentration (Appendix D).

EDTA (Ethylene diamine tetra acetic acid) titration method was used to determine the reacted Ca^{2+} ions by comparison of Ca^{2+} leftover in fly ash after the TPD process and Ca^{2+} available in fresh fly ash. The titration experiments were carried out for fresh fly ash and fly ash after the TPD process, as per the same EDTA titration procedure described in section 3.1.3. The SO_2 capture capacities due to reaction with free Ca^{2+} ions were calculated by taking the difference between the amount of free Ca^{2+} ions left in the fresh fly ash and fly ash after the TPD process (Appendix E).

3.2.5 Process simulation procedure for SO_2 capture

The process simulation for the scaled-up SO_2 capture system using fly ash was conducted using Aspen plus process simulation software. RPlug reactor model (Tubular reactor) coupled with IDEAL thermodynamic property method in Aspen plus software (Ideal gas law and ideal gas behavior) was used to model the reactor system for the SO_2 sulfation reaction with fly ash based on the kinetic parameters. The experimental results for the composition of fly ash were applied to define the component system for the simulation program in Aspen plus software and, the temperature at maximum yield of SO_2 capture revealed from the experimental results, was specified as the temperature for the scaled-up reactor system. The composition of flue gas was calculated and input to the simulation program.

Few assumptions were made in the SO_2 capture simulation process using fly ash. The SO_2 sulfation reaction with CaO in fly ash was considered as the only way of SO_2 capture and the sulfation reaction temperature was selected as 400 ºC based on the experimental results in this study. The total SO_2 amount in the flue gas without any control from Mae Moh coal fired power plant, Thailand was taken as 150 tonne/hr [38]. The flue gas was simulated as per the standard composition of flue gas from pulverized coal fired power plants as shown in Table 2.2 [35]. Due to the huge load of flue gas quantity, only 1 wt% of flue gas was assumed as the intake into the scaled-up reactor system for SO_2 capture using unqualified fly ash. Table 3.2 indicates the composition of flue gas input to the simulation program in Aspen plus software.

Table 3.2: Composition of flue gas input to the SO_2 capture simulation program

Component	**Composition (vol%)**	**Total mass flow rate (ktonne/year)**	**Mass flow rate into simulation (ktonne/year)**
Sulfur dioxide (SO_2)	6000 ppm	1,314	13.14
Carbon dioxide (CO_2)	12 vol%	18,174	181.74
Oxygen (O_2)	5 vol%	5,507	55.07
Moisture (H_2O)	5 vol%	3,098	30.98
Nitrogen (N_2)	75 vol%	72,282	722.82
Nitrogen dioxide (NO_2)	500 ppm	57.5	0.58
Total flue gas		100,432.5	1004.33

The unqualified fly ash quantity was assumed to be 10 wt% of the total annual fly ash production equivalent to 200 ktonne/year (i.e. 10 wt% of 2000 ktonne/year). The composition of fly ash was considered as per the experimental XRF results in this study. It was assumed that, only major components such as, SiO_2, Al_2O_3, Fe_2O_3, CaO are present in fly ash. The pre-exponential factor (A) at 400 ºC and the activation energy (E_a) for the reaction 3.2, between SO_2 and CaO in fly ash were obtained from a similar kinetic study available in the literature. The pre-exponential factor at 400 ºC was taken as, $A = 178\ min^{-1} = 2.97\ s^{-1}$ and, activation energy was taken as, $E_a = 13.9\ kJmol^{-1}$ [69].

$CaO + SO_2 + ½ O_2 \rightarrow CaSO_4$ Reaction 3.2

These values were input as the kinetic parameters for the power law reaction in Aspen plus simulation. Figure 3.7 shows the process flowsheet for the SO_2 capture process simulation in Aspen plus software. Two tubular reactors in parallel were selected for the simulation program where the total unqualified fly ash quantity was equally distributed into the packed beds of each tubular reactor. 0.05 wt% of the total flue gas quantity was fed into each tubular reactor to flow through each unqualified fly ash packed in the reactor bed.

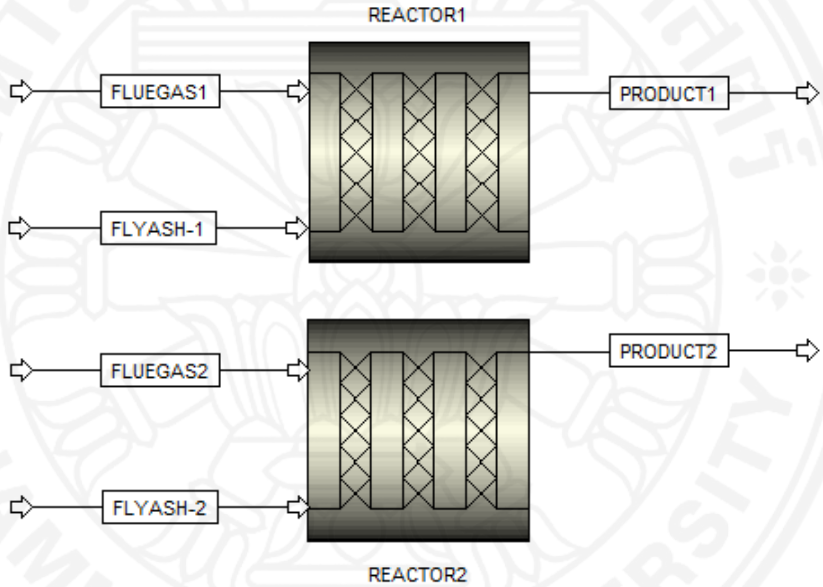

Figure 3.7: Process flowsheet for SO_2 capture process simulation in Aspen plus

Equation 3.1 to equation 3.5 indicate the mathematical formulas related to the Aspen plus simulation model with two packed bed reactors.

The power law kinetic expression for the reaction 3.2 was taken as,

$-r_{SO_2} = k[SO_2]$ Where, $k = A\left(exp\frac{E_a}{RT}\right)$ Equation 3.1

The initial design equation for the packed bed reactor,

$F_{A_o}\frac{dX}{dw} = -r_{SO_2}$ Equation 3.2

Isothermal reaction at 400 ºC was assumed and, the pressure drop in the packed bed reactor follows the Ergun Equation indicated by equations 3.3 and 3.4.

$$\frac{P}{P_0} = (1 - \alpha w)^{1/2} \qquad \text{Where,} \qquad \alpha = \frac{2\beta_o}{A_c(1-\varphi)\rho_c P_0} \qquad \text{Equation 3.3}$$

$$\beta_o = \frac{G(1-\varphi)}{\rho_o g_c D_p \varphi^3}\left[\frac{150(1-\varphi)\mu}{D_p} + 1.75G\right] \qquad \text{Equation 3.4}$$

Flue gas was assumed to behave like an ideal gas which follows the ideal gas law indicated by equation 3.5.

$$PV = nRT \qquad \text{Equation 3.5}$$

The symbols in the above equations represent the parameters and units as indicated in the list of symbols and abbreviations. Figure 3.8 shows the diagram for the steps of SO_2 capture process simulation.

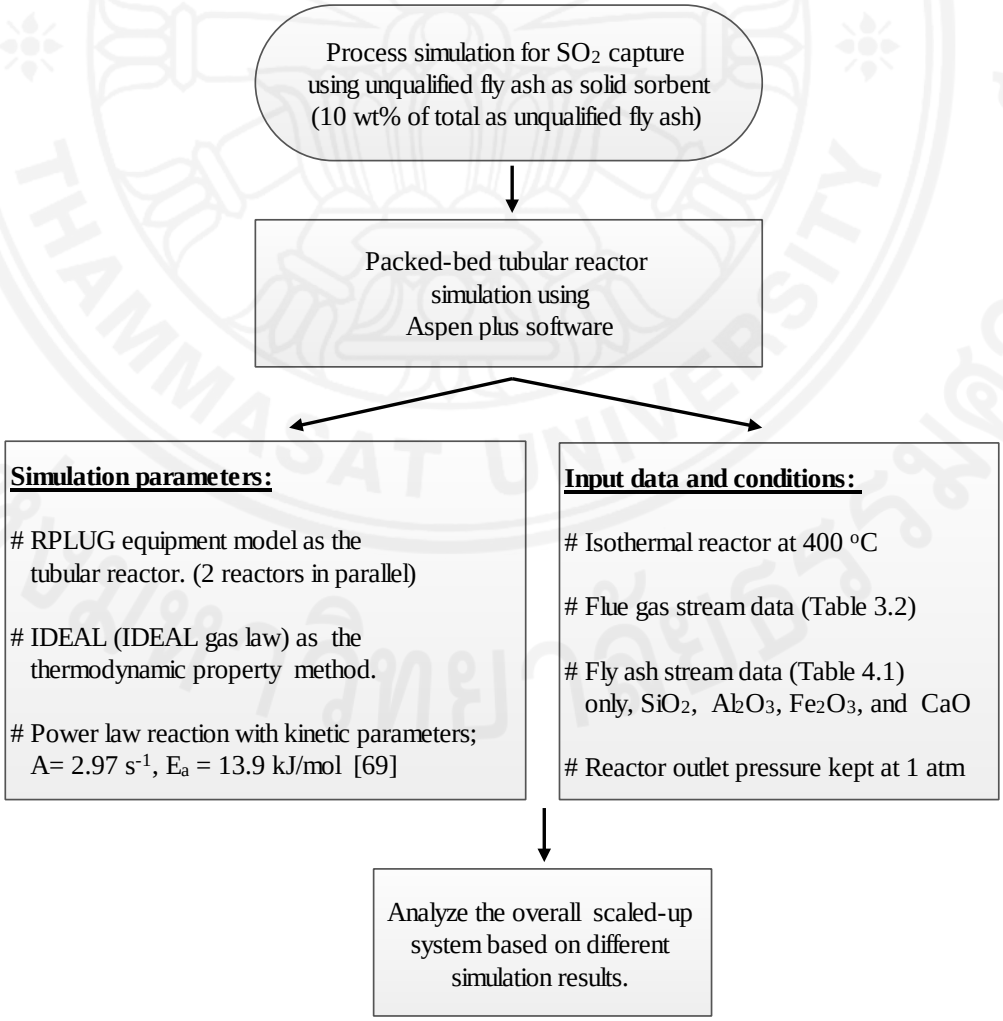

Figure 3.8: Steps of SO_2 capture process simulation procedure

Chapter 4
Results and Discussion

4.1 Properties of fly ash

Table 4.1 lists the composition of major components in fly ash obtained from Mae Moh coal fired power plant, Thailand which was analyzed by X-ray fluorescence spectrometer (XRF). The major components contained in fly ash are SiO_2, Al_2O_3, CaO, MgO and Fe_2O_3. These chemical compounds have high thermal stability with uniform properties at high temperatures [42]. Therefore, fly ash is feasible to be applied as a solid sorbent in a wide temperature range in order to capture CO_2 and SO_2. The amount of free lime (CaO) in fly ash is considerable. Therefore, free lime in fly ash can promote the carbonation reaction as well as sulfation reaction during CO_2 capture and SO_2 capture because, free lime can react with both CO_2 and SO_2 by forming the carbonate compounds and sulfate compounds respectively.

Table 4.1: Major components of fly ash from Mae Moh coal fired power plant

Species	Composition (wt %)
SiO_2	35.71
Al_2O_3	20.44
CaO	16.52
MgO	2.00
Fe_2O_3	15.54
SO_3	4.26
Free CaO	1.70
Others	3.83

4.2 CO_2 capture using fly ash

4.2.1 Effect of moisture content for CO_2 capture capacity of fly ash

Table 4.2 shows the CO_2 capture capacities by adsorption for fly ash obtained at different moisture contents at 30 ºC, 1 atm, and contact time of 30 minutes. 1 kg of fly ash was mixed with the required quantities of water vapor to prepare the samples with moisture contents of 5wt% and 10 wt%.

Table 4.2: Effect of moisture content for CO_2 capture performance of fly ash at 30 ºC, 1 atm, and contact time of 30 minutes

Moisture content of fly ash (wt %)	**CO_2 capture by adsorption using fly ash (µmol/g sorbent)**
0	2.90±0.30
5	3.34±0.10
10	3.75±0.30

The results indicate that, there is a slight increase of CO_2 capture capacity when the moisture content in fly ash goes up. The effect of moisture content for the CO_2 capture performance was only investigated for the CO_2 capture due to adsorption. In practical, fresh fly ash coming out from the combustion chamber of a coal fired power plant can be slightly wet. Literature reports that, flue gas and fly ash coming out from a pulverized coal fired power plant consists of approximately 6 wt% moisture [35]. Therefore, it is necessary to assume the availability of a reasonable moisture content like 5 wt% in the fly ash for the scaled-up CO_2 capture reactor system of the coal fired power plant.

4.2.2 Effect of pressure for CO_2 capture capacity of fly ash

Table 4.3 indicates the CO_2 capture capacities of fly ash with the variation of pressure inside the tubular reactor at 1 atm, 1.2 atm and 1.5 atm respectively while keeping other conditions constant at 30 ºC, 0 wt% moisture content in fly ash, and contact time of 30 minutes. The results point out that, CO_2 capture capacity increased simultaneous to the increment of adsorption pressure. When the pressure rises, the gas diffusion and adsorption over the solid sorbent becomes more convenient, resulting the increased CO_2 capture capacities higher pressures. However, in industrial applications, high pressure will affect to the cost of operation and capital investments including additional material cost for reactors. Studies reveal that flue gas pressure in coal fired power plants lies around 1.2 atm [35]. Therefore, it is fairly reasonable to apply 1.0 atm - 1.2 atm as the pressure condition for the scaled-up CO_2 capture reactor system of the coal fired power plant.

Table 4.3: Effect of the adsorption pressure for CO_2 capture capacity of fly ash at 30 ºC, 0 wt% moisture content, and contact time of 30 minutes

Pressure (atm)	**CO_2 Capture by adsorption using fly ash (µmol/g sorbent)**
1.0	2.90±0.30
1.2	3.23±0.02
1.5	4.29±0.01

4.2.3 XRD characterization of fly ash before and after CO_2 capture

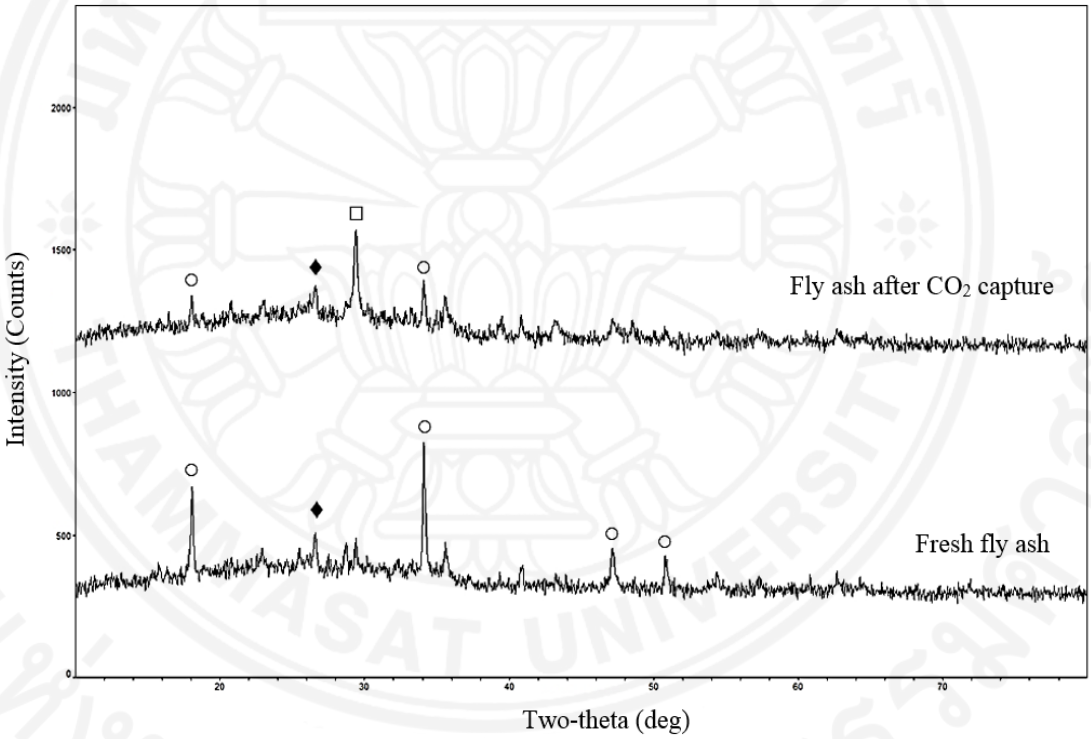

Figure 4.1: XRD patterns of the fresh fly ash before CO_2 capture and after CO_2 capture at 30 ºC, 1 atm, 5 wt % moisture

□: $CaCO_3$ (Calcite); ○: $Ca(OH)_2$ (Portlandite); ♦: SiO_2 (Quartz)

Figure 4.1 illustrates the XRD results of fly ash samples before and after CO_2 capture 30 ºC, 1 atm and 5 wt% moisture. The XRD profile of fly ash after CO_2 capture was compared with that of the fresh fly ash sample before CO_2 capture. The $CaCO_3$ phase (JCPDS No: 47-1743), $Ca(OH)_2$ phase (JCPDS No: 44-1481), SiO_2 phase (JCPDS No: 46-1045) were observed in the XRD patterns.

XRD results show that, XRD peaks corresponding to $Ca(OH)_2$ and SiO_2 are the major peaks available in fly ash before CO_2 capture. This reveals that free lime (CaO) available in fly ash get hydrated due to the moisture in fly ash and form $Ca(OH)_2$ initially. It is noticeable that, the height of the XRD peaks of $Ca(OH)_2$ got significantly reduced and XRD peak corresponding to $CaCO_3$ was appeared in the fly ash after CO_2 capture. Therefore, the XRD results of fly ash before and after CO_2 capture, confirm that, carbonation reaction ($CaO + CO_2 \rightarrow CaCO_3$) takes place during the CO_2 capture process using fly ash.

4.2.4 Effect of contact time for CO_2 capture performance of fly ash

Table 4.4: Effect of contact time for CO_2 capture capacity of fly ash at 30 ºC, 1 atm and 0 wt% moisture

Contact time for CO_2 capture (min)	**CO_2 capture by adsorption (µmol/g sorbent)**	**CO_2 capture by carbonation reaction (µmol/g sorbent)**	**Total CO_2 capture (µmol/g sorbent)**
1	2.80±0.10	204.60±0.40	207.41±0.50
5	2.81±0.10	224.70±0.40	227.51±0.50
30	2.90±0.10	226.40±0.40	229.30±0.50

Table 4.4 depicts the results obtained for CO_2 capture performance using fly ash when the contact time between CO_2 and fly ash in the tubular reactor is varied at 1 minute, 5 minutes and 30 minutes while keeping other conditions constant at 30 ºC, 1 atm pressure and 0 wt% moisture. According to the results, there is no significant change in the CO_2 capture capacity by both adsorption and carbonation reaction when the contact time was increased. However, fly ash shows a very low CO_2 capture capacity by adsorption than by carbonation reaction. The reason for this is, the high free lime (CaO) content in fly ash causes to capture more CO_2 by carbonation reaction. However, these results indicate that 1 minute would be a more practical selection for the space time in the actual reactor chamber. At 1 minute contact time, the corresponding total CO_2 capture capacity of fly ash was 207.40±0.50 (µmol/g sorbent).

4.2.5 Process simulation results for CO_2 capture

Table 4.5 shows the process stream flow results obtained from the Aspen plus simulation of the scaled-up reactor system for CO_2 capture. The simulation was made on the basis of using 90% of the entire annual quantity of fly ash as the qualified fly ash which is suitable for cementitious applications after CO_2 capture. The single scaled-up system comprising of two reactors in series, where each reactor was loaded with 900 ktonne of fly ash and, operated at 30 ^{o}C temperature, 1 atm pressure and 5 wt% moisture content. Simulation results show that, totally 16.48 ktonne CO_2/year can be captured using the annual qualified fly ash quantity of 1,800 ktonne and, the total CO_2 capture is equivalent to 0.09% of the annual CO_2 emission (18,174.18 ktonne/year) from Mae Moh coal fired power plant, Thailand.

Table 4.5: Process stream flow results from the Aspen plus simulation for the CO_2 capture process

Reactor	**Stream ID**	**Fly ash mass flow rate (ktonne/year)**	**CO_2 mass flow rate (ktonne/year)**	**CO_2 Capture (ktonne/year)**
Reactor 1	Input	900	18,174.18	8.24
	Output		18,165.94	
Reactor 2	Input	900	18,165.94	8.24
	Output		18,157.70	
Total	Input	1800	18,174.18	16.48
	Output		18,157.70	

The Aspen plus simulation conducted for scaled-up CO_2 capture was just a preliminary calculation in order to estimate the total CO_2 capture on the basis of experimental CO_2 capture capacity using the available fly ash quantity in Mae Moh coal fired power plant, Thailand. Further experimental investigations and rigorous simulations under the real flue gas conditions are required to analyze proper scaled-up reactor sizing for CO_2 capture using fly ash.

4.3 SO_2 capture using fly ash

4.3.1 SO_2 capture of fly ash at low temperatures

Table 4.6 reports the SO_2 capture capacities of fly ash at 50 ºC and 100 ºC. The SO_2 capture by fly ash can occur in two ways via adsorption and reaction with free Ca^{2+} ions. The total SO_2 capture capacity at 100 ºC is higher than the total SO_2 capture capacity at 50 ºC. The results indicate that, the temperature affects to both adsorption and reaction during the SO_2 capture by fly ash. Adsorption prefers low temperatures while, reaction boosts up at high temperatures. Unfortunately, SO_2 adsorption at low temperatures is reversible, which is not a desirable option to capture a toxic gas like SO_2. However, SO_2 capture capacity due to the reaction with free Ca^{2+} ions boosts up approximately by 50% when the temperature increases from 50 ºC to 100 ºC. Therefore, the reaction to convert SO_2 into an irreversible form at high temperatures is preferable for the SO_2 capture using fly ash.

Table 4.6: Average SO_2 capture capacities of fly ash at low temperatures

Temperature (ºC)	**SO_2 capture capacity by adsorption (µmol/g sorbent)**	**SO_2 capture capacity by the reaction (µmol/g sorbent)**	**Total SO_2 capture capacity (µmol/g sorbent)**
50	40.68	45.19	85.87
100	34.61	65.23	99.84

The free lime available in fly ash can play a major role to interact with SO_2 for sulfation reactions during the SO_2 capture process, where free lime and SO_2 can react to form $CaSO_4$. In practical, fresh fly ash coming out from a pulverized coal fired power plant consists of approximately 6 wt% of moisture content [35]. Due to the moisture, most of the free lime available in fly ash can easily turn into hydrated lime (calcium hydroxide) which may lead to high reactivities with SO_2 at low temperatures [16, 77]. The irreversible dehydration reaction of $Ca(OH)_2$ can occur at high temperatures and it can promote the reaction between CaO and SO_2 [69]. Reaction 4.1 shows the irreversible dehydration of $Ca(OH)_2$ and reaction 4.2 represents the SO_2 sulfation with CaO.

$$Ca(OH)_2 \rightarrow CaO + H_2O \qquad \text{Reaction 4.1}$$

$$CaO + SO_2 + \tfrac{1}{2} O_2 \rightarrow CaSO_4 \qquad \text{Reaction 4.2}$$

The temperature of flue gas after combustion from a pulverized coal fired power plant varies in the range of 110 °C – 150 °C [35]. As a result, the actual temperature that is suitable for SO_2 capture can exceed 100 ºC when the fly ash is directly applied to capture SO_2 from flue gas. Since, SO_2 is a toxic gas, the irreversible sulfation reaction is preferred for SO_2 capture. Therefore, investigation of the specific temperature to boost up the activity of irreversible sulfation reaction is required which will be discussed in the section 4.3.2.

4.3.2 SO_2 capture over fly ash by sulfation reaction

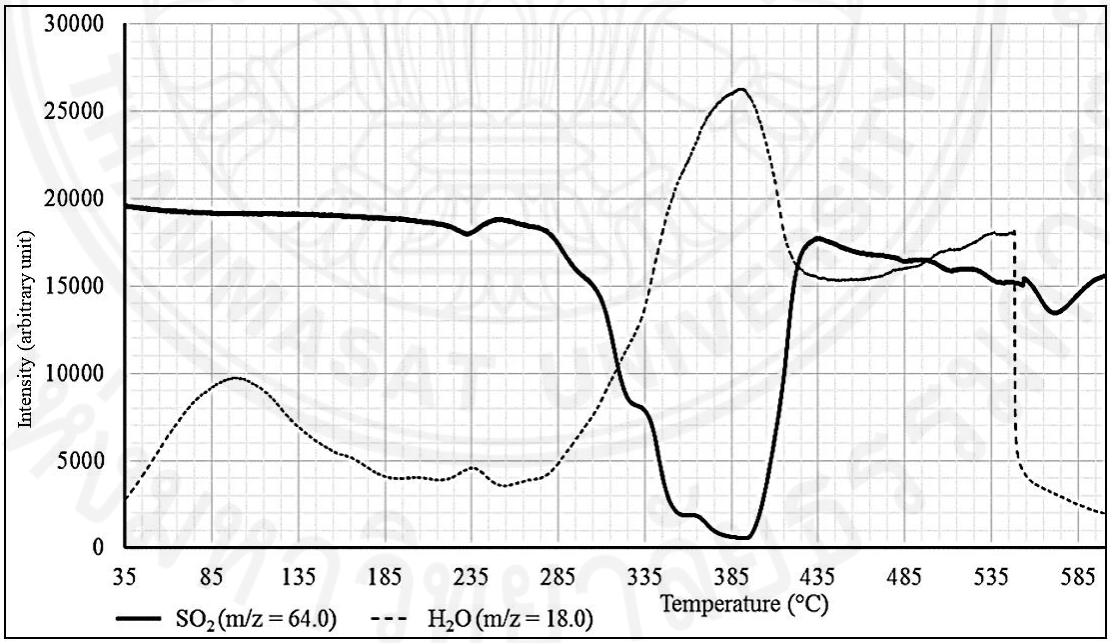

Figure 4.2: Mass spectrometry profiles of SO_2 (m/z = 64.0) and H_2O (m/z = 18.0) for temperature programmed reaction (TPR) over fly ash from 35 ºC - 600 ºC

Figure 4.2 illustrates the mass spectrometry profiles for TPR process over fly ash. The SO_2 (m/z = 64) mass spectrometry profile started to suddenly drop at 285 ºC and acquired the original position at around 435 ºC.

The drop-off in the SO_2 mass spectrometry profile indicates that, SO_2 can be effectively captured using fly ash at temperatures from 285 ºC to 435 ºC. The average SO_2 capture capacity during this temperature range was equivalent to 572.8 µmol/g sorbent and the highest yield of SO_2 capture occurred approximately at 400 ºC.

In addition, the mass spectrometry profile of H_2O vapour (m/z = 18) indicated two peaks at 100 ºC and 400 ºC. Initially, the moisture available in fly ash was released at 100 ºC and secondly, H_2O vapour was liberated corresponding to the SO_2 capture at 400 ºC. H_2O vapour emission at 400 ºC can be related to the reaction 4.1 indicated in section 4.3.1, which is the dehydration of $Ca(OH)_2$ in fly ash to form CaO. The CaO can further react with SO_2 as per the reaction 4.2 to form $CaSO_4$. The results from TPR affirm that, the irreversible reactions take place between fly ash and SO_2 with the highest yield of SO_2 capture at 400 ºC which is lower than the conventional desulfurization temperatures, usually over 700 ºC. However, a part of the H_2O vapour released at high temperatures can be due to the dehydration of different components in fly ash other than $Ca(OH)_2$. This can be the reason for the delay to drop the mass spectrometry profile of H_2O vapour (m/z = 18) after SO_2 capture is finished. In depth studies are required to confirm the behavior of H_2O vapour release from fly ash.

4.3.3 XRD characterization of fly ash before and after SO_2 capture

Figure 4.3 demonstrates the XRD results of three fly ash samples such as, fresh fly ash, after SO_2 capture at 330 ºC and after temperature programmed reaction (TPR) from 35 ºC to 600 ºC. The diffractograms of fly ash samples after SO_2 capture were compared with the diffractogram of the fresh fly ash sample before SO_2 capture.

The $CaSO_4$ phase (JCPDS No: 37-1496), $Ca(OH)_2$ phase (JCPDS No: 44-1481), SiO_2 phase (JCPDS No: 46-1045), $Fe_2^{+}Fe_2^{3+}O_4$ phase (JCPDS No: 19-0629) and Na_2SiO_3 phase (JCPDS No: 16-0818) were observed in the XRD patterns of three fly ash samples.

XRD patterns show that, the $CaSO_4$ (anhydrite) is the only sulfation product detected in the fly ash samples after SO_2 capture. The XRD peaks of $CaSO_4$ increased after TPR process compared to that of fresh fly ash. Therefore, this confirms that, $CaSO_4$ (anhydrite) forms as the sulfation product during the SO_2 capture at 400 ºC using fly ash.

XRD peaks of $Ca(OH)_2$ phase have been disappeared in the XRD pattern of fly ash after the TPR process while, the XRD peaks of $Ca(OH)_2$ phase are still available in the XRD pattern of fly ash after SO_2 capture at 330 ºC. This elucidates that, all the $Ca(OH)_2$ were consumed during the SO_2 capture at 400 ºC.

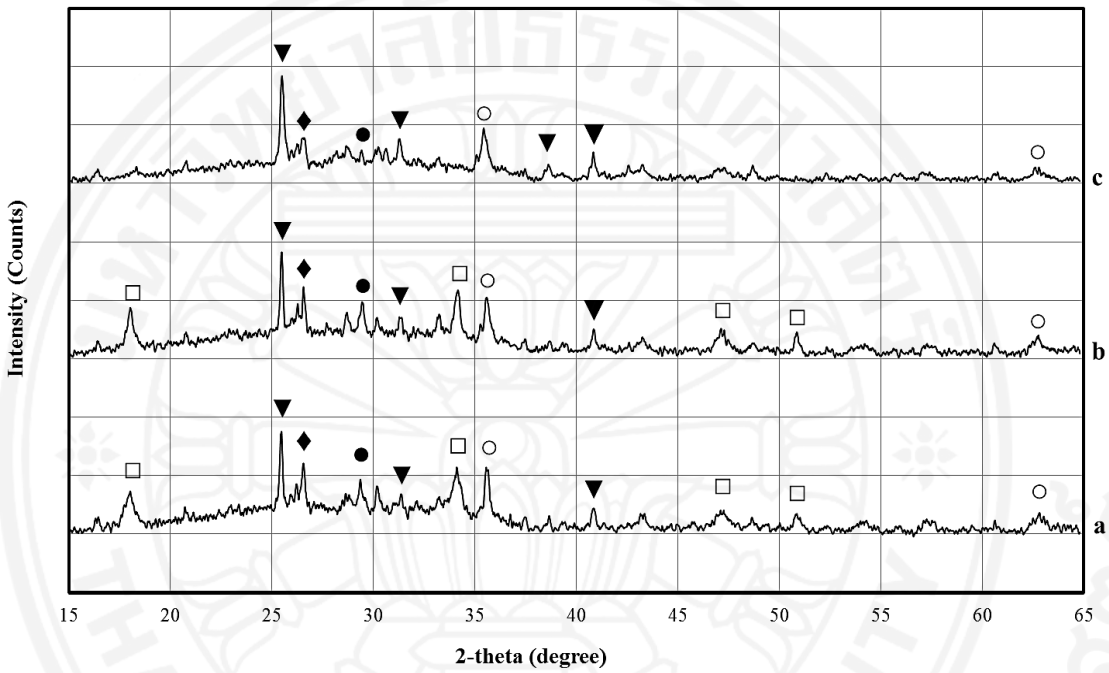

Figure 4.3: XRD patterns of the fly ash samples (**a**: Fresh fly ash; **b**: After SO_2 capture at 330 ºC; **c**: After temperature programmed reaction from 35 ºC - 600 ºC)
▼: $CaSO_4$ (Anhydrite); □: $Ca(OH)_2$ (Portlandite); ♦: SiO_2 (Quartz);
○: $Fe^{2+}Fe_2^{3+}O_4$ (Magnetite); ●: Na_2SiO_3 (Sodium Silicate))

Literature also reports that, the dehydration reaction of $Ca(OH)_2$ in fly ash (reaction 4.1) takes place at 400 ºC and it can boost up the reaction between CaO and SO_2 (reaction 4.2) [16, 77]. Therefore, the XRD results confirm that, the observation of water vapour release from 285 ºC to 435 ºC in section 4.3.2 happens due to the irreversible dehydration reaction of $Ca(OH)_2$ in fly ash which occurs with maximum $Ca(OH)_2$ conversion at 400 ºC without any $Ca(OH)_2$ leftover while, the SO_2 sulfation reaction with free lime (CaO) (reaction 4.2) takes place at the same temperature forming $CaSO_4$ (anhydrite) as the product.

In addition, Figure 4.3 shows that, the respective XRD peaks of SiO_2 and Na_2SiO_3 have been slightly reduced in the XRD pattern of fly ash after the TPR process compared to other two XRD patterns. However, further investigations are required to confirm the possibility of SO_2 adsorption into SiO_2 crystalline structures in fly ash during the SO_2 capture. The experimental results suggest that, fly ash from Mae Moh coal fired power plant, Thailand can be utilized for SO_2 capture at low temperatures to lower the load of desulfurization unit for flue gas emission from the same vicinity.

4.2.2 Process simulation results for SO_2 capture

Aspen plus process simulation was carried out for the scaled-up packed bed reactor system according to the assumptions as described in section 3.2.5. The simulation was performed on the basis of using 10% of the entire annual quantity of fly ash as the unqualified fly ash which is not suitable for cementitious applications. The scaled-up reactor system comprising of two tubular reactors in parallel, where each reactor was loaded with 100 ktonne of unqualified fly ash and, operated at 400 ^{o}C temperature under 1 wt% of simulated flue gas flow. Since, the flue gas quantity to be handled is large and the mass of fly ash in each packed bed should be kept at a constant value of 100 ktonne, the pressure drop in the packed bed of each reactor, becomes the key parameter that should be controlled for the scaled-up reactor system. The pressure drop in the packed bed varies with the other reactor design parameters such as, flue gas inlet mass flow rate, packed bed void fraction, reactor diameter, and reactor length. Therefore, a sensitivity analysis was initially carried out in Aspen plus in order to determine the suitable values for the necessary design parameters.

The Aspen plus sensitivity analysis results are shown in the graphs from Figure 4.4 to Figure 4.7. The reactor inlet pressure was assumed to be equal to the flue gas inlet pressure of 1.2 atm and the reactor system should be designed by minimizing the pressure drop in each packed bed where, the reactor outlet pressure should be equal to 1 atm (total pressure drop to be 0.2 atm). The results indicate that, flue gas inlet mass flow rate should be 42,500 kg/hr, packed bed void fraction should be kept at 0.9, reactor diameter should be 6 m and, the reactor length should be 8 m in order to maintain the reactor outlet pressure at 1 atm.

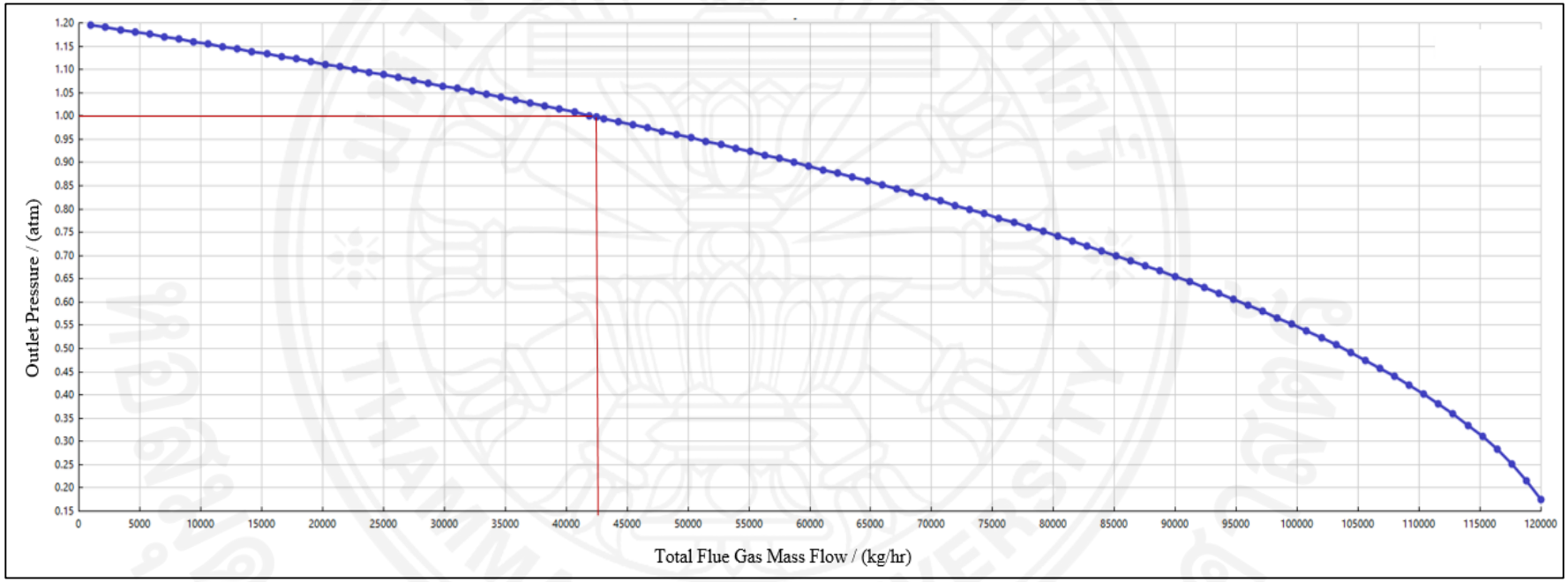

Figure 4.4: Aspen plus sensitivity analysis results for the variation of reactor outlet pressure with respect to the total flue gas mass flow into the scaled-up packed bed reactor system

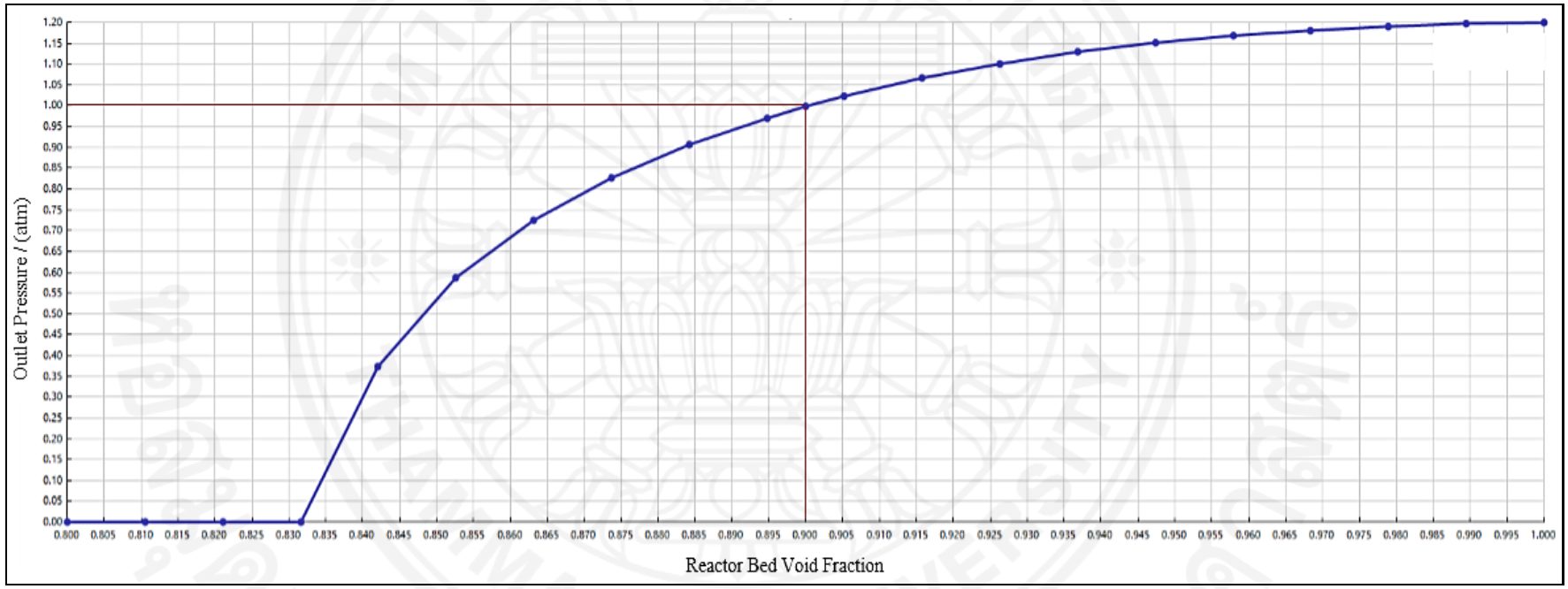

Figure 4.5: Aspen plus sensitivity analysis results for the variation of reactor outlet pressure with respect to the reactor bed void fraction in the scaled-up packed bed reactor system

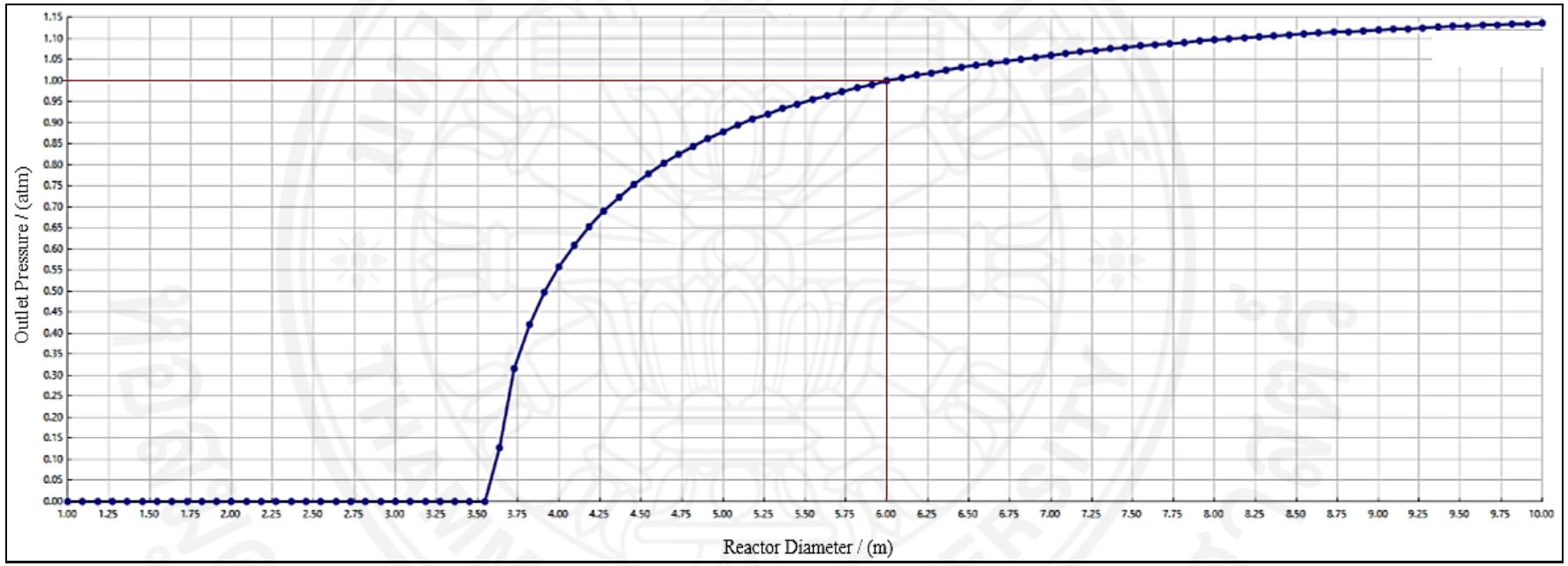

Figure 4.6: Aspen plus sensitivity analysis results for the variation of reactor outlet pressure with respect to the reactor diameter in the scaled-up packed bed reactor system

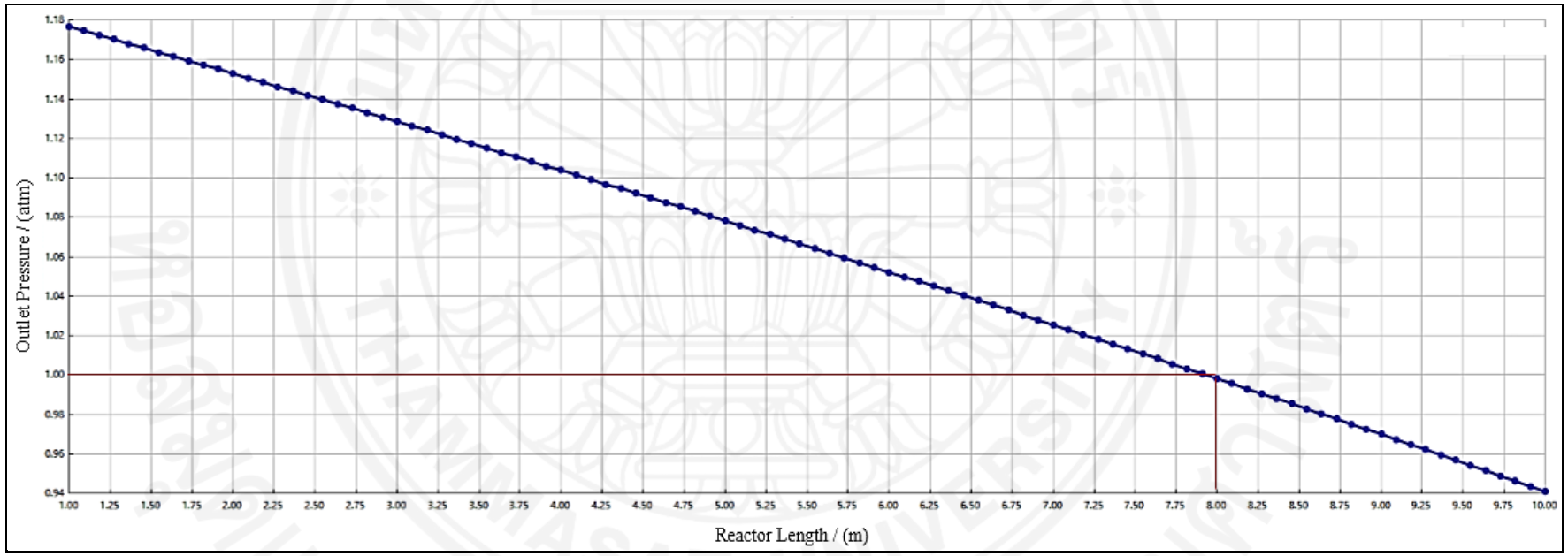

Figure 4.7: Aspen plus sensitivity analysis results for the variation of reactor outlet pressure with respect to the reactor length in the scaled-up packed bed reactor system

The Aspen plus simulation to evaluate the total amount of SO_2 capture from the scaled-up reactor system was conducted using the design parameter values found from the initial Aspen plus sensitivity analysis. Table 4.7 shows the results received from the Aspen plus simulation for the scaled-up packed bed reactor system under the conditions explained in section 3.2.4 and the design parameter values controlling the reactor outlet pressure at 1 atm.

Simulation results report that, totally 4.882 ktonne SO_2/year can be captured using the annual unqualified fly ash quantity of 200 ktonne and, the total SO_2 capture by the scaled-up packed bed reactor system is 0.37% of the annual SO_2 emission without any control (Total 1,314 ktonne SO_2/year without desulfurization unit) from Mae Moh coal fired power plant, Thailand. Therefore, the simulation results confirm that, the waste fly ash from Mae Moh coal fired power plant, Thailand can be applied for SO_2 capture to lower the load of desulfurization unit for flue gas emission from the same vicinity upto a certain extent.

Table 4.7: Process stream results from the Aspen plus simulation for the scaled-up SO_2 capture system

Reactor	**Total fly ash quantity (ktonne/year)**	**SO_2 capture (ktonne/year)**
Reactor 1	100	2.441
Reactor 2	100	2.441
Total	200	4.882

Furthermore, the results indicate that, total heat duty required to maintain the isothermal reactor system at 400 °C is 4,143.12 kW. This heat duty becomes a comparatively large value because, the volume of the reactor becomes larger with a diameter of 6 meters to control the pressure drop through the packed bed at 0.2 atm while being the reactor outlet pressure at 1 atm. According to the simulation results, the residence time through the reactor is 20.764 s which can reduce the activity of the sulfation reaction between fly ash and SO_2. However, increasing the residence time through the reactors is difficult due to the pressure drop barrier.

The simulation results reveal that, the performance of SO_2 capture in the scaled-up system for SO_2 capture using unqualified fly ash highly depends on the pressure drop variable and the packed bed reactor system may not be the most suitable design for the scaled-up SO_2 capture system. The simulation study for SO_2 capture suggests that, further investigations are required to verify the applicability of a fluidized bed reactor system for the scaled-up SO_2 capture system where, a better contact between fly ash and SO_2 in flue gas can lead to increased SO_2 capture. Therefore, further investigations are required to confirm the most suitable design for the scaled-up reactor system for SO_2 capture using fly ash.

Chapter 5
Conclusions and Recommendations

5.1 Conclusions

Fly ash from Mae Moh coal fired power plant of The Electricity Generating Authority of Thailand (EGAT) are available as qualified fly ash which can be used for cementitious applications and unqualified fly ash. The qualified fly ash can be utilized to capture CO_2 in the flue gas coming out from the same power plant as well as in further cementitious applications after CO_2 capture. Gas chromatogram analysis and EDTA titration results showed that, CO_2 capture over fly ash takes place via both surface adsorption and carbonation reaction. CO_2 capture capacity increases with the increment of moisture content and pressure. The total CO_2 capture capacity of fly ash at 30 ˚C, 1 atm and 5 wt% moisture content was equivalent to 208 μmol CO_2/g fly ash sorbent.

The scaled-up reactor system for CO_2 capture simulated in Aspen plus software matching with the qualified fly ash quantity equivalent to 90 wt% of annual fly ash production in 2008 from Mae Moh coal fired power plant, Thailand, was capable of yielding a total CO_2 capture of 16.48 ktonne CO_2/year at 30 ˚C and 1 atm which is 0.09% of the total annual CO_2 emission from the same coal fired power plant. The scaled-up CO_2 capture reactor system was consisted of two tubular reactors in series based on the total qualified fly ash quantity of 1,800 ktonne/year.

In addition, the feasibility of utilizing unqualified fly ash from Mae Moh coal fired power plant, Thailand was evaluated in this study for SO_2 capture at low temperatures to lower the load of desulfurization unit for flue gas emission from the same vicinity. Mass spectrometry measurements and EDTA titration results showed that, fly ash exhibits significant activities for SO_2 capture via both SO_2 adsorption and SO_2 sulfation reaction with free lime at low temperatures such as, 50 ºC and at 100 ºC. Different temperatures result in different interactions between SO_2 and fly ash. SO_2 adsorption at low temperatures becomes reversible when the temperature is increased which is not desirable for SO_2 removal.

However, irreversible SO_2 sulfation at high temperatures is preferable to capture a toxic gas like SO_2 using fly ash whereas, the reactivity between free lime in fly ash and SO_2 improves at high temperatures.

The irreversible SO_2 sulfation reaction with free lime effectively occurs from 285 ºC to 435 ºC with an average SO_2 capture capacity equivalent to 572.8 µmol/g sorbent while forming $CaSO_4$ as the sulfation product after SO_2 capture. The highest yield of SO_2 capture using fly ash occurs at 400 ºC. The reaction mechanism between fly ash and SO_2 consists of two reactions where, initially formed $Ca(OH)_2$ from free lime due to the moisture of fly ash, undergoes to the dehydration reaction with a huge release of water vapour and the irreversible sulfation reaction takes place between free lime and SO_2 at 400 ºC.

Aspen plus simulations were also conducted for the scaled-up SO_2 capture reactor system comprised of two packed bed tubular reactors in parallel at 400 ºC, by controlling the reactor outlet pressure at 1 atm (total pressure drop to be 0.2 atm). This reactor system was able to totally capture 4.882 ktonne SO_2/year which is equivalent to 0.37% of the annual SO_2 emission without any control (Total 1,314 ktonne SO_2/year without desulfurization unit) using the annual unqualified fly ash quantity of 200 ktonne from Mae Moh coal fired power plant, Thailand.

Figure 5.1 summarizes the overall process simulation results from this study for the CO_2 and SO_2 capture reactor systems using fly ash.

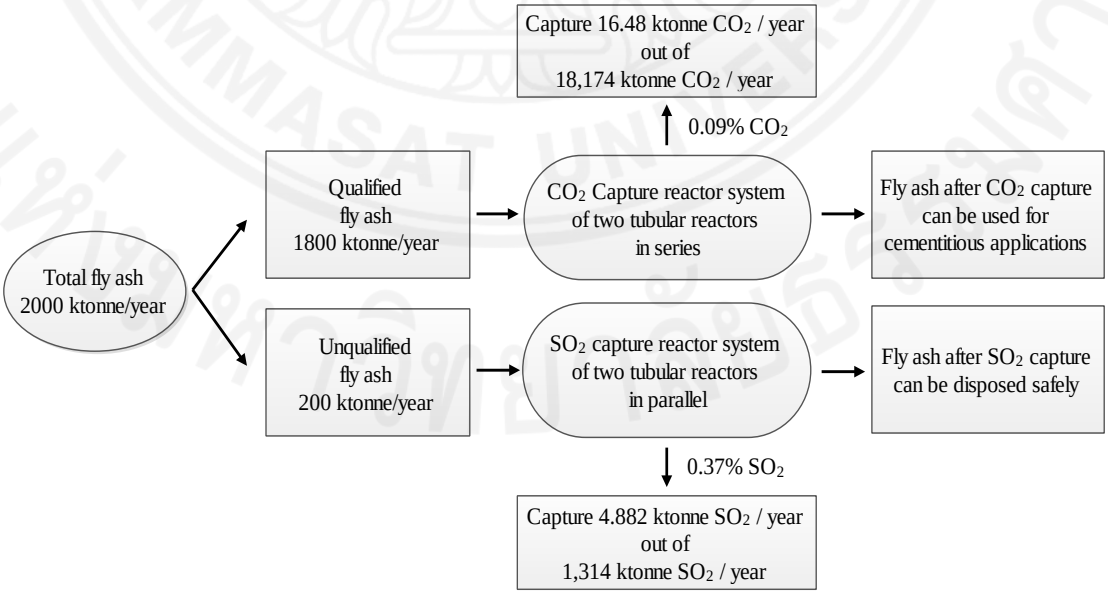

Figure 5.1: Summary of the proposed CO_2 and SO_2 capture systems using fly ash

5.2 Recommendations

The variations of compositions and conditions in the flue gas and fly ash from the coal fired power plant due to the seasonal variations of coal, were not considered for the simulation studies due to their complexity of fluctuation. The investigations of the CO_2 capture and the SO_2 capture performances which were executed in this study, are limited only for coal fly ash from Mae Moh coal fired power plant in Thailand. Since, the composition and characteristics of fly ash obtained from Mae Moh coal fired power plant in Thailand can differ from fly ash in another coal fired power plant, the results of this study can be applicable only for coal fired power plants with the similar quality of coal and operational conditions to the Mae Moh coal fired power plant in Thailand.

Furthermore, analysis was not carried out in order to compare the specified fly ash solid sorbent with other available CO_2 capture techniques, desulfurization techniques, and solid sorbents. Therefore, it is suggested to continue further investigations in order to confirm the most appropriate system of applying fly ash for CO_2 and SO_2 capture from coal fired power plants. The performance of SO_2 capture in the scaled-up system using unqualified fly ash highly depends on the pressure drop constraint in the packed bed reactor system that causes high heat duty and low residence time within the reactor bed. Therefore, future investigations are required to analyze the most suitable reactor type and design for the SO_2 capture.

In overall, the results from this study can be utilized as a basis for future investigations regarding CO_2 and SO_2 capture using fly ash as a solid sorbent as well as, the post capture applications of fly ash after CO_2 and SO_2 capture.

References

1. Mearns, E., Andrews, R. (2014). *Global Energy Trends – BP Statistical Review 2014, Energy Matters.* Retrieved October 24, 2014, from http://euanmearns.com/global-energy-trends-bp-statistical-review-2014/

2. Meshram, P., Purohit, B. K., Sinha, M. K., Pandey, B. D. (2014). Demineralization of low grade coal – A review. *International Journal of Renewable and Sustainable Energy Reviews*, *41*, 745-761.

3. WCA. (2014). *Coal Facts - WCA (World Coal Association, London, UK).* Retrieved November 20, 2014, from http://www.worldcoal.org/sites/default/files/coal_facts_2014%2812_09_2014%29.pdf

4. WCA. (2009, June). *Coal resource - Overview of coal. (World Coal Association, London, UK).* Retrieved November 20, 2014, from http://www.worldcoal.org/sites/default/files/coal_resource_overview_of_coal_report(03_06_2009).pdf

5. Kouprianov, V. I. (2002). Influence of lignite quality on airborne emissions from power generation in the Russian Far East and in Northern Thailand. *International Jounal of Fuel Processing Technology*, *76*, 187-199.

6. Wang, M., Lawal, A., Stephenson, P., Sidders, J., Ramshaw, C., Yeung, H. (2011). Post-combustion CO_2 Capture with Chemical Absorption: A State-of-the-art Review. *Chemical Engineering Research and Design*, *89*, 1609-1624.

7. Yang, H., Xu, Z., Fan, M., Gupta, R., Slimane, R. B., Bland, A. E., Wright, I. (2008). Progress in carbon dioxide separation and capture: A review. *Environmental Sciences*, *20*, 14 - 27.

8. Wolsky, A. M., Daniels, E. J., and Jody, B. J. (1994). CO_2 Capture from the Flue Gas of Conventional Fossil Fuel Fired Power Plants. *Environmental Progress*, *13*, 214-219.

9. Arenillas, A., Smith, K. M., Drage, T. C., Snape, C. E. (2005). CO_2 capture using some fly ash-derived carbon materials. *Fuel*, *84*, 2204–2210.

10. NLM. (1998). *SO_2 fact sheet in Hazardous Substances Data Bank (HSDB) by U.S National Library of Medicine's (NLM)*. Retrieved February 20, 2015, from http://toxnet.nlm.nih.gov/cgi-bin/sis/search2/f?./temp/~YZ2g1Q:3

11. Ward, P. L. (2009). Sulfur dioxide initiates global climate change in four ways. *Thin Solid Films*, *517*, 3188–3203.

12. Thanh, B. D., Lefevre, T. (2001). Assessing Health Benefits of Controlling Air Pollution from Power Generation: The Case of a Lignite-Fired Power Plant in Thailand. *Environmental Management*, *27(2)*, 303–317.

13. Burnard, K, Jiang, J, Li, B., Brunet, G., Bauer, F. (2014). *Emissions Reduction through Upgrade of Coal-Fired Power Plants : Learning from Chinese Experience by International Energy Agency*. Retrieved February 22, 2015, from https://www.iea.org/publications/freepublications/publication/PartnerCountrySeriesEmissionsReductionthroughUpgradeofCoalFiredPowerPlants.pdf

14. Brigden, K., Santillo, D., Stringer, R. (2002). *Hazardous emissions from Thai coal-fired power plants by Greenpeace Research Laboratories, Department of Biological Sciences, University of Exeter, Exeter, UK*. Retrieved October 12, 2014, from http://www.greenpeace.to/publications/Thai%20fly%20ash%20report%20FINAL.pdf

15. Dehghani, A., Bridjanian, H. (2010). Flue Gas Desulfurization Methods to Conserve the Environment. *Petroleum & Coal*, *4*, 220-226.

16. Barbara, Toole-O'Neil. (1998). *Dry Scrubbing Technologies for Flue Gas Desulfurization*. Ohio Coal Development Office, United States: Kluwer Academic Publishers, 862 pages.

17. Wang, L. K., Williford, C., Chen, W. Y., (2005), *Desulfurization and Emissions Control*, in *Handbook of Environmental Engineering Volume 2: Advanced Air and Noise Pollution Control*. The Humana Press Inc.,Totowa, New Jersy, US, 35-93.

18. Tsuchiai, H., Ishizuka, T., Ueno, T., Hattori, H., Kita, H. (1995). Highly Active Absorbent for SO_2 Removal Prepared from Coal Fly Ash. *Industrial & Engineering Chemistry Research*, *34*, 1404-1411.

19. Tsuchiai, H., Ishizuka, T., Nakamura, H., Ueno, T., Hattori, H. (1996). Removal of Sulfur Dioxide from Flue Gas by the Absorbent Prepared from Coal Ash: Effects of Nitrogen Oxide and Water Vapor. *Industrial Engineering Chemistry Research*, *35*, 851-855.

20. Restrepo, A, Miyake, R, Kleveston, F, Bazzo, E. (2012). Exergetic and environmental analysis of a pulverized coal power plant. *Energy*, *45*, 195-202.

21. Barman, N. B., Cebolla, V. L., Mehrotra, A. K., Mansfield, C. T. (2001). Petroleum and Coal. *Analytical Chemistry*, *73*, 2791-2804.

22. O'Keefe, J. M. K., Bechtel, A., Christanis, K., Dai, S., DiMichele, W. A., Eble, C. F, Esterle, J. S., Mastalerz, M., Raymond, A. L., Valentim, B. V., Wagner, N. J., Ward, C. R., Hower, J. C. (2013). On the fundamental difference between coal rank and coal type. *Coal Geology*, *118*, 58-87.

23. Pintana, P., Tippayawong, N. (2013). Nonisothermal Thermogravimetric Analysis of Thai Lignite with High CaO Content. *The Scientific World Journal*, 1-7.

24. Tangtermsirikul, S. (2005). *Development of fly ash usage in Thailand*, in *The International Workshop on Project Management, Kochi, Japan*. Retrieved February 13, 2015, from https://ssms.jp/wp-content/uploads/PDF/ssms2005/SMS05-003_Tangtermsirikul.pdf

25. Xianchun, L., Rathnam, R. K., Jianglong, Y., Wang, Q., Wall, T., Meesri, C. (2010). Pyrolysis and Combustion Characteristics of an Indonesian Low-Rank Coal under O_2/N_2 and O_2/CO_2 Conditions. *International Journal of Energy and Fuels*, *24*, 160-164.

26. Xianglin, S. (2001). *Coal Combustion and Combustion Products. Coal, Oil shale, Natural bitumen, Heavy oil and Peat - Vol 1, Encyclopedia of Life Support Systems (EOLSS).* Retrieved 08 March, 2015, from http://www.eolss.net/sample-chapters/c08/e3-04-03-01.pdf

27. Xiaohui, P., Boshu, H., Yan, L., Wang, C., Song, W., Jingge, S. (2013). Process simulation of oxy-fuel combustion for a 300 MW pulverized coal-fired power plant using Aspen Plus. *International Journal of Energy Conversion and Management, 76*, 581-587.

28. Huilin, L., Guangbo, Z., Rushan, B., Yongjin, C., Gidaspow, D. (2000). A coal combustion model for circulating fluidized bed boilers. *Fuel, 79*, 165–17.

29. Actruba, J. Z. (2009), *How does a circulating fluidized bed boiler work, in Bright Hub Engineering web page,* Retrieved October 09, 2014, from http://www.brighthubengineering.com/power-plants/26547-how-does-a-circulating-fluidized-bed-boiler-work/

30. Corella, J., Toledo, J. M., Molina, G. (2006). Steam Gasification of Coal at Low-Medium (600-800 °C) Temperature with Simultaneous CO_2 Capture in Fluidized Bed at Atmospheric Pressure: The Effect of Inorganic Species. 1. Literature Review and Comments. *Industrial Engineering Chemistry Research*, *45*, 6137-6146.

31. Kolev, N., Schaber, K., Kolev, D. (2001). A new type of a gas–steam turbine cycle with increased efficiency. *Applied Thermal Engineering*, *21*, 391-405.

32. BBC. (2005). *Clean coal technology: How it works, BBC News*. Retrieved October 19, 2014, from http://news.bbc.co.uk/2/hi/science/nature/4468076.stm

33. Robert, W. S. (2014). *A Coal-Fired Thermoelectric Power Plant: Georgia Power's Plant Scherer*. Retrieved 10 October, 2014, from http://water.usgs.gov/edu/wupt-coalplant-diagram.html

34. Ren, S., Hou, Y., Wu, W., Tian, S., Liu, W. (2012). CO_2 capture from flue gas at high temperatures by new ionic liquids with high capacity. *Journal of Royal Society of Chemistry Advances, 2*, 2504-2507.

35. Zevenhoven, R., Kilpinen, P. (2001). *Control of pollutants in Flue Gases and Fuel Gases Vol 4*. Helsinki University of Technology, Finland. 298 pages.

36. Ministry of Industry. (Dated 7th October, 2004). *The Notification of the Ministry of Industry "Emission Standard of the Power Plant", Royal Government Gazette Volume 121, Special Parts 113D, Ministry of Industry, Thailand*. Retrieved, February 25, 2015, from https://www.jetro.go.jp/thailand/e_activity/pdf/moinoti36.pdf

37. MEP. (2012). *Emission Standards of air pollutants for thermal power plants, Ministry of Environmental Protection, China*. Retrieved February 25, 2015, from http://english.mep.gov.cn/standards_reports/standards/Air_Environment/Emission_standard1/201201/t20120106_222242.htm

38. Simachaya, W. (2008). *Lessons Learned for Air Pollution Control in Thailand - Air Quality & Noise Management Bureau Pollution Control Department.* Retrieved January 23, 2015, from http://www.egcfe.ewg.apec.org/publications/proceedings/CleanerCoal/HaLong_2008/Day%201%20Session%201B%20-%20Wijarn%20Simachaya%20Lessons%20Learned%20Thailand.pdf

39. Moretti, A. L., Jones, C. S. (2012, October). *Advanced Emissions Control Technologies for Coal-Fired Power Plants (Report No. BR-1886) in Power-Gen Asia (Babcock & Wilcox Power Generation Group, I. B., Ohio, U.S.A., Ed.), Bangkok, Thailand*. Retrieved October 17, 2014, from http://www.babcock.com/library/Documents/BR-1886.pdf

40. Cao, D., Selic, E., Herbell, J. (2008). Utilization of fly ash from coal-fired power plants in China. *Journal of Zhejiang University SCIENCE A, 9(5),* 681-687.

41. Sua-iam, G., Makul, N. (2014). Utilization of high volumes of unprocessed lignite-coal fly ash and rice husk ash in self-consolidating concrete. *Journal of Cleaner Production, 78,* 184-194.

42. Ahmaruzzaman, M. (2010). A review on the utilization of fly ash. *Progress in Energy and Combustion Science, 36,* 327-363.

43. Hui, L., Liu, G., Cao, Y. (2014). Content and Distribution of Trace Elements and Polycyclic Aromatic Hydrocarbons in Fly Ash from a Coal-Fired CHP Plant. *International Jounal of Aerosol and Air Quality Research, 14,* 1179-1188.

44. Gines, O., Chimenos, J. M., Vizcarro, A., Formosa, J., Rosell, J. R. (2009). Combined use of MSWI bottom ash and fly ash as aggregate in concrete formulation: Environmental and mechanical considerations. *International Jounal of Hazardous Materials, 169,* 643-650.

45. Berrymana, C., Zhuam J., Jensena, W., Tadrosb, M. (2005). High-percentage replacement of cement with fly ash for reinforced concrete pipe. *Cement and Concrete Research, 35,* 1088– 1091.

46. Kaewmanee, K., Krammart, P., Sumranwanich, T., Choktaweekarn, P., Tangtermsirikul, S. (2013). Effect of free lime content on properties of cement–fly ash mixtures. *International Jounal of Construction and Building Materials, 38,* 829-836.

47. Lee, K. T., Mohamed, A. R., Bhatia, S., Chub, K. H. (2005). Removal of sulfur dioxide by fly ash/CaO/$CaSO_4$ sorbents. *Chemical Engineering Journal*, *114*, 171–177.

48. Maroto-Valer, M., Andresen, J. M., Zhang, Y., Lu, Z. (2004). *Development of Fly Ash derived Sorbents to Capture CO_2 from Flue Gas of Power Plants by The Energy Institute, The Pennsylvania State University, US*. Retrieved February 07, 2015, from http://www.osti.gov/scitech/servlets/purl/924619-Xmuum3/

49. Valer, M. M. M., Lu, Z., Zhang, Y., Tang, Z. (2008). Sorbents for CO_2 capture from high carbon fly ashes. *Waste Management*, *28*, 2320-2328.

50. Zhang, Z., Wang, B., Sun, Q. (2014). Fly Ash-derived Solid Amine Sorbents for CO_2 Capture from Flue Gas. *Energy Procedia*, *63*, 2367 – 2373.

51. Montes-Hernandez, G., Perez-Lopez, R., Renard, F., Nieto, J. M., Charlet, L. (2008). Mineral sequestration of CO_2 by aqueous carbonation of coal combustion fly ash. *Journal of Hazardous Materials, Elsevier*, *161(2-3*), 1347 - 1354.

52. Freund, P., Bachu, S., Simbeck, D., Thambimuthu, K., Gupta, M. (2005). *Annex I: Properties of CO_2 and carbon based fuels in IPCC Special Report on Carbon dioxide Capture and Storage by Cambridge University Press, New York, US*. Retrieved June 05, 2015, from https://www.ipcc.ch/pdf/special-reports/srccs/srccs_wholereport.pdf

53. Plaza, M. G., Pevida, C., Arenillas, A., Rubiera, F., Pis, J. J. (2007). CO_2 capture by adsorption with nitrogen enriched carbons. *Fuel*, *86*, 2204–2212.

54. Gray, M. L., Soong, Y., Champagne, K. J., Baltrus, J., Stevens, R. W., Toochinda, P., Chuang, S. S. C. (2004). CO_2 capture by amine-enriched fly ash carbon sorbents. *Separation and Purification Technology*, *35*, 31-36.

55. Bachelor, T. T. N., Toochinda, P. (2012). Development of low-cost amine-enriched solid sorbent for CO_2 capture. *Environmental Technology*, *33(23)*, 2645–2651.

56. Liu, Z., Wang, L., Kong, X., Li, P., Yu, J., Rodrigues, A. E. (2012). Onsite CO_2 Capture from Flue Gas by an Adsorption Process in a Coal-Fired Power Plant. *Industrial & Engineering Chemistry Research*, *51*, 7355−7363.

57. Fogler, H. S. (2006). *Elements of Chemical Reaction Engineering, Fourth Edition, Prentice-Hall International series in the physical and chemical engineering sciences*. Prentice Hall PTR, 1080 pages.

58. Kazuya, G., Katsunori, Y., Takayuki, H. (2013). A review of efficiency penalty in a coal-fired power plant with post-combustion CO_2 capture. *Applied Energy*, *111*, 710–720.

59. Stendardo, S., Foscolo, P. U. (2009). Carbon dioxide capture with dolomite: A model for gas–solid reaction within the grains of a particulate sorbent. *Chemical Engineering Science*, *64*, 2343 - 2352.

60. Symonds, R. T., Lu, D. Y., Hughes, R. W., Anthony, E. J., Macchi, A. (2009). CO_2 Capture from Simulated Syngas via Cyclic Carbonation/Calcination for a Naturally Occurring Limestone: Pilot-Plant Testing. *Industrial Engineering Chemistry Research*, 48, 8431–8440.

61. Ashar, N. G. (2015). *Advances in sulfonation Techniques, Chapter 02 - Chemical and physical Properties of Sulfur Dioxide and Sulfur Trioxide SpringerBriefs in Applied Sciences and Technology*. Retrieved August 15, 2015, from www.springer.com/cda/content/document/9783319226408-c2-1.pdf

62. Foo, H., Teong, L. K., Fernando, N., Mohamed, A. R. (2011). Flue Gas Desulphurization at Low Temperatures Using Coal Fly Ash/Ca-Based Sorbent: Determination of Rate Limiting Step. *Journal of Advanced Chemical Engineering*, *1*, 12 Pages.

63. EPA. (2003). *Air Pollution Technology Fact Sheet (Report No. EPA-452/F-03-016) by United States Environmental Protection Agency*. Retrieved March 10, 2015, from http://www3.epa.gov/ttncatc1/dir1/ffdg.pdf

64. Crnkovic, P. M., Milioli, F. E., Pagliuso, J. D. (2006). Kinetics study of the SO_2 sorption by Brazilian dolomite using thermogravimetry. *Thermochimica Acta*, *447*, 161–166.

65. Fang, F., Li, Z., Cai, N., Tang, X., Yang, H. (2011). AFM investigation of solid product layers of $MgSO_4$ generated on MgO surfaces for the reaction of MgO with SO_2 and O_2. *Chemical Engineering Science*, *66*, 1142–1149.

66. Suchecki, T. T., Walek, T., Banasik, M. (2004). Fly Ash Zeolites as Sulfur Dioxide Adsorbents. *Polish Journal of Environmental Studies*, 13(6), 723-727.

67. Avila, I., Fernando, E. M., Crnkovic, P. M. (2005, November). *A Kinetics Study on the Sorption of SO_2 by Limestone through Thermogravimetry*. 18th International Congress of Mechanical Engineering. Ouro Preto, MG, Brazil. Retrieved January 20, 2015, from http://www.abcm.org.br/anais/cobem/2005/PDF/COBEM2005-1894.pdf

68. Lee, K. T., Bhatia, S., Mohamed, A. R. (2005). Kinetic Model for the Reaction between SO_2 and Coal Fly Ash/CaO/$CaSO_4$ Sorbent. *Journal of Thermal Analysis and Calorimetry*, *79*, 691–695.

69. YuRan, L., HaiYing, Q., ChangFu, Y., XuChange, X. (2007). Kinetic model of CaO/fly ash sorbent for flue gas desulfurization at moderate temperatures. *Fuel*, 86, 785-792.

70. Moshiri, H., Bahram, N. B., Ebrahim, H. A., Taheri, M. (2014). A Comprehensive Kinetic Study of the Reaction of SO_2 with CaO by the Random Pore Model. *Chemical Engineering Technology*, *37(12)*, 2037–2046.

71. Fernandez, J., Renedo, M. J., Pesquera, A., Irabien, J. A. (2001). Effect of $CaSO_4$ on the structure and use of $Ca(OH)_2$/ fly ash sorbents for SO_2 removal. *Powder Technology*, *119*, 201–205.

72. Tsuchiai, H., Ishizuka, T., Nakamura, H., Ueno, T., Hattori, H. (1996). Removal of Sulfur Dioxide from Flue Gas by the Absorbent Prepared from Coal Ash: Effects of Nitrogen Oxide and Water Vapor. *Industrial Engineering Chemistry, 35(3)*, 851-855.

73. Henry, F., Teong, L. K., Fernando, N., Mohamed, A. R. (2011). Flue Gas Desulphurization at Low Temperatures Using Coal Fly Ash/Ca-Based Sorbent: Determination of Rate Limiting Step. *Journal of Advanced Chemical Engineering*, *1*, 10 pages.

74. Lee, K. T., Bhatia, S., Mohamed, A. R. (2005). Kinetic Model for the Reaction between SO_2 and coal Fly Ash/CaO/$CaSO_4$ sorbent. *Journal of Thermal Analysis and Calorimetry*, *79*, 691–695.

75. Chiung-Fang, L., Shin-Min, S., Ren-Bin, L. (2002). Kinetics of the reaction of $Ca(OH)_2$/Fly ash sorbent with SO_2 at low temperatures. *Chemical Engineering Science*, *57*, 93–104.

76. Johnson, B. (2010, August). *An unbiased comparision of FGD Technologies: Wet, Spray Dry and CDS*, in *Worldwide Pollution Control Association.* IL Regional Technical Conference, Illinois, USA. Retrieved September 15, 2015, from http://wpca.info/pdf/presentations/IL2010/An%20Unbiased%20Comparison%20of%20FGD%20Technologies%20-%20Wet%20vs%20Spray%20Dryer%20vs%20CDS.pdf

77. Ogenga, D. O., Siagi, Z. O., Onyango, M. S., Mbarawa, M. (2008). An Overview of the Use of Ca(OH)/Fly Ash in Flue Gas Desulphurization. *R & D Journal of the South African Institution of Mechanical Engineering*, *24(3)*, 4-8.

Appendices

Appendix A

Physical properties of fly ash

No	Physical Property of Fly Ash	Value	Reference
1	Particle diameter	50 - 100 μm	[42]
2	Specific surface area	1.47 m^2/g fly ash	[69]
3	Specific pore volume	3.48×10^{-3} cm^3/g fly ash	[69]
4	Specific gravity	1.7 – 2.4	[24]
5	Blaine fineness	1800 – 4000 cm^2/g	[24]
6	Loss on ignition (%)	0.1 – 5	[24]
7	Bulk density	860 - 1500 kg/m^3	[24]

Appendix B

Chemical and physical properties of CO_2 [52]

No	Chemical and Physical Property of CO_2	Value
1	Molecular weight	44.01 $g.mol^{-1}$
2	Critical temperature	31.1 ºC
3	Critical pressure	73.9 bar
4	Critical density	467 $kg.m^{-3}$
5	Triple point Temperature	-56.5 ºC
6	Boiling (sublimation) point (1.013 bar)	-78.5 °C
7	Triple point pressure	5.18 bar
8	Gas density (1.013 bar at boiling point)	2.814 $kg.m^{-3}$
9*	Gas density	1.976 $kg.m^{-3}$
10*	Specific volume	0.506 $m^3.kg^{-1}$
11*	C_p	0.0364 $kJ.mol^{-1}.K^{-1}$
12*	C_v	0.0278 $kJ .mol^{-1}.K^{-1}$
13*	C_p/C_v	1.308
14*	Viscosity	13.72 $\mu N.s.m^{-2}$
15*	Thermal conductivity	14.65 $mW.m.K^{-1}$
16*	Solubility in water	1.716 $vol.vol^{-1}$
17*	Enthalpy	21.34 kJ mol^{-1}
18*	Entropy	117.2 $J.mol.K^{-1}$

* STP stands for standard temperature and pressure, which is 0°C and 1 atm.

Appendix C

Chemical and physical properties of SO_2 [10]

No	Chemical and physical property of CO_2	Value
1	Molecular weight	64.06 $g.mol^{-1}$
2	Color	Colorless
3	Physical state	Gas (or Liquid)
4	Melting point	- 72.7 ºC
5	Boiling point	-10 ºC
6	Density	2.927 $g.L^{-1}$ (Gas)
7	Odor	Strong odor, Suffocating
8	Odor threshold	Low: 1.175 $mg.m^{-3}$ (0.45 ppm) High: 12.5 $mg.m^{-3}$ (4.8 ppm) Irritating: 5 $mg.m^{-3}$ (1.9 ppm)
9	Solubility	Water at 0 ºC: 22.8 g/100 cc Water at 20 ºC: 11.3 g/100 cc Water at 90 ºC: 0.58 g/100 cc Organic solvents: Acetic acid, Alcohol, chloroform, ether
10	Vapor pressure at 20 ºC	3000 mmHg
11	Flammability limits	Nonflammable
12	Conversion factor	2.62 $mg.m^{-3}$ = 1 ppm

Appendix D

Calculation procedure for GC/MS results

Step 1

1. Calculation of conversion factor after calibrating the gas chromatograph (GC) of CO_2 and mass spectrum (MS) of SO_2 with the standard gases,

$$\text{Mole quantity of the standard gas (mol)} = \frac{\text{Pressure (P)} \times \text{Volume (V)}}{\text{Gas constant (R)} \times \text{Temperature (T)}}$$

Basis: 1 L of the standard gas,

$$\text{The standard gas volume (V)} = \frac{\text{vol \% Concentration of the standard gas}}{100}$$

$$\text{Conversion factor} = \frac{\text{Mole quantity of the standard gas (mol)}}{\text{Peak area of the standard gas (area)}}$$

Step 2

2. Calculation of CO_2 or SO_2 capture capacity due to adsorption,

$$CO_2 \text{ or } SO_2 \text{ capture capacity } \left(\frac{\mu\text{mol}}{\text{g}}\right)$$

$$= \frac{\text{Conversion factor } \left(\frac{\text{mol}}{\text{Area}}\right) \times \text{ Desorption peak area (area)}}{\text{Sorbent sample weight (g)}} \times 10^{-6} \left(\frac{\mu\text{mol}}{\text{mol}}\right)$$

Appendix E

Calibration curve of CO_2 for gas chromatograph

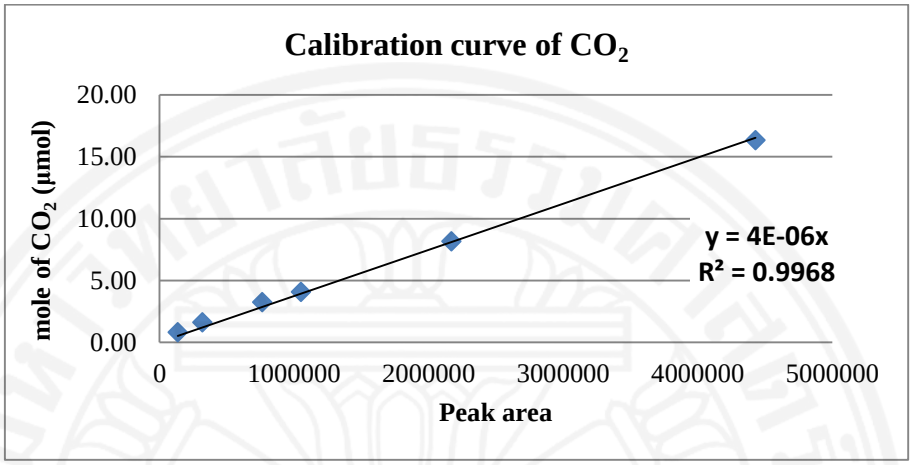

Volume of CO_2 (mL)	Peak area	Average peak area	Mole of CO_2 (µmol)
0.02	155,308	135,007	0.82
	110,336		
	143,091		
	128,518		
	137,780		
0.04	281,433	317,658	1.63
	298,469		
	321,023		
	353,990		
	333,375		
0.08	789,883	762,874	3.27
	757,566		
	768,354		
	768,364		
	730,204		
0.1	1,162,362	1,049,999	4.09
	1,163,759		
	963,683		
	1,019,533		
	940,657		
0.2	2,187,249	2,169,921	8.17
	2,174,072		
	2,147,921		
	2,189,646		
	2,150,717		
0.4	4,443,763	4,429,862	16.35
	4,459,467		
	4,432,390		
	4,381,829		
	4,431,861		

Appendix F

Calibration of SO_2 for mass spectrometry

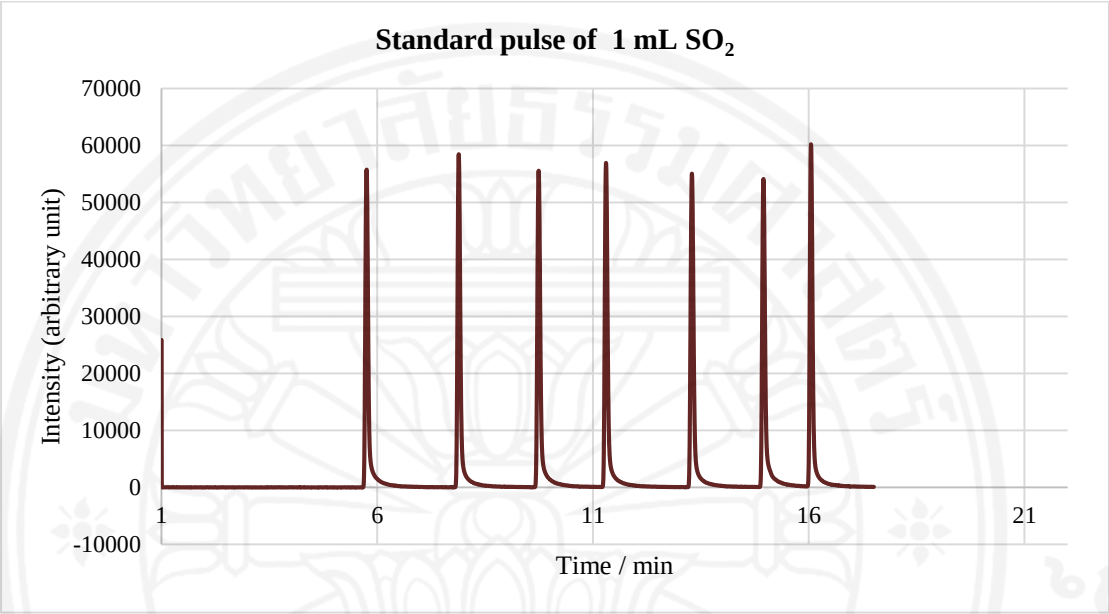

Peak	Peak area	Average peak area	mol of SO_2 (µmol)
1	28,974		
2	29,103		
3	29,741		
4	29,066	29,074.8	1.76
5	29,074		
6	28,739		
7	28,825		

Appendix G

Calculation procedure for EDTA titration results

Step 1

1. Calculation of Ca^{2+} ions available in each fly ash sample,

Concentration of Ca^{2+} ions in fly ash sample solution $(C_1)\left(\frac{mol}{L}\right)$;

$$C_1 = \frac{\text{Concentration of EDTA solution } \left(0.025\ \frac{mol}{L}\right) \times \text{ Titration volume of EDTA}(V_1)}{\text{Titration volume of fly ash sample solution } (V_2)}$$

Ca^{2+} ions available in total fly ash sample $\left(\frac{\mu mol}{g}\right)$

$$= \frac{C_1\left(\frac{mol}{L}\right) \times \text{Total volume of fly ash sample solution (L)}}{\text{Mass of the fly ash sample (g)}} \times 10^{-6}\left(\frac{\mu mol}{mol}\right)$$

Step 2

2. Calculation of CO_2 or SO_2 capture capacity due to reaction with Ca^{2+} ions,

CO_2 or SO_2 capture capacity $\left(\frac{\mu mol}{g}\right)$

$$= Ca^{2+} \text{ ions in fly ash sample (before capture} - \text{ after capture)} \left(\frac{\mu mol}{g}\right)$$